SAPIENZA
UNIVERSITÀ DI ROMA

Tesi di Dottorato

XXIX Ciclo

Sistemi a microonde dedicati ad applicazioni del Ground Penetrating Radar e alla spettroscopia dielettrica

Dottorato in Modelli Matematici per L'Ingegneria
Elettromagnetismo e Nanoscienze

Dipartimento Di Ingegneria Dell'informazione
Elettronica E Telecomunicazioni (DIET)

Dottorando
Santo Prontera

Relatore
Prof. Fabrizio Frezza

Introduzione

Parte I

La presente tesi di dottorato espone il lavoro svolto durante i previsti tre anni del corso di Dottorato di Ricerca, del XXIX ciclo in Modelli Matematici, Elettromagnetismo e Nanoscienze.

Introduzione sul GPR

L'interesse della presente tesi di dottorato si evidenzia su due argomenti, il primo riguarda lo studio e la caratterizzazione di uno specifico radar, il GPR (Ground Penetrating Radar) dispositivo di indagine non invasiva impiegato primariamente per lo studio dell'adiacente sottosuolo o anche di strutture visivamente non accessibili. Il termine radar deriva dalla denominazione inglese "radio detection and ranging" impiegata universalmente per indicare apparecchiature le quali effettuano, a mezzo di onde elettromagnetiche, rilevamenti della posizione o del movimento di oggetti. Il principio di funzionamento è basato sull'analisi delle riflessioni delle onde elettromagnetiche trasmesse nel terreno o nella struttura da esaminare.

Il GPR usa lo stesso principio dei radar convenzionali, ma con alcune differenze significative. In un radar convenzionale l'onda elettromagnetica irradiata si propaga in aria per molti chilometri, nel GPR si propaga nel suolo o in altri materiali solidi raggiungendo distanze di pochi metri o anche decine di metri. La risoluzione dei radar convenzionali è dell'ordine delle decine o

centinaia di metri, il GPR ha risoluzioni dell'ordine delle decine di centimetri e con alcuni tipi di antenne si possono avere risoluzioni dell'ordine dei centimetri.

L'osservazione è realizzata con varie tecniche elettromagnetiche, fornisce con elevata efficienza ed esattezza e in modo quasi continuo indicazioni sulla composizione della struttura indagata. Nello specifico è possibile discriminare interfacce di elementi dotati di differente costante dielettrica.

Con il termine Ground Penetrating Radar si intende, nella più generica delle accezioni, anche la tecnica con cui si conduce l'indagine.

Il successo di questa tecnica di indagine scaturisce dalla compattezza e dalla manovrabilità del sistema, dall'economia dei costi e dai tempi di esecuzione e soprattutto dalla sua caratteristica non distruttiva e da una semplice interpretabilità dei risultati.

L'utilizzo di questa tecnologia consente infatti di rilevare e localizzare nel mezzo investigato la presenza di oggetti, quali manufatti archeologici, danneggiamenti di generiche strutture viarie, strade ponti, gallerie, servizi interrati, condotte idriche, fognarie e del gas, cavità, svolgere attività di sminamento, misure di spessori, o evidenziare discontinuità correnti, in maniera molto facile ed economica.

Cenni storici

Le prime applicazioni delle tecniche GPR risalgono agli anni 30, con applicazioni nella ricerca archeologica. In particolare il primo esperimento condotto con questa tecnologia, fu quello per la determinazione della profondità di un ghiacciaio (1951). Nell'immediato dopo guerra si è verificato un rapido ed intenso sviluppo di questa tecnica, soprattutto con l'impiego

delle tecnologie di derivazione militare, quali i metal detector ed il radar. Per l'epoca le strumentazioni utilizzate erano complesse, ingombranti e richiedevano lunghi tempi per l'acquisizione dei dati.

Negli ultimi anni, i notevoli progressi tecnologici dell'elettronica di base e dell'informatica hanno rivoluzionato la tecnologia dedicata a queste apparecchiature, fornendo prodotti di contenute dimensioni, portatili e di facile impiego.

Le antenne sono di ridotte dimensioni, lavorano a frequenze che vanno in funzione dell'applicazione da 20 MHz ad alcuni GHz, consentono di ottenere risoluzioni maggiori per gli oggetti rilevati, i sistemi GPS abbinati allo strumento forniscono mappature automatiche e dettagliate per le scansioni su vaste aree. I software utilizzati per il post processing garantiscono immagini delle scansioni effettuate di notevole qualità.

Attività sul GPR in Italia

In ambito del progetto COST Action TU1208 "Civil engineering applications of Ground Penetrating Radar", è stato fatto un censimento sulle attività che coinvolgono l'uso GPR in Europa, in questo capitolo della tesi si mettono in evidenza le attività svolte in Italia, quali progetti di ricerca, siti di test, aziende produttrici, Università coinvolte etc.

In particolare nel nostro paese già partire dagli anni 80 i progetti di ricerca e le varie iniziative, finanziate da enti istituzionali, Ministero dell'Università e della Ricerca, consorzi pubblici quali, Consorzio Nazionale Interuniversitario per le Telecomunicazioni (CNIT), aziende Selex-ES e Telespazio S.p.A., hanno sviluppato molteplici tecnologie di radar "stepped frequency" e "ultra-wide band" (UWB), usati sia in ambito civile, archeologico o militare.

Una importante azienda Italiana, fondata negli anni 80 è la IDS S.p.A. che da oltre 30 anni è la principale fornitrice di innovative tecnologie e soluzioni ingegneristiche per le diverse applicazioni cioè: navale, aeronautico, georadar e militare.

Dal 1999 l'IDS ha iniziato la commercializzazione a livello mondiale di sistemi GPR basati su sistemi array multi-frequenza e multi-canale e tutt'oggi è una delle aziende leader in questo settore, una società multi-nazionale con una rete di agenzie e uffici in posizione strategica non solo in Italia, ma anche nei paesi europei e in tutto il mondo.
Alcuni siti test dislocati sul territorio Italiano sono: In Frosinone, dedicato prevalentemente allo sviluppo e uso della tecnologia GPR in applicazioni archeologiche, il secondo è localizzato in Pescate provincia di Lecco, principalmente impiegato per studiare antiche strutture sepolte. Il sito di Ispra in provincia di Varese, è prevalentemente usato per scopi militari e dedicato soprattutto al rilevamento di mine antiuomo. Un altro sito di test molto importante per la ricerca di base, si trova in provincia di Lecce.
Le facoltà scientifiche di molte Università Italiane, sono ampiamente coinvolte nello studio e nella promozione del GPR. Interessanti corsi universitari sono organizzati dall'Università di Roma Tre, Università di Genova, la Seconda Università di Napoli, Politecnico di Milano, Università Mediterranea di Reggio Calabria, Università di Pisa, Università di Siena, Università della Basilicata, Università degli Studi di Bari e dall'Università degli Studi di Messina.

Il sistema analizzato

Il dispositivo analizzato in camera anecoica, è l'insieme del sistema radar GPR: GSSI (Geophysical Survey Systems, Inc.) SIR2000, Figura 1, abbinato all'antenna radar: Radar Team SUB-ECHO HBD 300, Figura 2

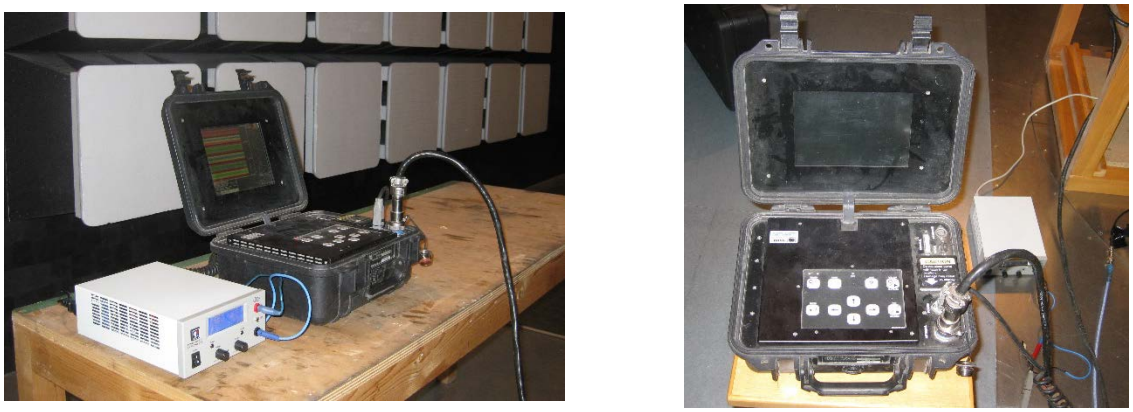

Fig. 1– sistema radar GPR GSSI SIR2000

Fig. 2 – Antenna Radar Team SUB-ECHO HBD 300

Segnale irradiato dal sistema

Il GPR lavora con l'emissione di brevi impulsi elettromagnetici, ripetuti con continuità ed emessi da un'antenna in prossimità della superficie da indagare. L'impulso elettromagnetico si propaga in profondità del terreno, quando incontra una discontinuità dielettrica tra due mezzi, una parte dell'energia

incidente viene riflessa ed una parte prosegue nel secondo mezzo. Le onde riflesse dalla discontinuità ritornano in superficie e vengono captate dall'antenna ricevente ed analizzate dal sistema, la parte di impulso trasmesso procede oltre la discontinuità stessa e può subire altre riflessioni su eventuali discontinuità più profonde. La caratteristica generale di un GPR è quella di un radar che trasmette segnali con una caratteristica banda UWB (Ultra Wide Band) in un range di frequenze che va da 10 MHz a circa 5 GHz. La durata del segnale trasmesso è dell'ordine dell'inverso della banda, che a sua volta è dell'ordine della frequenza centrale dell'antenna in uso. Se siamo a centro banda 20 MHz la durata è quindi dell'ordine di 50 ns, se siamo a 200 MHz la durata dell'impulso è dell'ordine di 5 ns e se siamo a 2 GHz la durata è dell'ordine di 0.5 ns.

In questo caso il segnale trasmesso è un tipico segnale impulsato con una durata temporale dell'ordine di circa 2.70 ns, Figura 3, ed è emesso dal sistema con una determinata frequenza di ripetizione (Pulse Repetion Frequency) PRF Figura 4.

Individuare queste caratteristiche di emissione in fase di misura richiede molta accortezza, in quanto bisogna discriminare fra tutti gli altri segnali ambientali e i disturbi casuali.

Il GPR è di dimensioni contenute e può essere fisicamente traslato gradualmente lungo un prefissato tracciato rettilineo in superficie e ottenere così una rappresentazione bidimensionale o "radargramma", un grafico che rappresenta lo spostamento lungo una direzione in funzione dei tempi di ricezione del segnale riflesso.

L'energia media irradiata è molto bassa, confinata nel sottosuolo, raggiunge svariati metri di profondità, in funzione della frequenza usata, il tipo di terreno etc. e in parte è assorbita istantaneamente. Tutte queste

caratteristiche sono esclusive di un dispositivo GPR, in confronto ad altri dispositivi di esplorazione quali il metal detector o un generico sensore di movimento, che lavorano a piccole profondità e limitate gamme di frequenza.

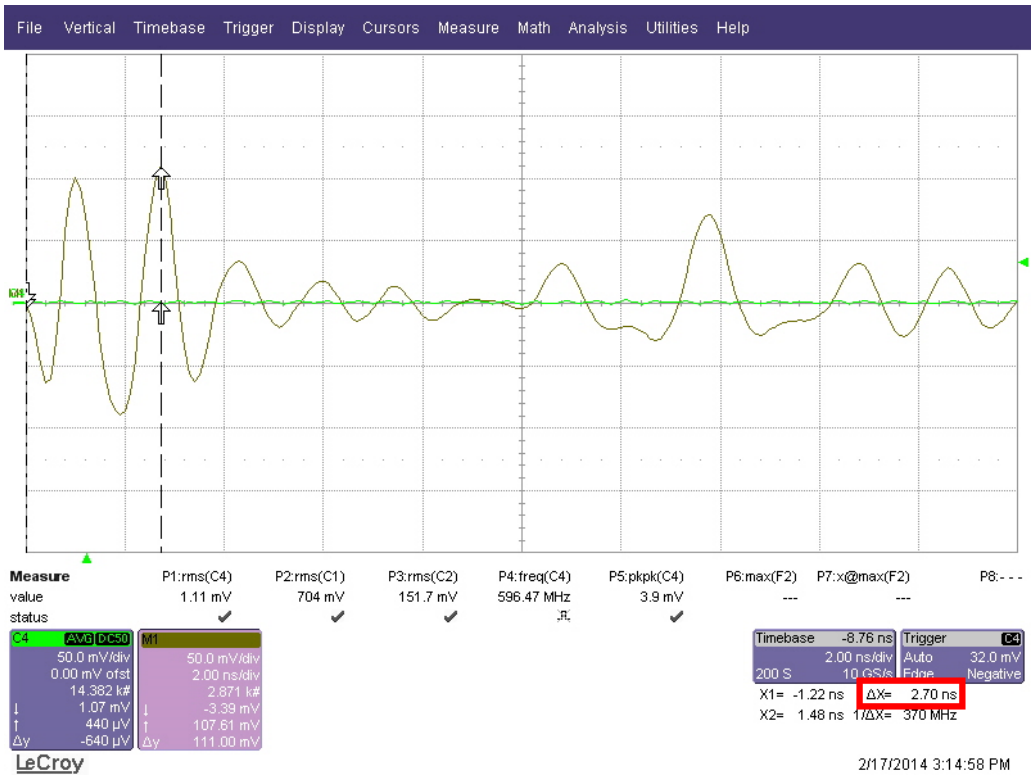

Fig. 3 – L'impulso radar trasmesso è la derivata prima di un impulso gaussiano "mexican hat" ha una durata temporale di 2,70 ns

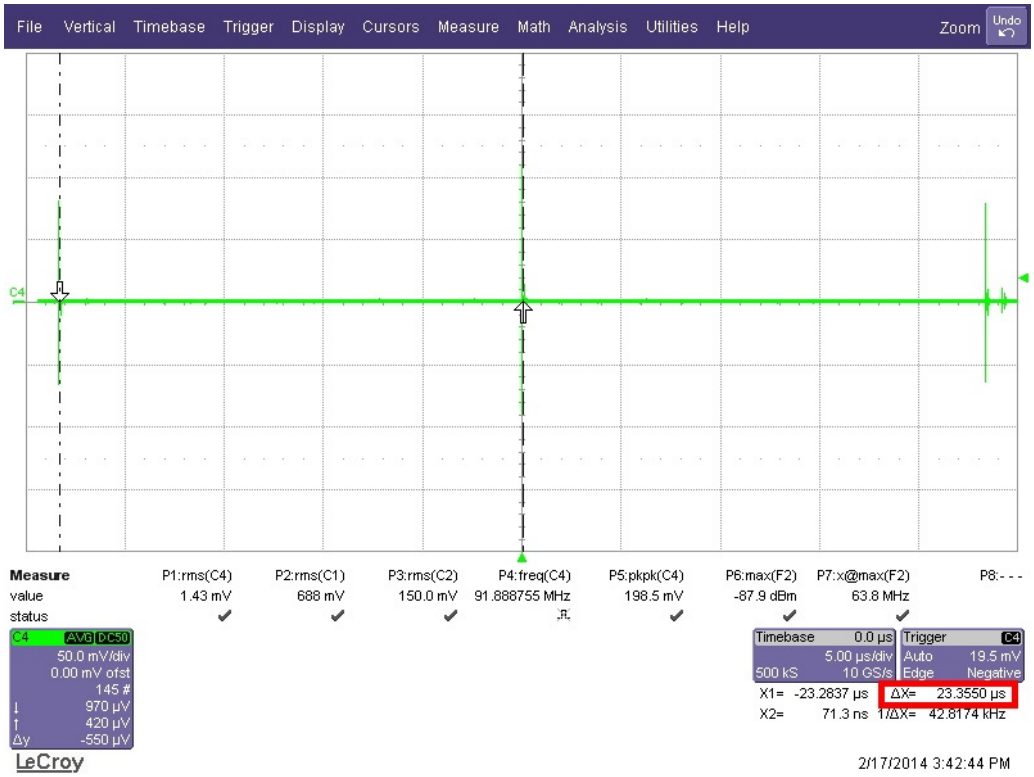

Fig. 4 – Ripetizione temporale dell'impulso emesso, PRF di 23,3 ns

Inoltre l’antenna lavora a stretto contatto con il terreno ispezionato e le proprietà elettriche del terreno stesso hanno una forte influenza sulla impedenza di ingresso dell'antenna del dispositivo e delle sue caratteristiche di radiazione.

Con le suddette considerazioni, il segnale di trasmissione deve avere una durata molto breve nel tempo e l'antenna deve essere in grado di trasmettere il segnale con la minima distorsione per evitare di degradare gli echi di ritorno e falsare l’acquisizione. Queste specifiche richiedono quindi una antenna a larga banda, direttiva e con una basso “ringing” d’antenna.

Il tempo di acquisizione per ogni punto di osservazione viene settato dall'operatore. Nella maggior parte dei casi è sufficiente un fondo scala minore di 100 ns, ma le eccezioni sono diverse. In generale il tempo di acquisizione totale per un sistema GPR è inferiore a 100 ns.

Nello specifico, il primo degli argomenti trattati è rivolto allo studio dell’esposizione elettromagnetica che interessa l’operatore durante l’utilizzo del dispositivo GPR, in particolare sono state considerate le due componenti che intervengono nel processo di esposizione, la radiazione che scaturisce dal back lobe dell’antenna in fase di trasmissione e la radiazione identificata sotto forma di segnale riflesso dal terreno illuminato sottoposto ad indagine, Figura 5.

Lo studio è stato realizzato in due differenti scenari operativi, in un ambiente non anecoico e non schermato e quindi riproducente una tipica situazione di lavoro in campo libero, sia in un ambiente alquanto controllato, cioè anecoico e schermato. In particolare per quest’ultimo scenario è stata scelta la camera semianecoica “VECUVIA” presso l’ente ENEA, Centro Ricerche Casaccia in Roma, Figura 6 e le sue efficienze di schermatura, Figura 7.

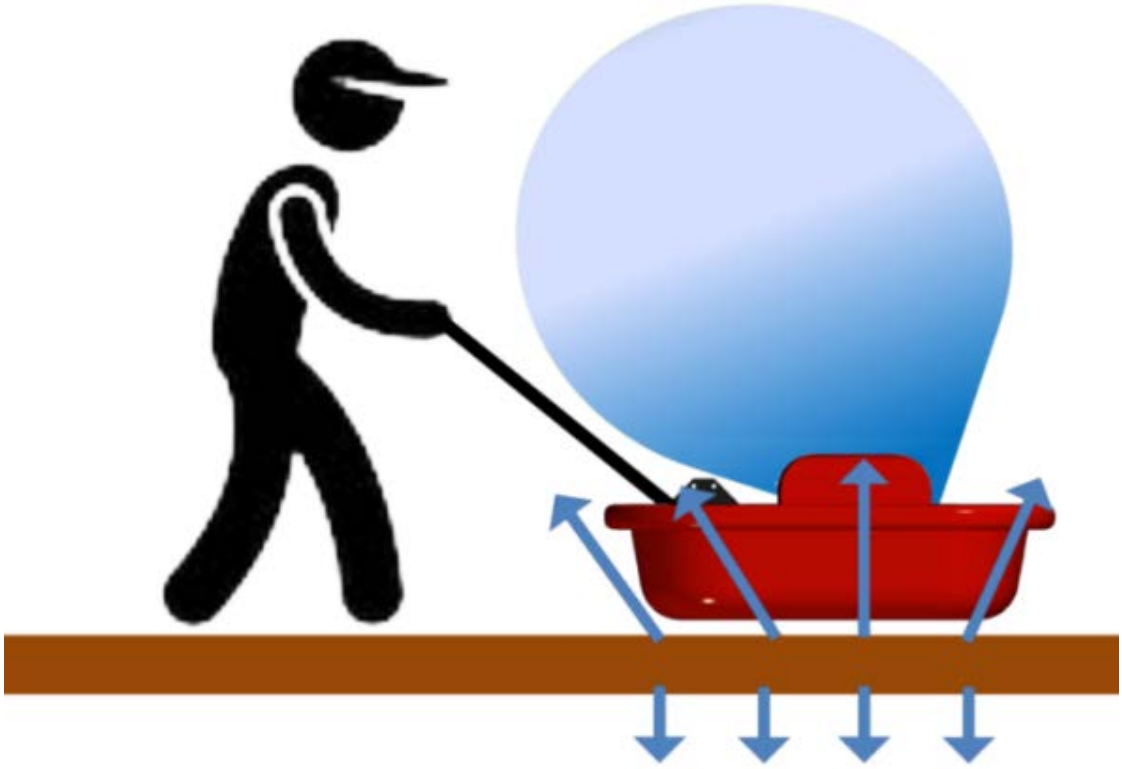

Fig. 5 – Esposizione elettromagnetica dell'operatore durante l'uso del GPR

In seguito lo studio è stato completato, sempre nella suddetta camera semianecoica, con l'analisi delle caratteristiche operative del sistema radar GPR: GSSI (Geophysical Survey Systems, Inc.) SIR2000 e della sua antenna radar. Si è accertato sperimentalmente il valore del campo elettrico emesso ad una individuata distanza, la forma dell'impulso emesso, il pattern d'antenna sia sul piano verticale che orizzontale. E sono stati effettuati una serie di test per verificare come apparati di telefonia mobile o altre analoghe fonti possibili di interferenze possono contaminare i dati raccolti dal GPR.

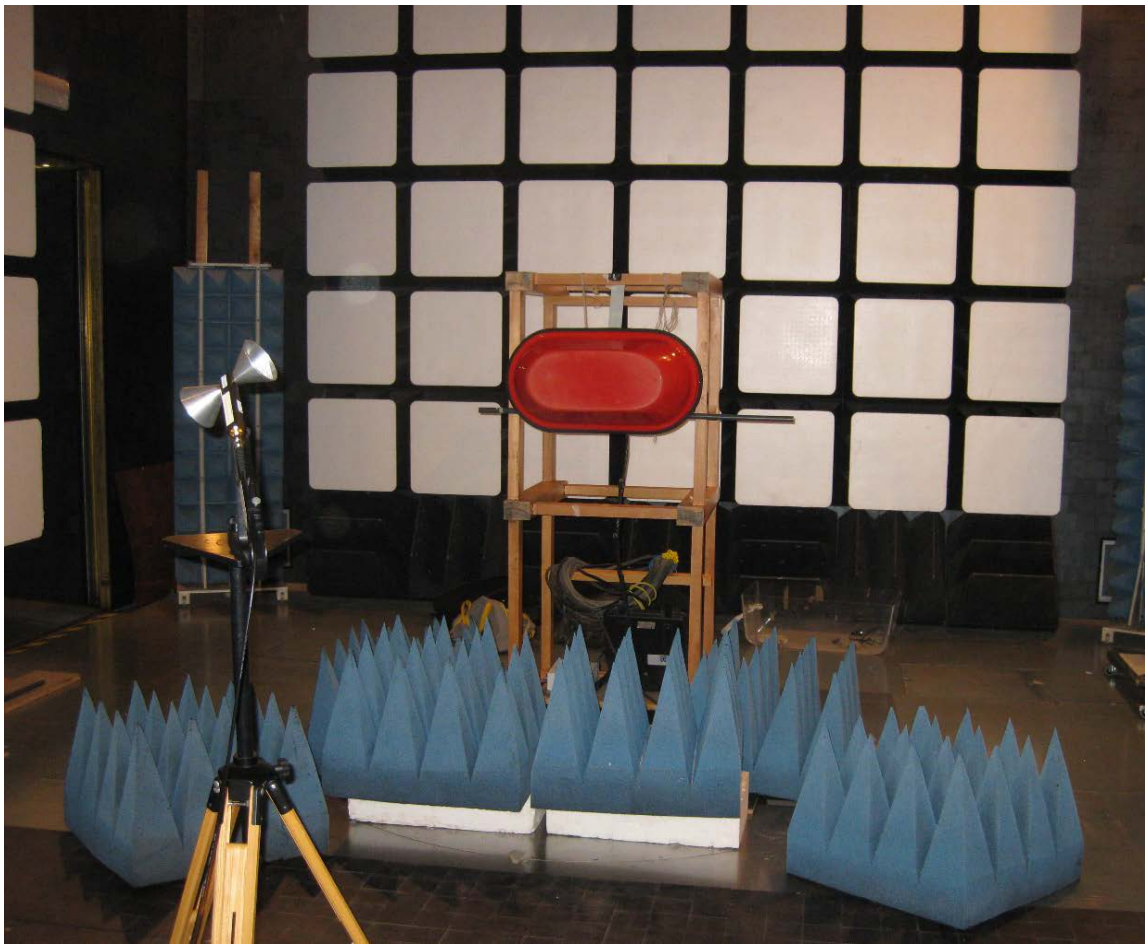

Fig. 6 – Setup in camera semianecoica "VECUVIA" del sistema radar e della sua antenna

Efficienze di schermatura camera semianecoica VECUVIA	
Campo Elettrico	
300 kHz – 30 MHz	120 dB
30 MHz – 400 MHz	105 dB
400 kHz – 18 GHz	100 dB
Campo Magnetico	
10 kHz	60 dB
100 kHz	90 dB

Fig. 7 – Camera semianecoica "VECUVIA", efficienze di schermatura

Modellizzazione di una griglia metallica per applicazioni GPR

Questa parte del lavoro è dedicata alla simulazione di scenari bidimensionali e alle tematiche di scattering elettromagnetico, tipiche condizioni in cui si trova ad operare il GPR. I risultati di questa attività sono stati conseguiti con l'uso un noto software freeware che utilizza i metodi di calcolo alle differenze finite (FDTD), GprMax.

In particolare si focalizza l'attenzione su un oggetto, un modello di griglia metallica formata da cilindrici metallici lunghi e sottili, sepolti nel terreno o incorporati in una struttura, questa è la tipica attività di controllo della qualità del cemento armato o applicazioni simili.

La migliore modellizzazione di una griglia metallica si ottiene considerando un elevato numero di fili metallici, ma è anche importante valutare il raggio del filo metallico e la spaziatura stessa della griglia. A tal proposito si fa riferimento alla cosiddetta regola (Equal Area Rule) EAR, regola dedotta dall'osservazione empirica e descrive come la superficie totale dei fili deve essere uguale alla superficie dell'oggetto da modellare.

Alcuni autori hanno studiato l'affidabilità della regola EAR comparando la radiazione di campo magnetico trasverso, generata da un cilindro nel vuoto con una corrente sulla sua superficie o illuminato da un'onda piana monocromatica trasversa magnetica e confrontato con un modello a griglia metallica. Deducendo così che il modello a griglia è compatibile con la regola EAR. Inoltre i fili troppo spessi si comportano male come quelli troppo sottili.

Tutti i mezzi coinvolti sono assunti lineari ed isotropi, dispersivi, gli oggetti metallici si presume siano perfettamente conduttivi. In questa simulazione non sono state incluse le strutture fisiche sia del ricevitore che

del trasmettitore, la sorgente è rappresentata da una linea di corrente ed è stato calcolato il campo elettrico incidente sul ricevitore.

La propagazione degli errori numerici è contenuta, decretando il passo di discretizzazione spaziale di un fattore 10 volte più piccolo della lunghezza d'onda minima del campo elettromagnetico. La frequenza massima da considerare nella simulazione, è tre volte la frequenza centrale dell'impulso.

Per evitare l'effetto di frammentazione a scala del bordo degli oggetti continui, le forme circolari sono approssimate con un numero di almeno 20 celle per il loro raggio.

E' necessario limitare lo spazio computazionale, inserendo delle forme Perfectly Matched Layer (PML) per i bordi in modalità di Absorbing Boundary Conditions (ABS), usando 10 strati e ponendo sorgenti e target almeno 15 cellule distanziate dallo strato più interno.

Lo scenario è visualizzato in Figura 7a, dove un perfetto conduttore cilindrico dal raggio di R=50mm è inglobato in un dielettrico rappresentante il suolo e avente una ε_r=4. La sorgente è posizionata nell'interfaccia suolo-aria ed emette un campo elettrico parallelo all'asse del cilindro. La struttura wire-grid da modellare è descritta in Figura 7b, ed è composta da N cilindri di raggio r disposti circolarmente con il loro asse adagiato sulla superficie del cilindro. Con un N molto grande il comportamento si avvicina all'oggetto modellato. L'obbiettivo è di verificare la validità di EAR, in questo caso la regola impone la condizione r=R/N=3,125mm.

Una buona attendibilità di questo criterio risulta dalle Figure 8 e 9. I B-scan del campo elettrico sono rappresentati nelle Figure 8c e 8d, ottenuti spostando la sorgente in M = 80 posizioni equidistanti lungo l'interfaccia aria-suolo, il campo elettrico è calcolato sull'interfaccia ad una distanza d = 50 mm dalla sorgente.

Si evidenziano delle differenze tra i risultati relativi al cilindro a sezione circolare e il suo modello wire-grid. In particolare il modello wire-grid provoca un consistente numero di riflessioni secondarie.

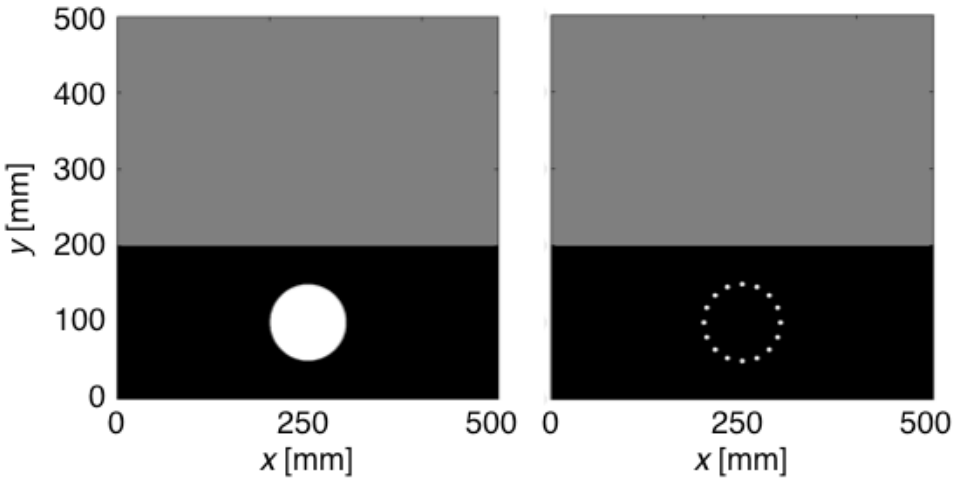

a) b)

Fig. 7 – (a) conduttore cilindrico dal raggio di R = 50mm inglobato in un dielettrico, (b) N cilindri di raggio r disposti circolarmente

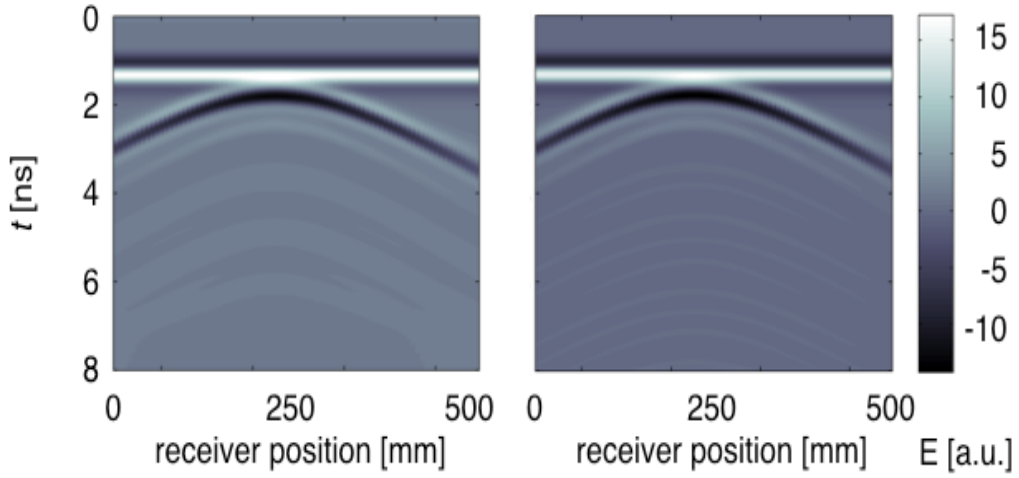

c) d)

Fig. 8 – (c) B-scan ottenuta dal cilindro, (d) B-scan del modello wire-grid

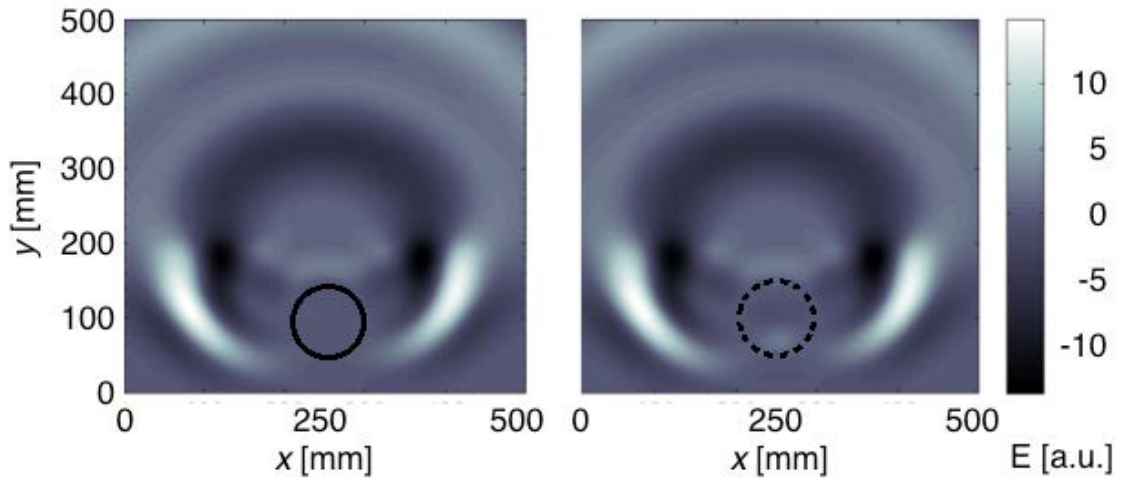

a) b)

Fig. 9 – (a) B-scan con sorgente posizionata in x = 240 mm, y = 250 mm per il cilindro, (b) B-scan con sorgente posizionata in x = 240 mm, y = 250 mm per il modello wire-grid

Il campo irradiato nel sottosuolo (e in particolare all'interno del target), da un'antenna in posizione fissata, Figura 9a e 9b, sono calcolati ponendo la sorgente è in x = 240 mm, y = 250 mm, si deduce che il campo interno del modello wire–grid non svanisce ed è molto più sensibile di quello esterno, questo suggerisce che un maggior numero di fili dovrebbero comporre il modello quando si desidera un buon effetto di schermatura.

La Figura 10a descrive i risultati della configurazione riferita alla Figura 7b, per varie lunghezze del raggio del wire-grid minore, uguale o maggiore che R/N. In particolare è tracciato l'errore di A-scans definito come la grandezza della differenza tra l'esatto A-scan (calcolati in presenza del cilindro circolare) e A-scan ottenuto per il modello a griglia metallica.

L'analisi svolta è di particolare interesse per la simulazione elettromagnetica di scenari Ground Penetrating Radar. I risultati si ripercuotono anche sulle applicazioni di schermatura elettrica e nella misura delle proprietà elettromagnetiche dei materiali attraverso l'uso di schermi coassiali

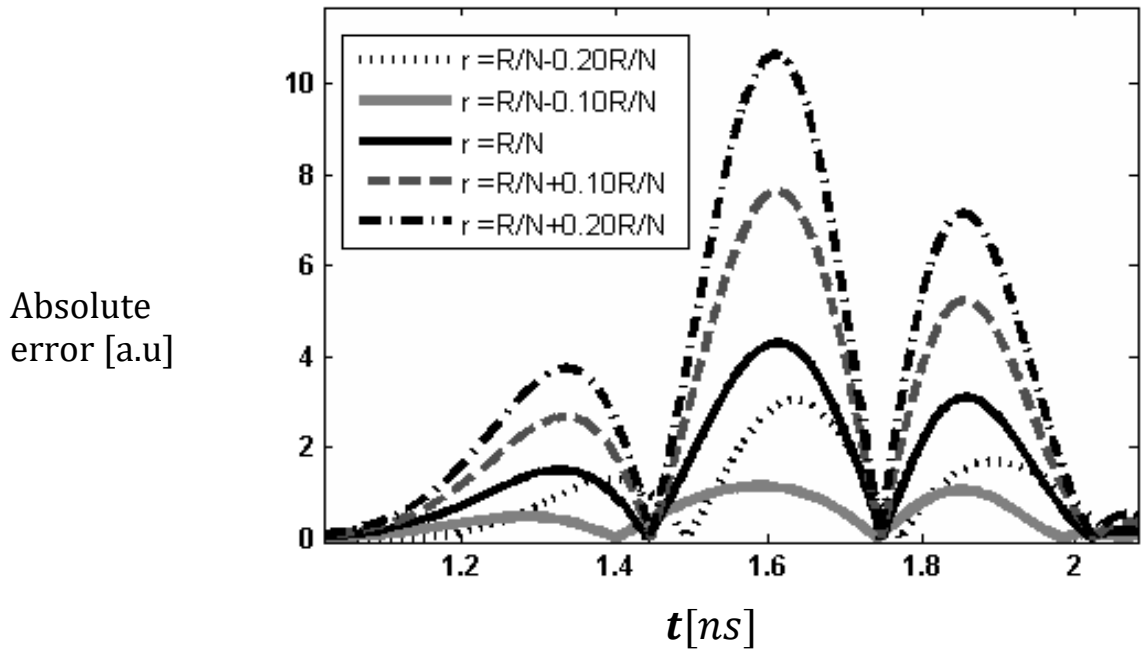

(a)

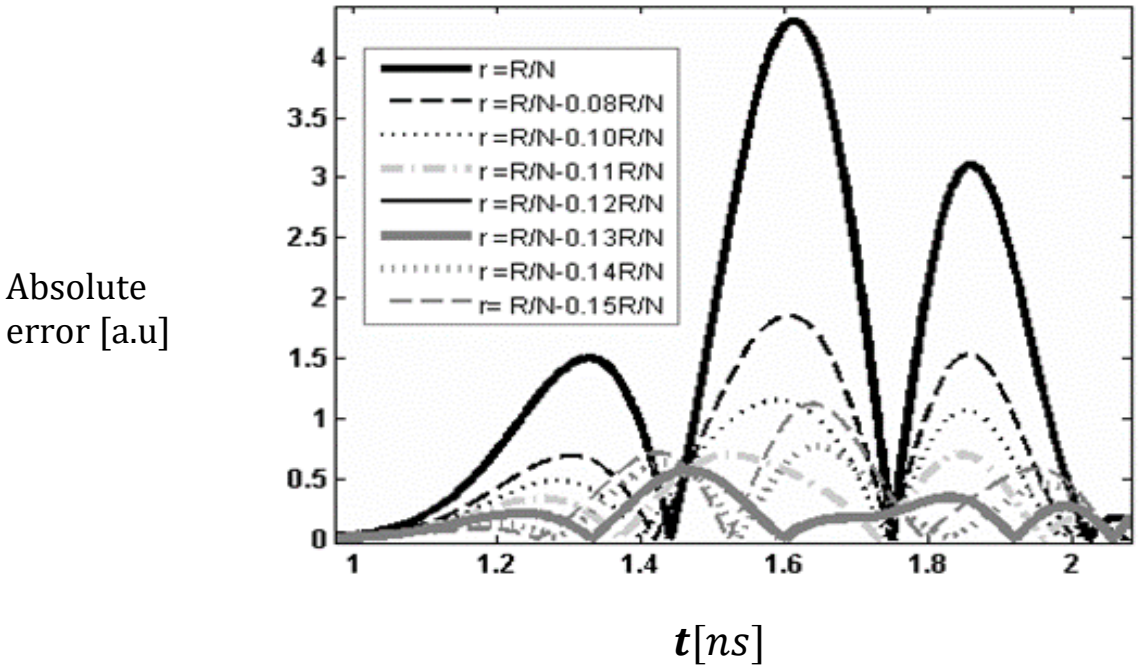

(b)

Fig. 10 – (a) Risultati riferiti alla configurazione della Figura 7b, con errore assoluto sulla A-scan, con N = 16 e per diversi valori del raggio dei fili, (b) Affinamento dell'analisi presentata in Figura 10 (a).

Parte II

Tecniche elettromagnetiche per la valutazione della permettività dielettrica di materiali

Il secondo argomento della tesi è dedicato all'analisi sperimentale della permettività dielettrica complessa di un generico materiale coeso. Lo studio è stato condotto per mezzo di una tecnica riflettometrica in guida d'onda a sezione rettangolare e un (Vector Network Analyzer) VNA. La frequenza di lavoro scelta è quella (Industrial, Scientific and Medical) ISM Band, cioè 2.45 GHz. L'indagine sperimentale è stata svolta presso il Laboratorio di Microonde del Dipartimento di Ingegneria Elettronica dell'Università degli Studi di Roma La Sapienza.

Le tecniche di spettroscopia dielettrica operanti nella banda delle microonde sono sempre più di largo impiego per la misura della permettività complessa di un campione di materiale. La conoscenza di questo importante parametro infatti può fornire informazioni sulla sua qualità e definire l'interazione del materiale e l'effetto di riscaldamento corrispondente.

Una applicazione del riscaldamento a microonde, soprattutto alla ISM Band è dedicato alla manutenzione del manto stradale, infatti, riscaldando l'asfalto attraverso l'uso di microonde, è possibile effettuare riparazioni in loco di fori o fessure presenti sulla superficie stradale. Inoltre l'uso delle microonde potrebbe anche essere impiegato durante la fase di produzione, in sostituzione ai forni convenzionali usati per l'essiccazione e il riscaldamento dei leganti minerali dell'asfalto e nel riciclo della pavimentazione con l'asfalto

rigenerato e bitume. Lo studio della permettività complessa del conglomerato bituminoso, posso far capire come realizzare un sistema dedicato al riscaldamento e all'analisi del sistema.

Il sistema è stato sviluppato con l'uso di una guida d'onda, in particolare la WR430 con una banda di frequenze che va da 1,7 GHz a 2.6 GHz e quindi compatibile con la ISM Band. Nella guida sono stati inseriti e misurati i materiali tipici che compongono l'asfalto. Figura 11 guida d'onda WR430 Figura 12a setup di misura WR430, Figura 12b sezione della guida WR430 con materiale granulare in misura. Nel disegno di Figura 11 si possono notare due finestre di pressurizzazione che svolgono il compito di

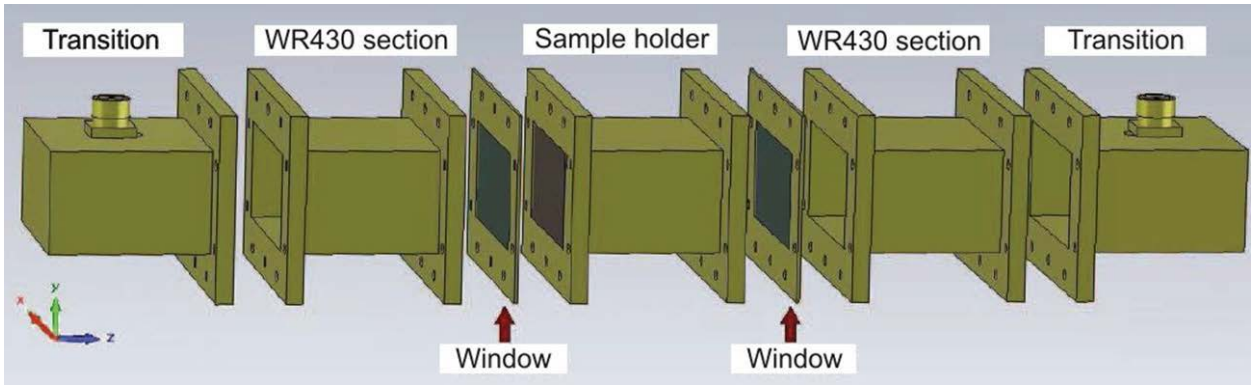

Fig. 11 – Schema guida d'onda WR430

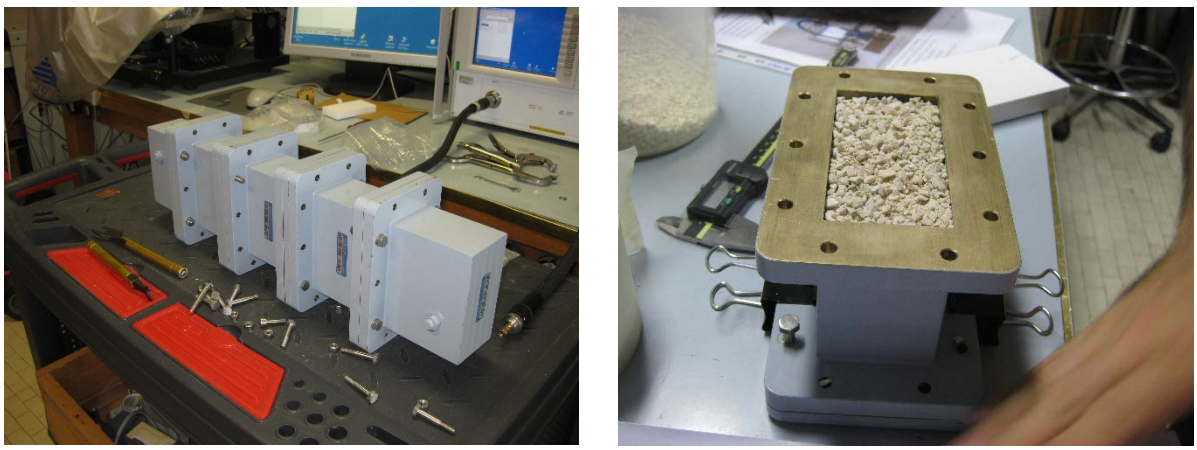

a) b)

Fig. 12 – (a) Setup di misura, (b) Aggregato inserito in guida d'onda per la misura

contenere il materiale granulare, poiché la guida è concepita per campioni con forma di parallelepipedo adatto al suo vuoto interno.

Il campione viene collocato all'interno della guida d'onda e un'onda elettromagnetica viene lanciata alla porta della guida d'onda.

Misurando i parametri di scattering alle porte della guida d'onda, è possibile derminare la permittività complessa del campione in misura, attraverso un algoritmo di misurazione appropriato.

Per questo tipo di misura è stato impiegando il modello sviluppato dalla (National Institute of Standards and Technology) NIST, è risultato essere il più preciso per materiali non magnetici come quelli trattati in questa misura.

Il sistema WR430 è stato caratterizzato facendo il confronto con misurazioni di riferimento di solidi a bassa permittività dal comportamento abbastanza piatto su tutta la banda di frequenza delle microonde. Misurazioni effettuate con sistema di guida d'onda WR90, che utilizza componenti commerciali dalla permittività nota. Il sistema è stato caratterizzato usando i seguenti materiali: PVC a bassa densità, teflon, plexiglas e policarbonato. La scelta è ricaduta su questi materiali per la facilità di preparazione del campione da inserire nella guida d'onda e la bassa permettività che rappresenta al meglio i composti granulari. Si è giunti che il confronto con i risultati ottenuti con il sistema WR430 e il sistema commerciale WR90 sono in buon accordo, le differenze percentuali tra le permittività misurate attraverso i due sistemi sono inferiori a 1%.

Il passo successivo è stato quello di misurare la permettività di materiali granulari utilizzati tipicamente per asfalto autostradale, con diverse miscelazioni e inumiditi a diverso contenuto d'acqua. Le misurazioni sono state effettuate su due materiali che sono tipicamente utilizzati nel settore

dell'asfalto, roccia calcarea e aggregati basaltici. Entrambi questi materiali sono stati selezionati in modo da ottenere pietre con un diametro compreso tra 2 e 4 mm.

I risultati di misura ottenuti, confermano la flessibilità e l'uso pratico del sistema in possibili applicazioni nell'industria per la manutenzione stradale. I costi per produrre i componenti della guida d'onda si aggirano intorno ai € 1000, la rendono una soluzione molto competitiva e conveniente.

La tecnica della spettroscopia dielettrica può essere applicata ai materiali granulari in genere, in particolare al settore agroalimentare con la misura di granaglie, farine alimentari etc.

Part I

Ground Penetrating Radar systems and applications

Chapter I.1

Ground Penetrating Radar Activities in Italy

Introduction

Ground Penetrating Radar (GPR) represents a well assessed technology, of huge interest in all those applicative contexts where non-invasive diagnostic surveys are required, such as infrastructure and cultural heritage monitoring as well as archaeological and subsurface prospecting [1–3]. It is worth noting that such applications are not only limited to archaeology: other fields in which GPR techniques have been applied include underground utilities mapping (i.e., pipes inside the soil), non-destructive inspection of structures (i.e., status of reinforcement bars in concrete structures), pavement inspections, bridge monitoring, railways engineering and landmine detection [4-7].

Basically, radar imaging is performed by transmitting an impulse of electromagnetic energy, which is then followed by capturing its echoes. The main characteristics of the surveyed object are then inferred from these echoes, which contain useful information that can be evaluated according to consolidated and novel signal processing techniques.

About the capability of this technique to reliably recover the features of an object unknown and not directly accessible, GPR allows us to achieve images

with a resolution ranging from centimeters or decimeters, depending on the wavelength and on the situation, to a few meters within the investigated region.

Results of a GPR measurement are usually represented by means of a 2D map, known as B-scan, from which expert users may detect and localize hidden objects and infer information about their geometrical features.

Nevertheless, the detection performances of GPR largely depend on a number of factors that can be grouped under the term “clutter”, which can partially or totally hide or distort the response of the buried objects. The main factors are:

- The antenna effects producing multiple reflections and signal distortion;
- The soil electromagnetic (EM) properties and their spatial distribution governing wave propagation velocity, attenuation, and scattering;
- The EM contrast between the soil and the object, determining the strength of the backscattered EM field;
- Soil roughness and inherent heterogeneities yielding diffuse scattering.

Therefore, there is a need to develop appropriate techniques for clutter reduction and objects imaging; this is a quite challenging task due to the complexity of the EM scattering phenomenon occurring in the a priori unknown antenna–air–soil–scatterer system.

Nowadays GPR is currently the key subject characterized by intensive research activities with respect to all the aforementioned applications, since it permits to detect both metallic and non-metallic objects by imaging rapidly and in a non-invasive way at least the shallow subsurface. Many works have been presented in literature about this topic and, due to the considerable interest in such type of activities, there have been a lot of research projects all over the world.

In COST Action TU1208 "Civil engineering applications of Ground Penetrating Radar" a census was done of the most significant activities involving GPR carried out in Europe and beyond. Information was also collected about available guidelines, test sites and training initiatives in the various Countries participating to the Action. Members were requested to answer eight questions. As a part of this PhD thesis, I worked at the development of the answers concerned with GPR activities carried out in Italy. A resume of these is presented in the following Sections of this Chapter.

1. Which are the most interesting (recent and ongoing) national research projects carried out in your Country?

More in details, such an interest in the GPR technology applied in several fields has been proved by different Italian research projects starting from the 1980s. Within this framework, the Italian community took part in both national and international initiatives, which have ranged from civil engineering to forensic and security applications.

To the best of the authors' knowledge, one of the first project the Italian community joined in was represented by the ARCHEO project, which goes back till the 1990s. This project, which was funded by the Italian Ministry for Universities and Scientific and Technological Research (MURST), had as main participants a lot of Italian researchers coming from different areas and institutions. In a few words, this project has been focused on the combination of several techniques for discovering and recognizing archaeological finds. In particular, a ground penetrating radar system has been developed by the Italian Consortium for Research on Advanced Remote Sensing Systems (CORISTA). The system has been designed to meet archaeological requirements and it has been conceived and realized as a stepped frequency ultra-wide band (UWB) radar, working both in gated and ungated mode [8].

The choice of a stepped frequency GPR has been adopted for this system due to the several advantages with respect to the traditional impulsive GPR systems, that have been witnessed since the seventies and up to now [9], while the possibility to use both gated and ungated modes is due to the aim of reducing the coupling between the transmitting and receiving antennas. Moreover, such radar was equipped with a positioning system [10-11] able to move independently the antennas without any intervention by the operator.

Some outdoor tests on the GPR were therefore performed in a controlled test site environment after laboratory tests [11]. In order to calibrate the system and assess its performances, a dedicated outdoor test facility was realized. In the framework of an agreement with the Italian Aerospace Research Centre (CIRA) located in Capua, southern Italy, a 25m × 25m pool with a depth of 5 m has been built up within the CIRA establishment and filled with river sand. Several objects, such as metallic sheets, plastic pipes, and tanks at different depth were buried as reference targets. For more details, the reader is invited to see Alberti et al. [8].

Another important step in ARCHEO project dealt with the theoretical analysis about the capability of the system to recover the features of unknown, buried objects. Such an analysis was realized by both Universities of Napoli “Federico II” and “Seconda Università” (SUN), which did not only focused on radar techniques based on traditional approaches, but also moved on a more innovative tomographic approach in order to improve the performances of the imaging system. Under this perspective, the whole structure of the project was split in different work packages which included the modeling of the electromagnetic features of the soil (WP 2), the analysis of different scattering models for the case of buried objects (WP 3-4), and the development of inverse scattering techniques (WP 5).

A more recent GPR project, which goes back till 2001-2004, was the SMART-RAD project, which was intended to response to specific limitations of existing systems in order to develop an innovative technology able to set forth the conditions for a widespread commercialization of GPR tools within a broad range of industrial sectors where efficient underground inspection was required [12].

Such a project had been funded by European Commission, and more in details by CORDIS (Community Research and Development Information Service). According to the guidelines proposed at that time, SMART-RAD was intended to be able to reliably detect buried objects and will have easy on-field data interpretation capability, such to be used by untrained operators. The system had a broad class of potential users in the construction and re-development industry, as efficient and cheap alternative to conventional ground inspection methods in construction or de-commissioning sites, reducing the risk of damages and accidents during excavation operations.

The main coordinator of the project was the Italian company D'Appolonia S.p.A., which managed all the activities of international participants, among which also another Italian institution, namely, the University of Pavia, took place. More recently, another project called ORFEUS (Optimized Radar to Find Every Utility in the Street) has been proposed. It was a collaborative research project, with financial support from the European Commission, which started in late 2006 with the overall aim of providing the capability to locate buried infrastructure accurately and reliably. Amongst the technical objectives of ORFEUS, a major task was the provision of a radar mounted on the drill heads of Horizontal Directional Drilling machines to provide a real-time indication of obstacles in the drill path to the operator, so that they can operate more safely below the ground. The bore-head radar has the capability to look in the forward and sideways directions and detect objects which come within the

cones of the antenna radiation patterns Figure 2. One of the main advantages was that information can be transmitted from the radar to the operator on the surface so that objects that would otherwise have been struck may be avoided. In addition to fulfil its primary detection role, the radar also provided information on the presence of objects that may cause problems for the drilling and subsequent pipe-laying operations. This included the angular position and distance of objects.

A comprehensive set of requirements was developed by the end-user group of the consortium at the beginning of ORFEUS, including criteria for detection distance, minimum detectable object size and resolution.

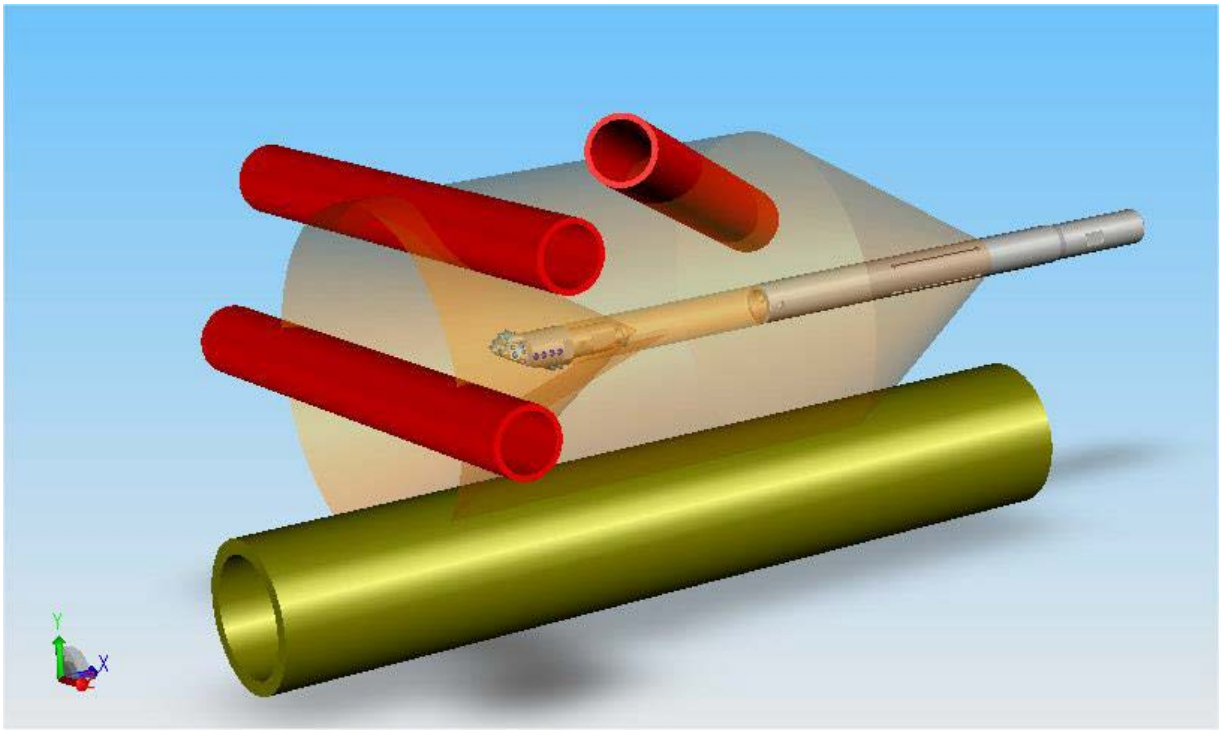

Fig. 2 – A possible operative situation for the bore-head radar.

An image of the final prototype is shown in Figure 3. In the last part of the project, the prototype was therefore tested firstly in artificial test sites, and then moved on more realistic scenarios. A simple test site Figure 4 was built at the IDS facilities in a sand pit large enough to avoid spurious signals generated by its walls interfering with the signal backscattered from the buried pipe “C”.

Two inspection holes were built to embed the antenna just above the pipe (hole “A”), or 20 cm shifted from that pipe (hole “B”). A metallic chain could be inserted in pipe C to make the reflected signal stronger; the inspection holes could be filled with sand to avoid interference from those not used during the experiment (e.g. hole A opposite).

Fig. 3 – General arrangement of the assembled prototype.

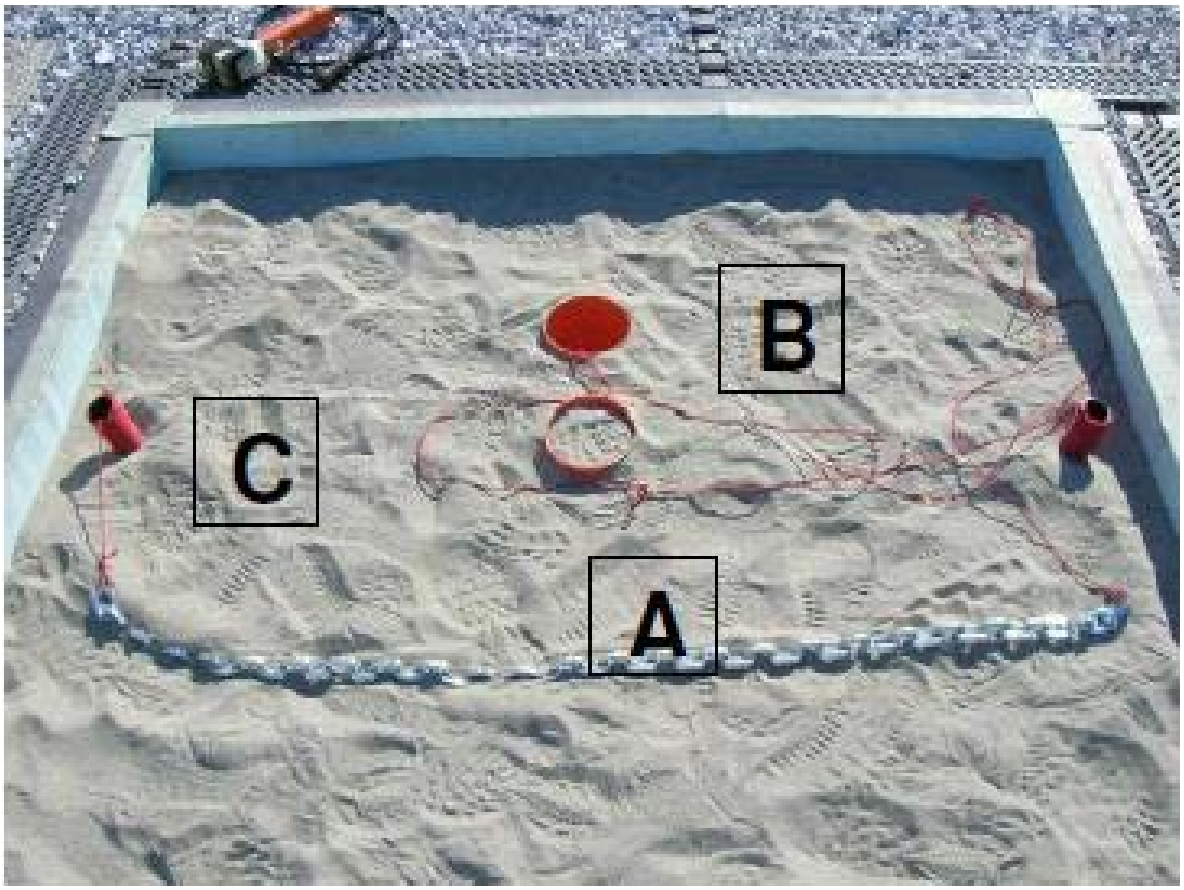

Fig. 4 – Artificial test site implemented at IDS.

A more sophisticated dedicated test site consisting of a wooden chamber was built near the facilities of Tracto-Technik in Lennestadt-Langenei Figure 5. Such chamber enabled to measure the penetration depth in different soils as well as the performance of the radar in detecting different obstacles of various size and layout.

Concerning the demining application of GPR, the D-BOX project has been developed for detecting and deactivating anti-personal landmines and cluster munitions remaining from armed conflicts [13]. It has started in January 2013 and it is currently ongoing. The aim of such a project consists in the development of an innovative, low-cost and easy-to-use demining toolbox, that could be used during all demining activities (from the preparation of the mission until the elimination of the mines including communication to general

public) to help operators and end-users to adopt the most safe conditions during demining activities.

Amongst all the partners of this project, it is worth citing the Italian groups of Consorzio Nazionale Interuniversitario per le Telecomunicazioni (CNIT), Selex-ES and Telespazio S.p.A., along with other international partners such as Astrium Polska, Delft University of Technology, Fraunhofer Institute and many more. In conclusion, GPR activities constituted and still do nowadays the main topic for many European and International projects, including a great variety of applications that ranges from civil to military ones. In this framework, the Italian community have played a considerable role, which is still covering.

Fig. 5 – Artificial test site built in Lennestadt-Langenei (Germany).

References

[1] D. Daniels, 2004, "Ground Penetrating Radar, 2nd Edition". The Institution of Engineering and Technology, UK.

[2] L. B. Conyers, D. Goodman, 1997 "Ground Penetrating Radar: An Introduction for Archaeologists". Alta Mira Press, Walnut Creek, London and New Delhi.

[3] A. S. Turk, K.A. Hocaoglu, A. A. Vertiy, 2011. "Subsurface Sensing". John Wiley & Sons Inc., ISBN: 978-0-470-13388-0.

[4] M. Ambrosanio and V. Pascazio, "A compressive sensing based approach for microwave tomography and GPR applications", International Geoscience And Remote Sensing Symposium, Quebec City, Canada, 2014.

[5] A. Benedetto, G. Manacorda, A. Simi and F. Tosti, "Novel perspectives in bridges inspection using GPR", Nondestructive Testing and Evaluation, vol. 27(3), 2012.

[6] A. Ihamouten, G. Villain, and X. Dérobert, "Complex permittivity frequency variations from multi-offset GPR data: hydraulic concrete characterization", IEEE Trans. Instrum. Meas., vol. 61, 6, 2012, pp. 1636-1648.

[7] S. Meschino, L. Pajewski, M. Pastorino, A. Randazzo, and G. Schettini, "Detection of subsurface metallic utilities by means of a SAP technique: Comparing MUSIC- and SVM-based approaches," J. Appl. Geophys., 2013.

[8] Giovanni Alberti, Luca Ciofaniello, Giovanni Galiero, Raffaele Persico, Marco Sacchettino, Grazia Maria Signore and Sergio Vetrella, "An Italian experience on stepped frequency GPR", Ann. of Geophysics, vol. 46, n. 4, pp. 707-717, August 2003.

[9] L. Robinson, W. B. Weirand, L. Yung,"Location and Recognition of Discontinuities in Dielectric Media Using Synthetic RF Pulses", Proc IEEE, vol. 62, 1, pp. 36-44, 1974.

[10] G. Alberti, L. Ciofaniello, M. Della Noce, S. Esposito, G. Galiero, R. Persico, and S. Vetrella, "Advanced stepped frequency GPR development", Proc. of the Conference on Subsurface Sensing Technologies and Applications II, at SPIE's Annual Meeting in July/August 2000, San Diego, USA.

[11] G. Alberti, L. Ciofaniello, G. Galiero, R. Persico, M. Sacchettino and S. Vetrella, "A stepped frequency GPR system working both in ungated and gated mode", Proc. of Workshop on "Radar a bassa frequenza", Napoli (Italy), September 2001.

[12] *http://cordis.europa.eu/project/rcn/55370_en.html*

[13] *http://www.d-boxproject.eu*

2. Outside the academic world, is GPR used in the management of your Country's resources and infrastructure?

The use of GPR for management of resources and infrastructures in Italy is a well established practice also outside the academic world. In more recent years, there has been an increasing interest in this geophysical technique, in large part due to the rapidity of execution and high resolution capability that modern GPR systems allow. These are key-features to the success of a non-destructive testing (NDT). Currently, an increasing number of major Italian companies operating in the civil engineering fields perform GPR surveys within its own business. The following is an overview of applications and case study from some of these Italian companies. The ANAS S.p.A. (acronym for Azienda Nazionale Autonoma delle Strade) is the management authority for the Italian road and motorway network of national importance. Amongst its activities, there are studies, research and experimental tests on the construction materials used for roads. These are carried out mainly at the experimental center called Centro Sperimentale Stradale (CSS) in Cesano, near Rome, Italy. Within this framework, it has been developed the so-called THETIS project, which stands for Thickness Evaluation Technology and Investigation radar System. THETIS is essentially a GPR system able to continuously detect the stratigraphy and thickness of the road layers. The system is equipped with radar antennas with different frequencies that allow the simultaneous investigation at different depths and with different resolutions.

The Sirti S.p.A. is a leading Italian company specialized in the design, implementation and maintenance of large telecommunication networks for mobile and internet connections as well as energy networks for railway

transport, underground railway, roads and motorways. It is well known that the maintenance of these network infrastructures absorbs huge amounts of money, also due to the inconveniences and interruptions caused to common activities. To this purpose, Sirti S.p.A has developed owned solutions that permit the time/space reduction of network realization limiting community impact. One of these relies on a GPR-based system capable to minimizing the costs and timing for scanning the subsurface. The so called S-GPR 3D (acronym of Sirti Ground Penetrating Radar in 3 dimensions) is a 3D GPR system developed by Sirti to obtain three-dimensional scans of the subsoil in real time, without the need for further post-processing of the data [1]. The S-GPR 3D is equipped with two antenna arrays, for overall 12 antennas per each array, which allow to obtain 3D scans with single pass along only one direction. Its dedicated software developed by Sirti in collaboration with Aresys s.r.l. takes advantage of algorithms that are routinely implemented in seismic reflection data processing [2]. After the standard pre-processing steps (band-pass filtering, gain, mean removal), the antenna records are continuously focused during acquisition, by means of Kirchhoff depth-migration algorithm, to build pre-stack reflection angle gathers while the migration step is performed using a set of different velocities around the typical soil velocity (generally 10 cm/ns). The comparison between the identified targets on different antenna records (i.e. different B scans) allows to greatly reduce the number of wrong detections and false alarms (their number has shown to be less than a couple for each kilometer of acquired data, implying a negligible decrease of overall acquisition productivity). Moreover, since the S-GPR is equipped with a GPS receiver, once identified the buried object, this can be directly georeferenced on a CAD map. All these features allow to implement a reliable subsoil mapping process in real-time, on a consumer laptop (based on, at least, an Intel Core 2 Duo

processor), and without the constrained need of skilled operators. This system has been successfully tested in-field during the realization of new infrastructures for optical network deployment in conjunction with new “mini-trenching” standard, which is characterized by reduced dimensions of digging (width and depth approximately of 5 cm and 30 cm, respectively). This limited extent of the area to be investigated was coupled with a multi-antenna GPR apparatus quite small, with central frequency of 900 MHz and different polarizations. The results obtained at different working sites showed a productivity index up to 1 km per hour (that includes the time required to mark the detected ducts directly on pavement during acquisition). In line with this, Sineco S.p.A is another important Italian company that makes extensive use of GPR-based diagnostic systems. It mainly operates in the field of engineering, with special reference to the NDT control and maintenance planning of major transport infrastructures. Its main mission is to provide support to road network operators in the control and surveillance of bridges, viaducts, galleries road and airport. To provide these services, has been performing pavement GPR (highway- airports-railways) and tunnel GPR surveys since more than 20 years ago. Within the framework of pavement surveys, Sineco S.p.A performs either standard GPR surveys to reconstruct the pavement structure up to depth of 2-3 meters and/or to detect morphological irregularities of the interfaces between layers, either signal attenuation analyses to evaluate the moisture/water accumulation, the presence of porous areas, density anomalies mapping and detection of inner distress in asphalt layers. Tunnels GPR survey are performed to locate cortical and/or inner discontinuities of the concrete (presence of voids, fractures, reinforcement rebars, steel ribs), to evaluate the thickness of concrete (up to 1 m depth) as well as the presence of moisture underneath the ground surface. In addition, Sineco S.p.A performs GPR investigations aimed at defining the state of

conservation of reinforced structure in deck bridges. Specific provided service are the reconstructions of 3D models of bridge deck (layers and rebars location), assessment of rebars geometry and depth, studies of amplitude maps of the main reflections surfaces (asphalt-concrete and upper rebars level) to evaluate anomalies or deteriorations (i.e., identifying metallic corrosion with weaker reflection). GPR surveys for utilities mapping (pipes, cables etc.) are also part of its core business. A recent case study on the activity routinely carried out by Sineco S.p.A., concerns the evaluation of the health state of a motorway bridge deck located along the A15 Parma–La Spezia motorway (Emilia Romagna, Italy) [3]. The main purposes of these surveys were the evaluation of the state of health of the bridge decks of the Rio Vizzana I bridge and the location of possible damaged areas among the concrete, steel rebar and asphalt pavement layers. Using a GPR radar system equipped with two rows of eight double polarized 2GHz antennas (mod. Ris Hi-Bright manufactured by IDS S.p.A.) the GPR survey of the entire area of the bridge deck (210 m^2, approximately) was performed in about half an hour. After data processing, the asphalt thickness and reinforcement rebar depth, rebar geometry, amplitude maps as well as moisture maps were successfully obtained. Such monitoring allowed to address the best strategy for a preventive intervention of restoration of the optimal structural conditions.

The Istedil S.p.A (acronym for Istituto Sperimentale per l'Edilizia) is an Italian company that develops its business in the field of monitoring surveys to assess and ensure the safety and quality state of civil structures. In doing this, Istedil S.p.A. routinely performs both 2D and 3D GPR surveys to acquire information on construction techniques, structural elements, rebars geometry and defects for both structures of great artistic value (where it is not possible to use invasive methods) and for civil large infrastructures. Two case studies below reported illustrate the type of activities carried out in this company [4]. The

first one is an example of application to a historic building of the architectural heritage of Rome (Italy): an eighteenth-century building originated from the expansion of a fifteenth-century building. Particularly, GPR surveys were aimed at identifying the structures of two slabs, namely, that of the first floor used as library, and that constituting the second floor. The acquisition phase was organized in order to investigate the structures transversely and longitudinally, using both a 1GHz antenna to investigate in detail the first 1.5 meters, and a 400 MHz antenna to have a global view of the structure. The obtained 2D radar scans showed characteristic hyperbolic paths within the first 20 cm in depth, at regular intervals of 80 cm, which were interpreted as linked joists. Below this upper slab, some voids were identified, especially in the neighborhood of the perimeter walls where they reached a maximum thickness of about 35 cm. The second reported case study is an example of a survey carried out to identify the position and geometry of rebars of a large complex of civil buildings in Rome (Italy). In order to define of the rebars, the GPR acquisition has been organized on a mesh of 4.4 m × 3.8 m, with perpendicular profiles equally the texture spaced of 20 cm. 3D processing allowed to obtain two depth slides (C scans), respectively at 5 cm and 15 cm, which showed very clearly the geometry of two distinct meshes of rebar. The C scan at 5 cm depth showed a mesh of rebars arranged regularly with a pitch of 20 cm. The C scan at 15 cm depth showed a second mesh of rebars composed in groups of 3 bars with a pitch of 15 cm, which repeated every 60 cm. A zone with moisture accumulation was also located.

The IDS (Ingegneria Dei Sistemi) S.p.A. georadar division from Pisa (Italy) is not a company operating in the field of civil engineering. More specifically, it is a company world leader in designing and providing GPR systems. Anyhow, within the framework of its research and development activities, the IDS S.p.A. georadar division has been involved in many kind of GPR surveys. In this

regard, one of the most significant and innovative applications is the GPR survey carried out to support the geotechnical study of the Gorsexio tunnel along the rail line Genova-Ovada, in Italy. The GPR survey was performed to study the fractures, stratigraphy and anomaly in the tunnel in order to evaluate the structure stability and the presence of area with a risk of water infiltration. Using both 200 MHz and 600 MHz antennas, the contact between tunnel structure and bedrock as well as the internal transition between two different layers of bricks were successfully determined along the entire tunnel structure. Fractures and fractured areas filled with water were also detected. Another interesting geotechnical GPR application is the study of the fractures and stratigraphy in a tunnel of limestone quarry located near to Bergamo, Italy. Using a low-frequency antenna with central frequency of 80 MHz, the GPR survey allowed to locate a dipping fault and to identify the contact between the fault and a geological transition. There are also a number of successful archaeological applications. A GPR survey conducted in Piazza dei Miracoli, Pisa, with an array of 200 MHz antennas dragged by hand has allowed to cover an area of 30.000 m^2 (total coverage) in one day. This survey has enabled to discover the presence of underground archaeological structures. A similar GPR survey was carried out at the Cavallino Archaeological park of Lecce, Italy, for the detection of buried structures. An area of 10.000 m^2 (total coverage) was covered in one day using a GPR system towed by a van. The survey allowed to discover the presence of underground structures. Finally, a very special application has been the GPR survey at the Pre de Bard Glacier (Valle d'Aosta – Italy) to define the glacier internal stratigraphy and the possible presence of erratic stones and/or crevasse. This special need was addressed using a 100 MHz antenna dragged by a helicopter.
Finally, it is worth mentioning the large number of small Italian companies providing geophysical services which regularly perform GPR investigations

throughout Italy for civil engineering, archaeological and environmental studies. The large number of applications and case studies in which they are currently involved, give a clear evidence of the continuing and widespread demand for GPR surveys within the Italian contest.

References

[1] Cottino E. and Di Buono N., A complete enabling solution for FTTx network infrastructure, Proceedings of 58th International Wire & Cable and Connectivity Symposium, Charlotte, North Carolina, USA, 2009.

[2] Molteni D., Mazzuchelli E., Cottino E. and Di Buono N., Real-time 3D GPR data processing for automated detection of buried services, Proceedings of 30° GNGTS Convegno Nazionale Gruppo Nazionale Geofisica Terra Solida, Trieste, 14-17 November 2011.

[3] Conti M., Use of Ground Penetrating Radar to evaluate the state of health of a motorway bridge deck, available at http://www.gruppo-sina.it/, 2012.

[4] Cassioli D., Marchetti D., Olini F., Orlandi O., Seri R. and Spina S., Esempi Di applicazione GPR (Ground Penetrating Radar) su beni architettonici e grandi complessi di edilizia civile e industriale nel centro Italia, Proceedings of 13° Congress AIPnD (Associazione Italiana Prove non Distruttive), Roma, 15-17 October 2009.

3. Do you have national guidelines, rules or protocols that can/have to be followed during GPR surveys?

The Italian body of laws and rules tackles the GPR applications only under an indirect and partial approach.

- At the national level, it is worth citing the law 109/94 (art. 16-17-19-20) [1] concerning the whole regulation of Public Works. In these articles, the need for geognostic surveys in civil preliminary projects is introduced, along with the possibility of subcontracting this activity to more specialized companies.

- At the regional/urban level, GPR is mentioned in the R.R. 28/02/2005 – n.3 [2], applying the former regional law L.R. 12/12/2003 – n.26 [3], that contains the guidelines for the development of the Urban Plans for the Management of Underground Utilities (Piano Urbano per la Gestione dei Servizi del Sottosuolo - PUGSS). The PUGSS is a document produced by the local administration (Region or Municipality), and represents a useful instrument able to coordinate public administrations and bodies managing the utilities located in the road sub-surface, such as electric or phone cables, optic fibers, water and gas pipes, sewers, etc. The main goal of this tool is to produce reliable reports about the presence of these utilities in the managed environment, in order to give proper information to the user. To achieve such results a wide database of surveys becomes necessary through this territory. Obviously, the high value of ratio benefit/costs resulting from NDTs could lead local administrations to undertake the use of these technologies for the aforementioned assessments through the PUGSS, with particular reference to the GPR.

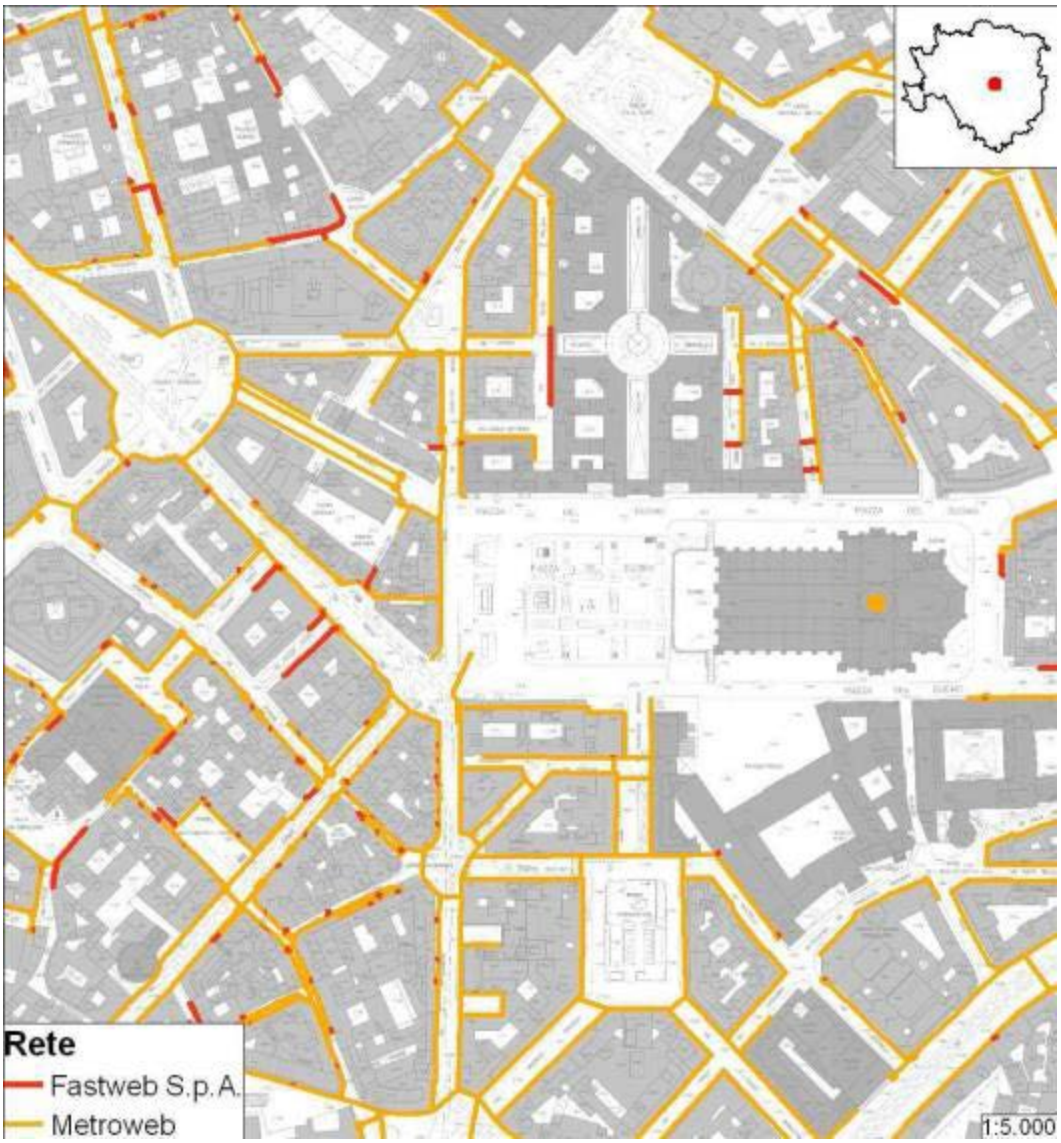

Fig. 6 – Phone – Internet cables network (PUGSS City of Milan).

- The main international reference, more technically speaking, is represented by the American Society for Testing and Materials International (ASTM International). This quality assurance body directly approaches GPR thematic through two different issues:
- ASTM D 4748-98 [4]: this guide by ASTM illustrates a test method covering the nondestructive determination of the thickness of the bound-layers in road pavements, i.e. the upper layers of a pavement made of bituminous or concrete materials, through the utilization of a short-pulse

radar equipment. The report focuses on the functioning principles of a short-pulse radar, and on the test equipment configuration, then faces more technical topics such as calibration and standardization, procedures, calculation, and reliability of results. In this document, it is also emphasized the importance of safety issues in GPR testing activities, since every radar apparatus involves a potential microwave radiation hazard.

- ASTM D 6432-99 [5]: this guideline concerns equipment, field procedures and data-interpretation for the electromagnetic evaluation of subsurface materials using the GPR method. The method illustrated can be used in geologic, engineering, hydrologic and environmental applications. Equipment configuration and parameters being measured are presented and then a table of representative values for different materials is shown. The method limitation are hence properly explained. Lastly, the test procedure is presented in details, and involves the following steps: (i) qualification of personnel, (ii) planning the survey, (iii) selection of the approach, (iv) survey design, (v) survey implementation, (vi) quality control, (vii) interpretation of GPR Data, (viii) interpretation of results and (ix) data processing.
- Although a general lack of normative technical protocols is shown by the Italian normative framework, the aims of the aforementioned guides have been gathered and exploited in a national guideline, even if concerning the only utilities-detection activities. An executive work in this field, indeed, can be considered well-developed and compliant to the standards of quality, if the prescription contained in the guidelines package CEI 306-8 [6], emitted by Italian Electro- technical Committee in 2004, are properly followed.
- The CEI regulation, as mentioned, concerns the utilization of GPR technology in the field of infrastructural activities, with the aim of

detecting the underground utilities for avoiding any possible damage and consequent time and money-loss. In this fields, moreover, the regulations illustrate the possibility of using GPR with the goal of determining the lithological characterization of the surveyed soil, which define its drilling attitude. This document aims to properly define (i) the correct test-performance modality, (ii) the right results interpretation, (iii) the equipment characterization and (iv) the minimum requested standards for the surveys.

- Since the field of civil engineering applications of GPR cannot be narrowed to the only utilities detection, private guidelines concerning a wider set of applications have been published by radar manufacturers or scientific associations.
- The most important example of the first ones are of course the Guidelines emitted by Ingegneria Dei Sistemi S.p.A. [7]. This document contains important general information not only related to civil engineering applications. In details:

- Theoretical principles of GPR
- The IDS equipment
- The RIS system (see point 5)
- Archeological applications
- Cultural heritage applications
- Generic Civil Engineering applications
- Geological surveys
- Focus: Railway embankments
- Focus: Road Pavements

Concerning the civil engineering applications, this document gives example and guidelines for activities of (i) assessment of geometry of pipes and voids

in walls; (ii) rubble stone filled masonry detection; (iii) geometry of rebars in structures; (iv) evaluation of inner structure in columns or pillars; (v) cracks presence and evolution in brick and concrete structures. The IDS Guidelines provide useful advices for users in terms of IDS equipment set-up and data evaluation. This represents a helpful tool for a proper interpretation of radar data, especially for less experienced technical users.

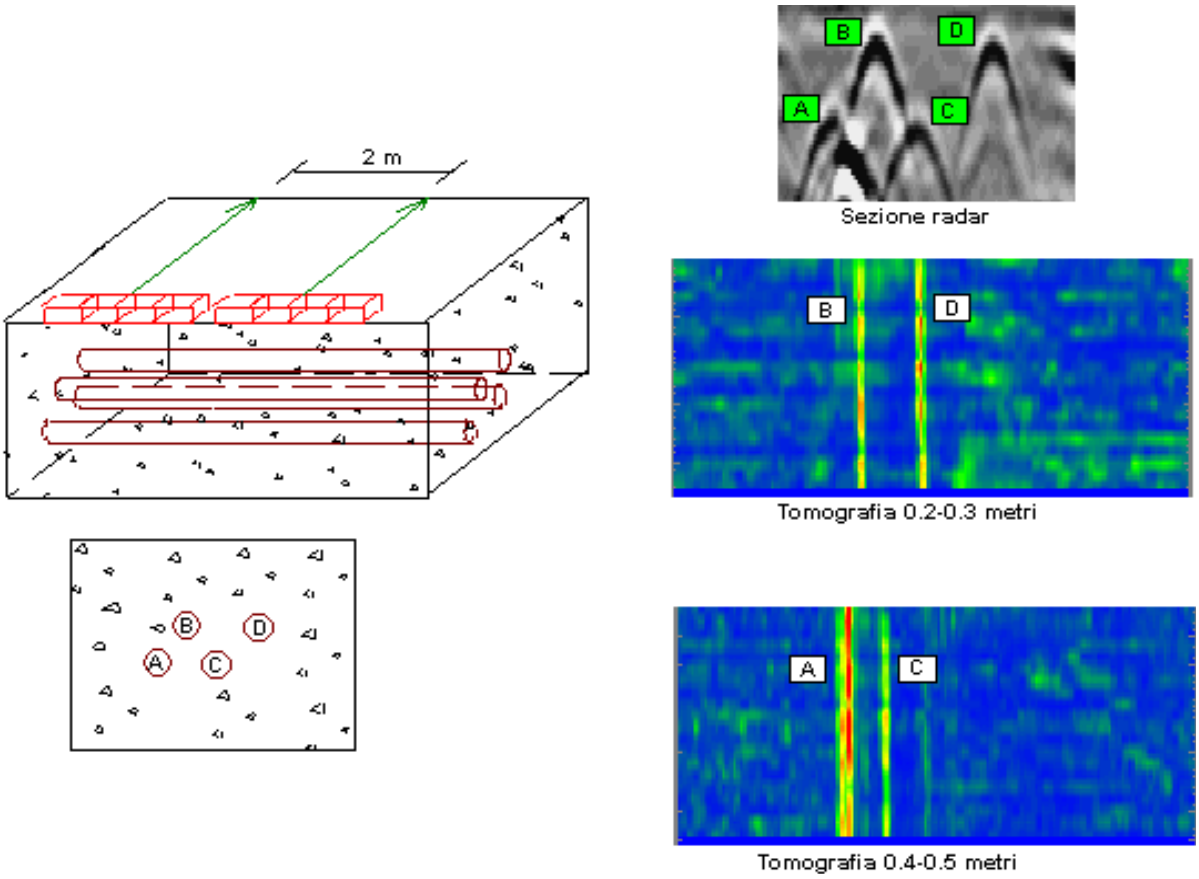

Fig. 7 – Pipelines detection example in IDS Guidelines.

In Chapter 2, indeed, operative aspects are faced and the interpretation of back-scattered signal from different kind of targets is approached. Principles of data processing are then given, and concepts of frequency filtering, Fourier analysis and data migration are introduced.

An important source of operative advices for GPR application is the document published in 2012 by Associazione Società di Geofisica (ASG), which is an

association involving many companies operating in the geophysics fields [8]. This Report contains a very wide set of prescription about sub-surface surveys, such as (i) seismic assessments, (ii) electrical explorations, (iii) Georadar evaluations and (iv) electro-magnetic surveys. Lastly, a semi–non-destructive approach is herein faced (coring). Particularly concerning the GPR, helpful information are given about the principles of the tool functioning and about the theoretical background. The most common central-frequencies are presented in dependence on the requested survey and then a common GPR-equipment is characterized. A very useful chapter is the one concerning the tool calibration (i.e., Chapter 3) which could lead, if wrongly developed, to an improper data interpretation. Principles of data processing are given and the concept of filtering is explained. More in detail, relevant filters like Horizontal High Pass (HHPF), Horizontal Low Pass (HLPF), Band Pass (BPF), Background removal, Notch and Flattering filters are briefly introduced.

Summarizing the state of the art of the regulation concerning the aforementioned GPR activities, laws and regulations in which this kind of surveys are provided were firstly presented. In this context, the role of the municipal administration is becoming increasingly important, due to some strategic plans called PUGSS, through which the mapping of utilities networks in urban field can be more easily managed. After having introduced the most known international references, the only officially recognized regulation in the narrowed field of buried utilities detection was then presented. Lastly, two guidelines regarding the whole set of civil engineering application of GPR were reported, developed by private manufacturers or professional association.

References

[1] D.L. February 11st 1994, n. 109, concerning: “Legge quadro in materia di lavori pubblici”.

[2] R.R. February 28th 2005, n.3, concerning: “Criteri guida per la redazione del PUGSS comunale”.

[3] L.R. December 12nd 2003, n.26, concerning: “Disciplina dei servizi locali di interesse economico generale”.

[4] ASTM D 4748-98: Standard Test Method for Determining the Thickness of Bound Pavement Layers Using Short-Pulse Radar, American Society for Testing and Materials, 1998.

[5] ASTM D 6432-99: Standard Guide for Using the Surface Ground Penetrating Radar Method for Subsurface Investigation, American Society for Testing and Materials, 1999.

[6] CEI 306-8, Impiego del radar per introspezione del suolo per prospezioni ad opera di posa di servizi ed infrastrutture sotterranee, Comitato Elettrotecnico Italiano, 2004.

[7] Linee Guida: La tecnologia IDS nel settore GEORADAR, IDS Ingegneria Dei Sistem S.p.A.

[8] Linee Guida per indagini geofisiche, Associazione Società di Geofisica, 2012.

4. In your opinion, how could a wider and more effective use of the GPR technique be promoted in your Country?

Ground-penetrating radar (GPR) uses a high-frequency (e.g. 40 MHz to 1500 MHz) EM pulse transmitted from a radar antenna to probe the subsurface. The transmitted radar pulses are reflected from various interfaces within the ground, and this return is detected by the radar receiver. Reflecting interfaces may be soil horizons, the groundwater surface, soil/rock interfaces, man-made objects, or any other interface having a contrast in dielectric properties. The dielectric properties of materials correlate with many of the mechanical and geologic parameters of materials. The objective of GPR surveys is to map near-surface interfaces at high resolution. Resolution and depth of investigation depends on the antenna frequency used in the survey: the lower the

frequency of the antenna, the greater the depth of investigation but the lower the resolution.

GPR covers a wide range of applications, such as the monitoring urban and rural roads, highways, bridges, tunnels and the detection of underground cavities and voids. It is also used for performing quality checks of reinforced concrete in existing works, for analysing geological structures, for mapping soil properties, and for characterizing materials under a geotechnical perspective, such as for the design of structural foundations. In addition, one of the most widespread applications of GPR concerns the detection of buried structures such as pipelines, electrical cables, gas and water pipes.

Combined with other geophysical techniques it can provide useful information about many features of the subsurface. Given the broad range of applications, the promotion of the technique can bring undoubtedly a huge benefit to the community.

Why should you use the GPR?

First of all, it represents an effective, non-destructive and non-invasive technique. Moreover, GPR surveys are carried out rapidly, and large areas can be covered in a short time.

The planning of the work is undoubtedly a key point of a project and sometimes this feature is overlooked, both at the design stage that during its development.

Who can benefit more from the use of this technique?

Public authorities (regions, provinces, municipalities, public service managers), constructors, police agencies, institutions of land protection, industries, citizens can benefit from the use of GPR.

How to promote the GPR?

All the stakeholders such as manufacturers of the test equipment, software developers, geophysical researchers, public authorities, public organizations, geologists) should be involved to promote GPR.

They should encourage the use of GPR and show the usefulness of this technique, for its ability to detect targets and to solve problems. Public service managers should be aware of the importance of a continuous monitoring of the plumbing in water distribution, gas, electric energy.

If a leak is effectively detected, it is possible to act locally, repairing the rift, saving money and lowering the social costs for the community.

Constructors and designer should duly consider geophysical features of the subsurface in order to properly design the building foundation. In particular, cavities, joints, fractures, loosely compacted layers, filling materials, localized anomalies must be carefully taken into account. At the same time, a careful monitoring of the structure is important during the life cycle of a building to repair possible fractures and damages and to ensure safety conditions for safeguarding people's life.

GPR is relatively easy to use although, as all the other geophysical techniques, it requires suitable levels of both experience and expertise to do it effectively and without any improvisation.

All the work steps should be done properly, from a suitable set-up for field activity, types of antennas, proper signal acquisition, signal processing, modeling, cartographic representation of the maps, final interpretation and finally editing the report. Particularly, the GPR modeling is a complex problem and requires an accurate calibration procedure, combining observed data with a-priori known characteristics of the soil. A great effort is required to manufacturers of the test equipment, software developers, geophysical researchers, universities, public organizations to work in cooperation, in

order to update constantly the community about the development of this technique. In addition, a wide exchange of knowledge and experience about different scientific-technical GPR-based techniques in various applications is required, in order to highlight the strengths and limitations of current GPR systems. Meetings, workshops, training courses should be regularly organized in order to clarify the effectiveness and the progress beyond the state of the art of this technique, to transfer research activities, to disseminate the results of the last research activities, to detail study cases.

Software developers should be encouraged to develop open source tools and share them amongst the GPR community.

Researchers from different field of applications that use GPR should regularly follow training courses in order to enhance the quality of their work.

An interesting example of cooperation between the stakeholders is provided by EuroGPR *http://www.eurogpr.org/joomla/,* an association made up of users and manufacturers of GPR equipment, intent on raising standards within the GPR industry and looking out for the rights of our members, giving them voice at a pan-european level on matters such as licensing, health and safety and market access.

5. Do you have GPR manufacturers in your Country? Which systems they produce?

In Italy, IDS Ingegneria dei Sistemi S.p.A., Pisa, Italy, is no doubt the most important GPR manufacturer, Figure 8a.

IDS S.p.A. was founded in 1980, and has over 30 years' experience in delivering innovative technologies and providing engineering solutions for different applications in the field of Earth sciences and beyond. Basically, it includes many divisions, namely, naval, aeronautical, air navigation, georadar, as well as a military department.

In 1999, the IDS began the worldwide commercialization of GPR products, especially concerning the manufacturing of multi-frequency and multi-channel array systems, thereby paving the way for becoming one of the leader companies in this field, and improving, amongst others, utilities detection performances of different GPR systems. In 2007, IDS S.p.A. has introduced on the market the first Ground-Based interferometric SAR IBIS.
The network offices in Italy are the following, each one with specific division:

- Pisa: Headquarters
- Roma: Air Navigation Division
- Napoli: Firmware development
- La Spezia: Ship Technological Mast design
- Lamezia Terme: Special materials for wind farms to mitigate their impact on air navigation.

Nowadays the IDS has become a multi-national company with a network of agencies and offices strategically placed not only in Italy, but also in European Countries (i.e., UK), and worldwide (i.e., North America, Brazil and Australia Figure 8b).
IDS S.p.A. has established and well-documented activities in the GPR products, since it has been investing more than 20% of its turnover in research and development programmers.

a) b)

Fig. 8 – The IDS S.p.A. Headquarter in Pisa (a), the network of agencies and offices of IDS in the globe (b).

The Company relies on nine Labs working together within an integrated environment to design and develop framework products: Computational Electromagnetic and Antenna Design, Electromagnetic System Design and Framework, Computational Geometry and Systems, Radar Systems, Signature Technologies, Avionics, Air Navigation Systems, Measurement and Structural. IDS S.p.A. products concern the fields of civil and transportation engineering, geology and environmental applications, as well as archaeology. Figure 9 represents an overview of the main GPR equipment manufactured by IDS S.p.A.

(a)Stream EM

(b)Opera duo

(c)RIS MF Hi-Mod

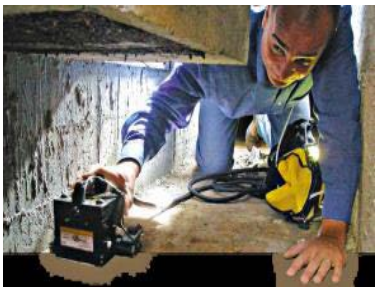

(d)Aladdin

(e)IDS RIS Hi-BrigHT

(f)SafeRailSystem (SRS)

(g)RIS Hi-Pave

(h)RIS ONE TR 25

(i)Stream X

(l)IBIS-FL

(m)IBIS-FM

(n)GPR TWR

Fig. 9 – The main GPR products manufactured by IDS.

As regards civil engineering, the multi-channel GPR system (also known as stream) is very useful in case of extensive road surveys, for detection and mapping, especially of pipes or utilities. The Company has realized two

different types of multi-channel GPR: one of these is used for civil engineering applications, namely, the stream EM; the second one, i.e., the stream X, is used instead for archaeological surveys.

The stream EM Figure 9a is employed for extensive utility mapping. The system is linked to a car or a vehicle, thereby it is capable to reach an operating speed of approximately 15 km/h. Data collection can be performed in longitudinal direction (without the need of moving the array in the transversal directions) along with the detection of utilities and connections. It guarantees high productivity, high modular structure, high detection capability and it avoids any blocking of the road traffic. Another important advantage is that it enables to export the data collected into CAD/GIS work environment.

For civil engineering purposes, several GPR devices have been manufactured by the Company. For utilities detection and mapping, IDS proposes two types of GPR systems: Opera Duo Figure 9b and RIS MF Hi-Mod Figure 9c. In case of analyses for monitoring the inner status of structures, the RIS Aladdin GPR can be specifically employed Figure 9d. Such system is particularly suited for collecting images of concrete rebar. It is also very useful both in the case of shallow detections and for the monitoring of deep structures.

In case of bridge surveys, the RIS Hi-BrigHT can be used to measure pavement and concrete slab thickness, to detect moisture damages, to locate deck slab and protective concrete damages; to map drainage and other buried pipes and to determine reinforcement cover depth. A relevant picture of this system is given in Figure 9e.

The Transportation Engineering Department of IDS S.p.A. is focused on the use of GPR to railway and road engineering applications. As regards the railway transport, the Safe Rail System GPR Figure 9f can provide a continuous mapping of the railway ballast structural conditions and thickness, and give useful information about its moisture content, the presence of local and

widespread failures at the ballast bed basis level, and it is also capable to distinguish between clean and fouled ballast and detect those sections with drainage problems.

Concerning the road transportation area, the RIS Hi-Pave GPR system Figure 9g ensures a continuous mapping of both asphalt and load-bearing layers status, as well as the presence of cavities. This RIS system can be also used for airport applications.

Applications in geology and environmental fields require the use of different GPR devices with specific characteristic. In particular, the GPR devices have to be fast and very handy to be driven in extremely conditions and, at the same time, to cover large areas. In Figure 9h, an example of a common system with large antennas RIS ONE TR25 MHz is shown. Concerning the archaeological field applications, IDS S.p.A. has provided another type of multi-channel device: the Stream X Figure 9i. It can be dragged by hand or towed by a vehicle, with a speed greater than 15 Km/h. It is suitable for working on rough terrain, with a real time Navigator for a fast and complete area coverage. It guarantees a higher investigation depth thanks to the high stacking factor and high performance low frequency antennas. In addition, the stream EM allows for a post processing software with automated transfer to CAD/GIS.

IDS S.p.A. is also the pioneer of the Interferometric radar. This technology is also a radar used to structural displacement applications. They realized two different models. The first one, namely, the IBIS-FL system Figure 9l is generally used for static monitoring of large structures, for example landslides or slope displacement; the second one, IBIS-FM Figure 9m is rather employed in case of mine slope instabilities or collapses. Both these systems are able to display the vibration and the DAM displacements.

Considerable efforts have been spent in time by IDS in the Forensic and Public Security field. They realized a GPR used for the location of cavities, tunnels,

buried bodies and a new generation of GPR TWR (Through Wall Radar) Figure 9n for the detection of people behind walls, very useful for military issues.

6. Do you have GPR test sites in your Country?

Although there is a lively research movement concerning the use of GPR in Italy, the amount of test sites is still meager, to the best of the authors' knowledge. We can recognize two test sites used for archaeological researches, located in Frosinone [1] and Pescate [2]. The first one enabled researchers to achieve a wide knowledge of the use of GPR technology in archaeological applications, while the second was mainly employed to study ancient buried structures.

The test site of Ispra [3], in Northern Italy, was used for military scopes, within the framework of a European research project concerning the detection of anti-personnel mines. Overall, the main test site built up for training GPR-based research in civil engineering activities was realized at the University of Salento, Lecce Figures 10 and 11. The test site area is located inside the University Campus, about 4 kilometers from the city center. The campus coasts the Lecce-Monteroni route, and has a dimension of about 2000 m^2.

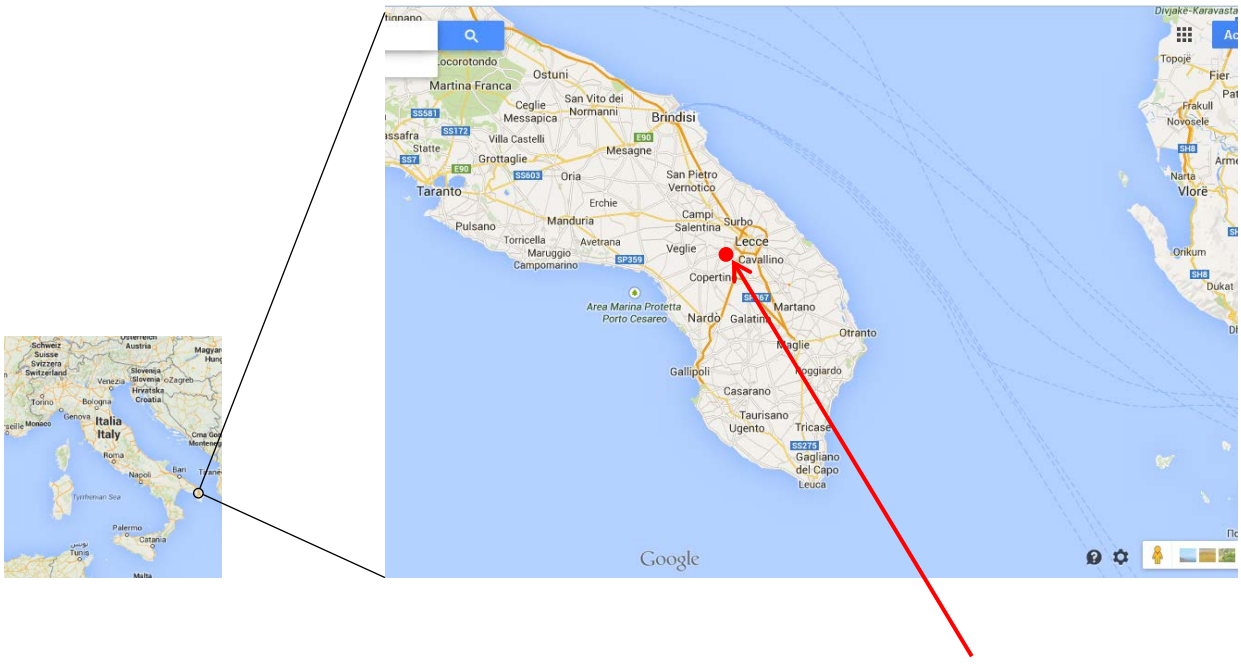

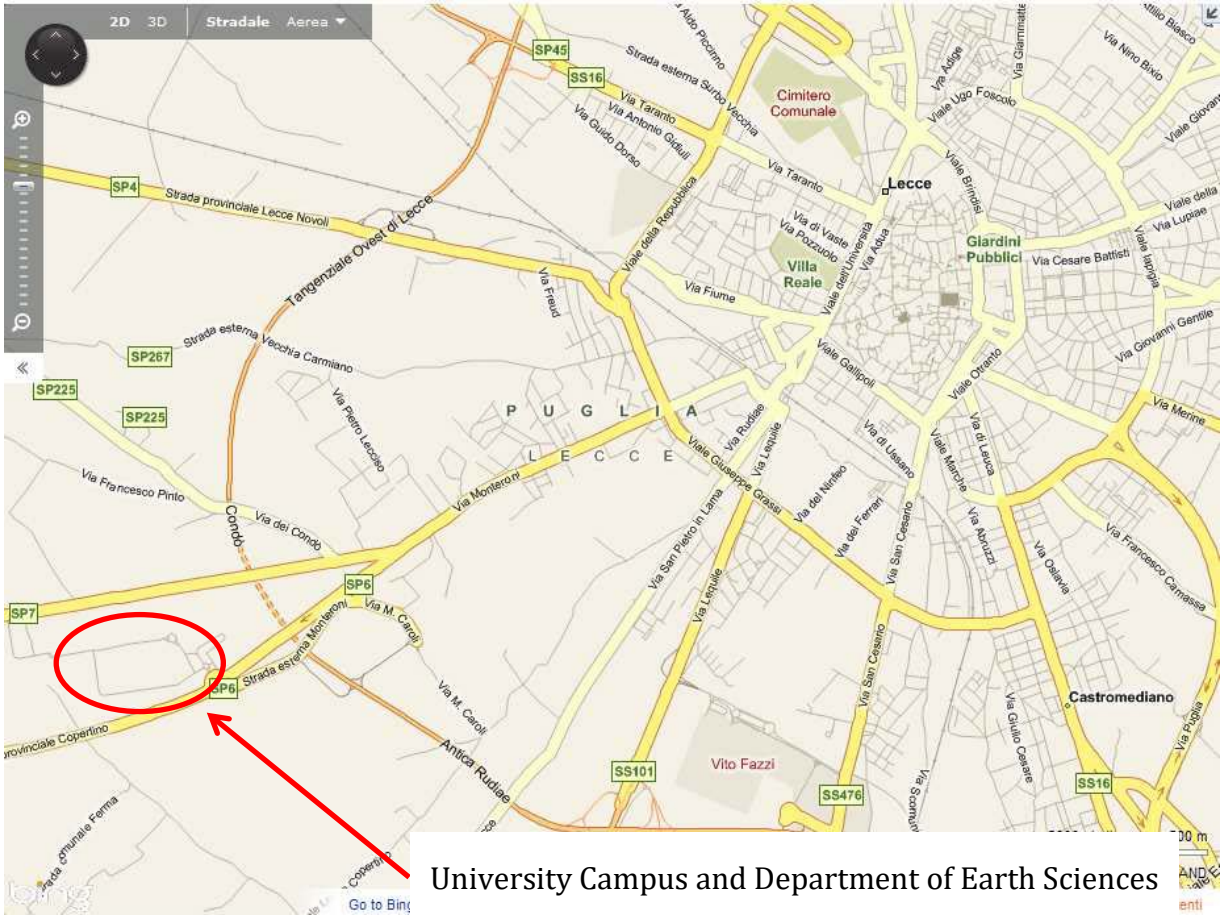

Fig. 10 – Map of Lecce and location of the University Campus (marked in red)

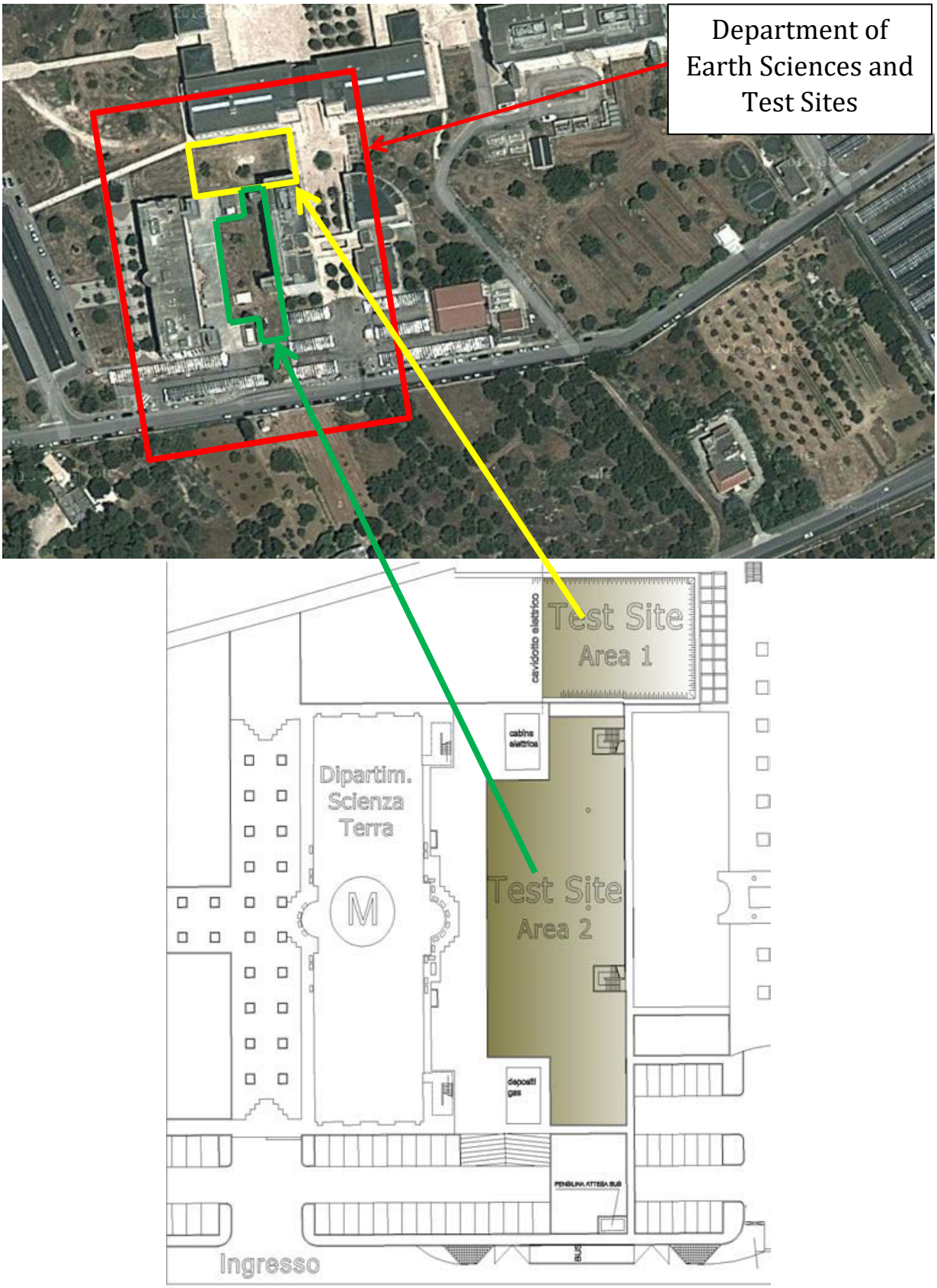

Fig. 11 – Map of location Department of Earth Sciences in University Campus and Test Sites

Therefore, as shown in Figures 12 and 13, it was possible to recognize 20cm diameter PVC pipes (1), 100cm Styrofoam sphere useful to simulate cavity (2), different walls manufactured with the so called Pietraleccese (3), a typical southern Italy material, or with Calcarenite (4), a Styrofoam Parallelepiped able to simulate a tomb (5). On other hand, Figures 14 and 15, shows a buried limestone road (6) to simulate ancient road, a metal barrel (7) and brick-walls above the ground (8).

In general, test sites areas are very useful to promote and develop the application of geophysical techniques, and can favour the cooperation between private companies and the academic world.

Finally, the test site will have a strong educational value, giving the opportunity to students of different levels (undergraduate, graduate and professional), to verify the accuracy of each method in detecting and estimating depth, size and nature of a target buried in the near subsurface.

Overview test site area 1

Buried targets in test area 1

Fig. 12 – Details test site area 1

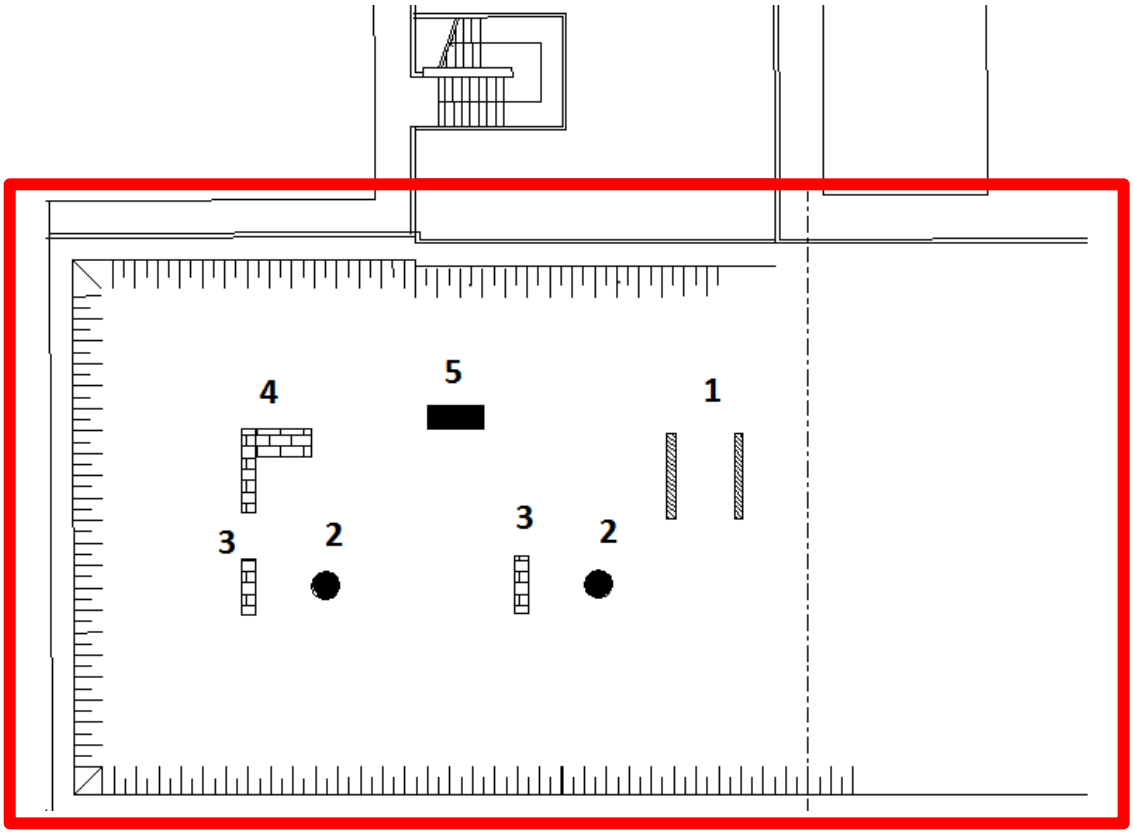

Legenda

1) PVC pipes 20 cm diameter

2) Styrofoam sphere 100cm diameter (to simulate cavity)

3) “Pietra leccese” wall

4) Calcarenite “tufo “ wall

5) Styrofoam Parallelepiped (to simulate a tomb)

Fig. 13 – In evidence plan of building and test site 1

Overview test site area 2

A simulated ancient road

A polystyrene sphere, simulating a cavity, with a tuff wall simulating a foundation

metallic bin

foundation walls in "Leccese" stone

Buried targets in test area 2

Fig. 14 – Details test site area 1

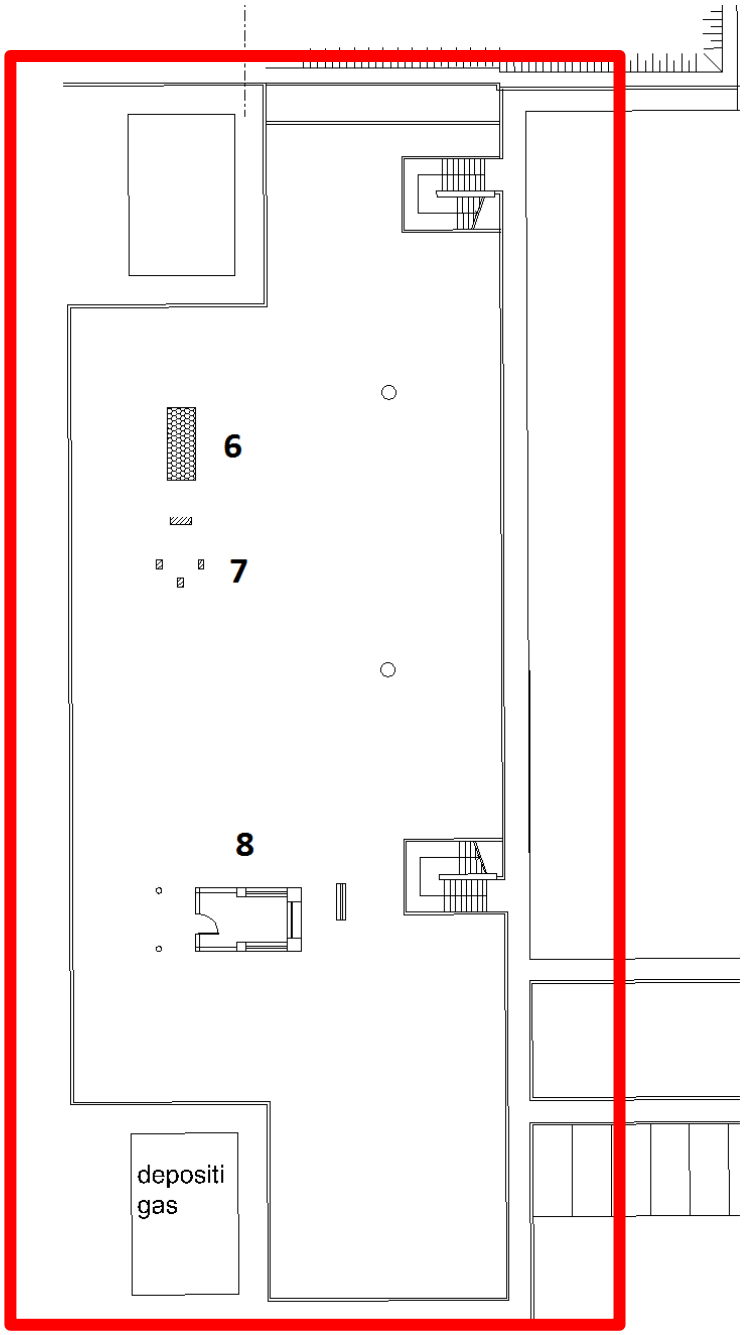

Legenda

6) Limestone road (to simulate an ancient road)

7) Metal barrel

8) Walls above the ground

Fig. 15 – In evidence plan of building and test site 2

The test site was opened during the XIII International Conference “GPR 2010”, held on June 2010. It is composed of two main areas. In order to simulate archaeological and urban subsurface scenarios, several objects and targets made by different materials and geometries, manmade and natural, have been buried. Moreover, small walls of buildings with different types of constructions, both ancient and modern, have been also built. The main goal of the test site is to offer to the manufacturing companies the opportunity to acquire radar data on such targets and to show to the scientific community as well as to the customers about the potential of their own systems [4]. The test site is also available for testing new or existing geophysical instruments and verify their target detection capability, both in terms of data acquisition strategy and signal processing effectiveness. Different objects were buried in both test site areas to simulate civil engineering and archaeological targets.

References

[1] Goodman D., Piro S., GPR remote sensing in Archeology, Geotechnologies and the environment, 2013.

[2] Lualdi M., Zanzi L., GPR investigation to reconstruct the geometry of the wooden structures in historical buildings, Proceedings of Ninth International Conference on Ground Penetrating Radar, 2002.

[3] HOPE project, Development of anti-personnel mines, Joint Research Centre (JRC), 2001.

[4] Negri S., Quarta T. A. M., Ground Penetrating Radar survey for civil-engineering applications: results from the test site, Proceedings of 14th onference on Ground Penetrating Radar (GPR), Shanghai, China, June 4-8, 2012.

7. Which are the most interesting university courses and training activities involving GPR?

At the moment, the most interesting training activities in Italy involving GPR are:

- The COST Action TU1208 co-organized, jointly with Action TD1301 "Development of a European-based Collaborative Network to Accelerate Technological, Clinical and Commercialization Progress in the Area of Medical Microwave Imaging" and with the European School of Antennas, a Training School on "Microwave Imaging and Diagnostics: Theory, Techniques, Applications."

- The training school "Civil Engineering Applications of Ground Penetrating Radar" held in Italy took place at the School of Engineering of the University of Pisa. The Training school has been organized within the framework of the COST Action TU1208, chaired by Dr. Lara Pajewski.

- 33rd EARSeL Symposium 3-5 June 2013 - Matera, ESA Course on Remote Sensing Applications for the Study and Observation of Archaeological sites in the framework of the 4th EARSeL Workshop on Cultural and Natural Heritage. 3 - 5 June 2013 - Matera, Italy.

Several courses on GPR are held by Scientific Faculties in many Italian Universities. In each of these faculties, the GPR methodology is taught in specific courses from both a theoretical and a practical approach, taking into account also different applications according to the main curricula of the degree course in the relevant scientific faculty.
The most interesting University courses are organized by Roma Tre University, University of Genoa, the Second University of Naples, Politecnico di Milano, University Mediterranea of Reggio Calabria, University of Pisa, University of Siena, University of Basilicata, University of Bari and by the University of Messina.

Inside the Roma Tre University there are several courses involving the GPR technology, for example the “Laboratory of microwave antennas” within the faculty of Electrical Engineering. This course provides theoretical and practical elements for the experimental characterization of microwave circuits and antennas. It also offers an introduction to the use of GPR and of electromagnetic simulation software, as well as some elements for electromagnetic subsurface investigations and diagnostic facilities with ground penetrating radar techniques. Another course is “GPR Signal processing-Ground penetrating radar (GPR) signal processing” organized by the Applied Electronics Section of the Department of Engineering of the University Roma Tre non-destructive technique, currently performed by many agencies involved in the road management, which results particularly promising for interpreting soil characteristics.

Inside the University of Genoa and in the Departments of Marine Engineering, Electrical, Electronic and Telecommunications (DITEN) the course “ADVANCED ANTENNA ENGINEERING” is taught. It concerns an introduction to the most relevant theoretical and algorithmic aspects of the modern microwave imaging approaches. The Microwave Imaging is a practical resource for engineers, scientists, researchers, and professors in the fields of civil and industrial engineering, nondestructive testing and evaluation, geophysical prospecting, and biomedical engineering.

In the Second University of Naples within the Department of Industrial Engineering and Information there are the courses of “Microwave Engineering and RADAR” and “Biomedical Imaging”. This course aims to provide students with an updated overview on the different methods of characterizing Imaging Radar applications and in particular on Biomedical diagnostics. At the Department of Civil and Environmental Engineering of the “Politecnico di

Milano" the course "Laboratory of Geology and Applied Geophysics" is given. To cite a few amongst the topics covered, the non-destructive detection of civil engineering structures with the Ultrasound techniques and the Ground Penetrating Radar methodology is faced.

The Engineering Faculty of the University Mediterranea of Reggio Calabria, in collaboration with the Institute of the National Research Council Irea organizes the course of Electromagnetic Diagnostics. Such course aims at providing basic knowledge about the electromagnetic diagnostics in the "near field" and in the "far field" conditions, including techniques and applications. Through the study of the mechanisms of interaction between electromagnetic waves and the natural environment, the course provides the necessary tools to analyze and formulate an application problem of electromagnetic diagnostics and identify appropriate methods of solution.

The University of Pisa, within the Faculty of Engineering, organizes the course of "Non-destructive analysis of works of civil engineering with Ultrasound techniques and Ground Penetrating Radar." In addition, the degree course of EXPLORATION AND APPLIED GEOPHYSICS contains the course of Geomorphology Radar which aims to provide students with the basic principles of operation of the Ground Penetrating Radar (GPR), data processing techniques and applications in the main geo-morphological environments. The course regards also the practical use of the GPR and the data processing.

The University of Siena within the CGT-Center for GeoTechnologies, organizes several annual Short Course:

- "The Use of GPR for electromagnetic survey in archaeological contexts (GPRA)": the course includes an introduction to electromagnetic methods, with particular attention to the theoretical principles that rule the operation of GPR and its use in archaeological environments. The central

part of the course is dedicated to some investigation campaigns in which participants have the opportunity to plan and carry out a survey using a GPR geophysical methodology in an archaeological site with the aim to identify the anthropogenic buried elements. In addition, the course is focused on providing a general knowledge of the theory behind ground penetrating radar, including some information on data processing and interpretation, using specific software that are made available to all the participants.

- Free Short Lecture GPR Methodologies 1 (PCGPR). The course on GPR Methodologies is dedicated at investigating the use of GPR in urban areas, as well as in geological and archaeological sites. The practical approach that characterizes this course offers new incentives for increasing the interest of the participants, and it is aimed at attracting especially the professional world wherein a continuous update on both the methods and the instruments of investigation is strictly required.

- Methods of Prospecting with Penetrating Radar. The main aim of this course is to provide the knowledge necessary for the correct use of the GPR in different environments, with particular focus at the study of shallow depth subsurface (geology, archaeology, civil and environmental engineering).

The University of Messina organizes the Master Course of "Diagnostics Town & Country, the GPR method." Such course regards the general equations of the electric and magnetic field, the propagation velocity, the electromagnetic properties of the medium, the waves propagation in a dispersive medium, the parameters that affect the electromagnetic waves

propagation, and the problems of signal attenuation resolution. This course is addressed to graduates in Engineering, Architecture, Geology, Physics and Environmental Sciences. The course is part of the activities budgeted as part of the International Conference of Applied Geophysics for Engineering (AGE), which is held annually in Messina *http://ww2.unime.it/osservatorio/age5.*

It is proposed to provide specific knowledge on issues related to the characterization of the current levels of susceptibility to damage of the elements of urban and territorial system for the design of structures of strategic importance; with the main goal of creating a stronger interaction amongst researchers and users of those techniques applied in the field of structural diagnostics and evaluation of the seismic vulnerability of urban and regional planning. The training is also aimed at placement purposes through the creation of an experts list in Diagnostics Town & Country, to which reference may be made in relation to the specific needs of companies, individuals, municipalities, provinces, regions and in typically institutions responsible for the territory protection.

The Department of Science, degree in geosciences and georesources, of the University of Basilicata organizes the course on “Geophysical Prospection”. The course program includes geophysical methods for geological, hydrogeological and archaeological applications in order to provide an overall understanding of the main geophysical methods (shallow and deep ERTs, Self Potential, Induced Polarization, GPR, Magnetic and EM techniques) aimed at studying and modeling the subsurface in 2D/3D/4D at both the laboratory and field scale, and the proper use of these geophysical techniques as a function of the specific application (geology, hydrogeology, contamination, archaeology). The Department of Earth Science and

Geoenvironmental of the University of Bari “Aldo Moro”, organizes the course on “Geophysical Prospection”. The course regards geophysical methods for geological and hydrogeological applications.

In addition to the above University courses, some professional orders and sector companies, such as the Italian Geological Society regularly organize training school for the spreading of the GPR technique and its integration with other geophysical technologies. These courses are dedicated to students and professionals in the field of geosciences and engineering.

Amongst them, the "Course of GPR in the areas Geological Survey, Structural and Environmental", organized frequently by Novatest Srl is a 32-hour course aimed at providing information on the main survey methods, instrumentation and main features, applications in the construction industry, the technical rules of construction NTC2008, on the contribution of GPR to the study of geological problems, of structural and environmental, of road applications etc..

In addition, GeoSed organized a school last year, within the section of Geology Stratigraphy and Sedimentology in an annual convention, on GPR in Alghero at the Department of Architecture.

The school was mainly addressed to graduated students and fellows, GeoSed Association and Geological Italian Society Members. The purpose of the school was to provide basic knowledge on the operation and the processing of a radar system.

Fig. 16 – Localization of the Italian Universities involved in GPR activities.

They have shown how to used the Hi-Mode Duo GPR system with integrated antennas at 200 and 600 MHz or at 600 MHz and 900 MHz and also a single GPR antenna at 80 MHz. All these systems are built by IDS S.p.A. *www.idscorporation.com,* and marketed by Boviar *www.boviar.com.*

8. How often is the GPR used in combination with other NDT methods?

At the state of the art, the use of GPR in combination with other NDTs in Italy appears to be still lacking, both in terms of regulation and related scientific

works. Nevertheless, it is possible to identify some works concerning the coupling of GPR and Light Falling Weight Deflectometer (LFWD), in order to infer information about the mechanical properties of soils as a function of their electromagnetic properties evaluated through radar systems.

Such scientific approach was mainly tackled in Italy by the University of Roma Tre, and was aimed at evaluating the mechanical response of transport infrastructures pavements with a high productivity.

Benedetto and Tosti [1] investigated the relationship between the dielectric and strength properties of unbound materials. Basically, they assume that dielectric properties of materials are related to their bulk densities therefore, since it is known that mechanical characteristics of soils depend on particles interaction, dielectrics of materials can be somehow related to their mechanical properties.

GPR tests were performed both at the laboratory and field scale using ground-coupled radar systems. The goal of the study was indeed to assess the bearing ratio of soils in Runway Safety Areas (RSAs), in airport environment.

Light Falling Weight Deflectometer was used for validating the procedure through in-situ measurements. In addition, laboratory tests for CBR evaluation were performed. Field tests took place at the Roma-Urbe Airport in Rome, Italy. A vehicle of the Fire Department was preliminarily used to simulate runway overruns of an aircraft in the RSA surface, defined as the surface at the lateral boundary of the runway required to reduce the risk of damage in case of landing or takeoff overruns.

GPR measurements were carried out along two trajectories of possible overrunning. The procedure was validated through CBR tests and twenty-nine LFWD measurements Figures 17 (a - c) were performed every 10 m alongside the considered trajectory. Therefore, a promising empirical

relationship between the relative electric permittivity and the resilient modulus of soils was found. The comparison between measured and predicted data shows a reliable prediction of Young Modulus, paving the way for inferring mechanical properties of unbound materials through GPR measurements. Encouraging results were obtained, being the absolute residuals between observed and predicted elastic moduli lower than 5 MPa in most of the surveyed station points, and the variability of residual incidences mostly included within approximately the 20%.

Prediction of strength properties of RSA unpaved soils can provide both time-efficient and cost-effective solutions, thereby improving the airport operability and favoring the decrease of runway maintenance and construction costs. As mentioned, the potential of this model can be also exploited for road purposes. Concerning bound pavement structures, it is well known that the loss of strength and deformation properties of road pavements and materials plays a key role in road safety issues as it brings to deep and surface damages that may cause car accidents [2].

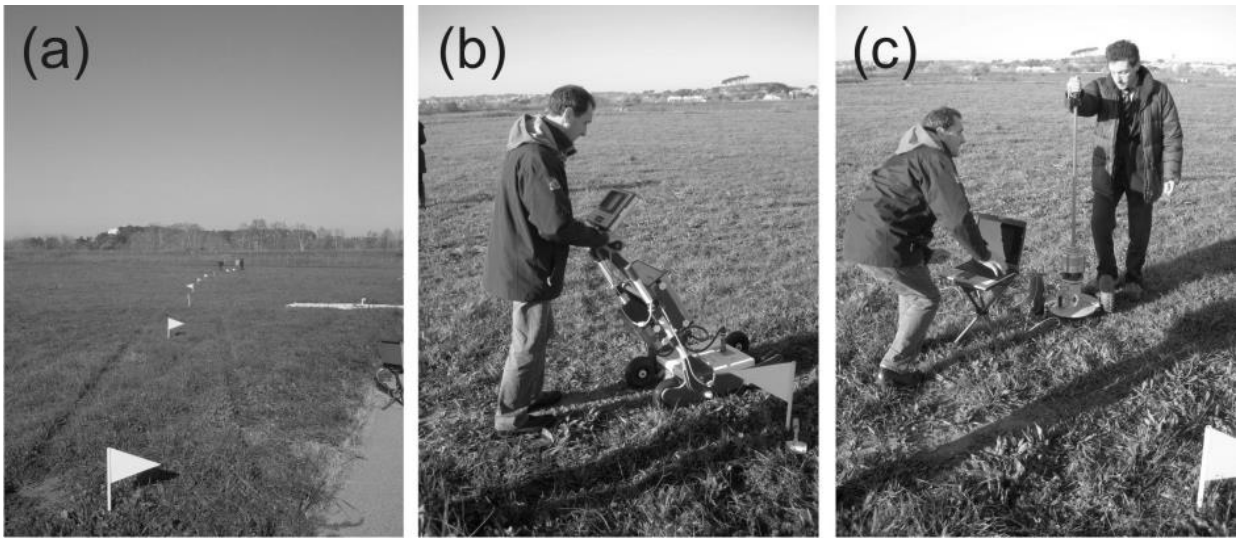

Fig. 17 – In-situ measurements at Roma Urbe Airport. (a) Trajectory of overrunning, (b) ground-coupled radar, 600 MHz and 1600 MHz central frequencies, (c) light falling weight deflectometer.

Overall, such event can be produced by several factors related to environmental conditions (e.g., annual precipitation, freezing index, moisture content of materials), type of material (e.g., fine or coarse grain size, subgrade soils susceptibility to frost), traffic loads, and construction aspects (e.g., pavement type, total thickness of layer structure, number of years since construction) [3].

Several traditional destructive techniques are used for evaluating strength and deformation properties both in laboratory and real road environment, although they can provide for time-consuming and low significant measurements.

In that respect, the use of falling weight deflectometer (FWD) has increased in the past decades [4-5], whereas more recently, the light falling weight deflectometer (LFWD) has been developed as a portable version of FWD to overcome accessibility problems of more cumbersome devices in roads under construction. A second Italian work, still by University of Roma Tre researchers, face these topics with the aim of retrieving the Young's modulus of a flexible pavement structure in a 4m×30m made up for this purpose [6].

Tosti et al. promisingly succeeded to develop a prediction model by relating electromagnetic data collected by GPR to LFWD measurements. The study represent a significant contribution to the research on preventing the risk of pavement surface damages due to the loss of strength of bound materials.

The surveyed test site is situated at the Department of Engineering of Roma Tre University in Rome, Italy (41° 51' 16.02" N, 12° 28' 06.02" E) Figure 18. The surveyed area is composed of one flexible pavement structure. The average elevation is 11.5 m above the sea level, with no slope and a straight extension of the path. The test site location was selected in order to avoid

surface metallic reflectors (e.g., sewer manholes) that might have provided unwanted EM reflections. Visual inspections of the pavement surface revealed relatively good conditions, with few early-stage cracked areas and a 62 m^2 repaved zone covering almost all of the last 12 m of the surveyed area.

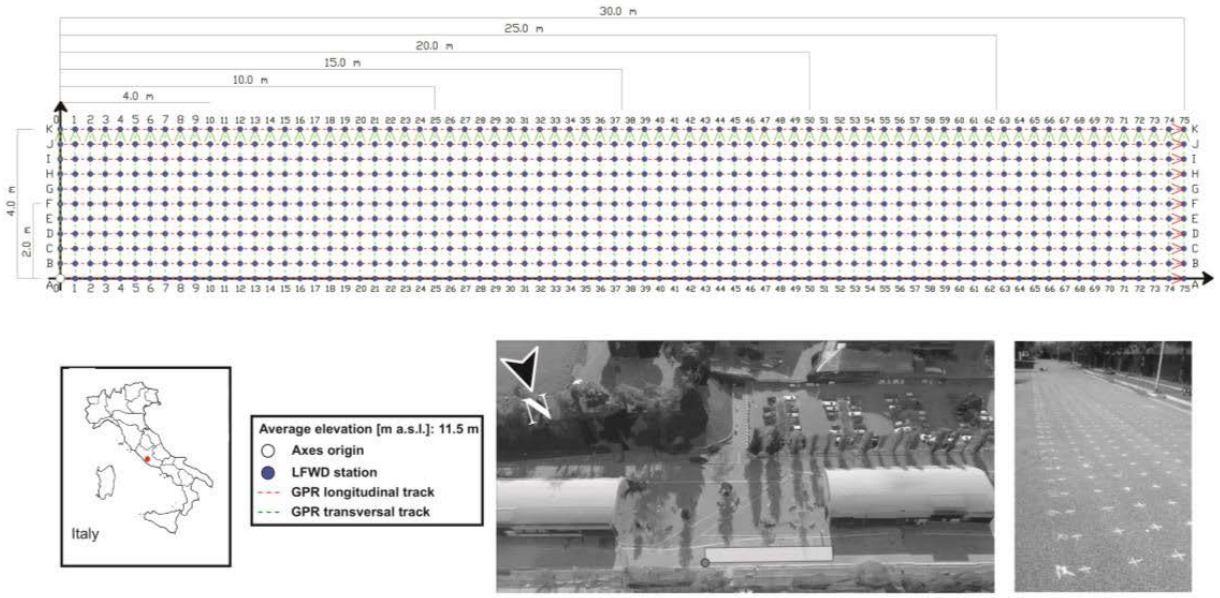

Fig. 18 – Test site for data acquisition carried out over a 4m×30m square regular grid mesh of 836 nodes.

A prediction model for inferring mechanical properties of the bound pavement structure through GPR inspections in order to prevent the risk of surface damages due to the loss of strength was finally developed.

The validation of this model demonstrates a relatively good agreement of both high and low strength values of observed and predicted elastic moduli. In addition, promising match is shown by comparing the two maps of elastic modulus, and a good consistency with visual surface inspections is proved.

The promising results achieved in the aforementioned studies open a wide research field at national level concerning the prediction of mechanical behaviour of both bounded and unbounded materials, through the coupling of two well known non-destructive technologies such as GPR and LFWD.

Moreover, it is worth noting that a deeper knowledge of the relationship between electromagnetic and mechanical properties of materials commonly used in civil engineering applications could represent a considerable break-through also in terms of achieving effective maintenance management programs. The attainment of the exact amount of deformation depending on the known forces acting in the considered system can indeed lead to predict the correct time beyond which it is necessary to start a maintenance activity to ensure the relevant safety levels with the lowest impact in costs outlay.

References

[1] Benedetto A., Tosti F., Inferring bearing ratio of unbound materials from dielectric properties using GPR: the case of Runaway Safety Areas, Airfield & Highway Pavement Conference, Los Angeles, USA, 2013

[2] Tighe, S., Li, N.Y., Falls, L.C., Haas, R, Incorporating road safety into pavement management, 79th Annual Meeting of the Transportation-Research-Board, Transportation Research Board Nat Research Council. pp. 1–10., 2000.

[3] Haas R., Hudson W.R., Zaniewski J., Modern pavement management. Malabar, FL: Krieger Publishing Company, 1994

[4] American Society for Testing and Materials (ASTM), Standard test method for deflections with a falling weight type impulse loading device, Annual Book of ASTM Standards 04.03, D4694.96., 2005

[5] Belt R., Morrison T., Weaver E., Long-term pavement performance program falling weight deflectometer maintenance manual, Report No FHWA-HRT-05-153. Georgetown Pike, VA, 2006

[6] Tosti F., Adabi S., Pajewski L., Schettini G., Benedetto A., Large-Scale Analysis of Dielectric and Mechanical Properties of Pavement using GPR and LFWD, Proceedings of 15th Conference on Ground Penetrating Radar (GPR2014), Brussels, Belgium, 2014.

Chapter I.2

Electromagnetic exposure of GPR operators and interference issues

Introduction

GPR systems operate from 10 MHz up to 5 GHz, with about a decade of bandwidth within that range, so placing themselves into the most extreme class of ultra-wideband (UWB) radars. In order to evaluate the electromagnetic emissions, comparing them to the limits that now exist in a number of jurisdictions, recent studies have focused on the basic steps needed to translate UWB GPR's results into regulatory parameters [1]. When analyzing a GPR we need to distinguish two functional aspects: operation as intentional radiator, and Electromagnetic Compatibility (EMC) requirements which equipment must satisfy. As deliberate radio frequency radiator, it can be assimilated to a Short Range Device (SRD), such as movement detectors and metal detectors, covered by the R&TTE Directive of European Commission [2]. Regarding EMC issues, emission requirements of equipment are defined by "Comité international spécial des perturbations radioélectriques" (CISPR) [3], and those of immunity by the International Electrotechnical Commission (IEC) committees. European Telecommunications Standards Institute (ETSI) published standards on

compatibility, and ground-and wall-probing radar applications, approved by the European National Standards Organizations in form of European Norm (EN). Specifically, ETSI Standard EN-302066-1 V1.2.1 [4] defines technical characteristics, and test methods, whereas ETSI Standard EN-302066-2 V1.2.1 [5] harmonizes requirements of an article of R&TTE Directive.

This chapter presents experimental test implementations for verifying how mobile phones and other common sources of possible interference can contaminate GPR data, and how to post-process the data in order to filter such interference effects. Among the interfering devices, XBee transceivers, based on IEEE 802.15.4 standard, are considered, since participants of Project 4.2 intend to combine them with a GPR, mounted on Unmanned Aerial Vehicle (UAV), for wireless communication of the detection and localisation of people buried under avalanche.

Considering that GPR systems:

- are not operated for extended duration and their mean radiated power is very low.
- are often used in areas where the density of population is low.
- are designed to radiate energy into the ground, where it is quickly absorbed Figure 1.
- are often equipped with a shut-off switch that automatically stops the radiation when the radar is lifted from the ground surface, or is not operated in the proper position.

interference is very rare and the human health protection issue is ignored. Nevertheless, when GPR application is exactly the people detection, this issue cannot be overlooked. Therefore, another focus of the work is to quantify the

exposure of GPR operators to electromagnetic waves emitted by the radar, for human health protection.

Fig. 1 – GPR radiates energy into the ground normally with reduced back-propagation toward operator.

1. EM Exposure of GPR Operators

Figure 2 shows the devices under test: the SIR2000, a GPR model by Geophysical Survey Systems, Inc. (GSSI), and the SUB-ECHO HBD 300 antenna by Radarteam Sweden AB factory.

SIR2000 is a single channel general-purpose system requiring a 12 V DC power input at 3 A. It can be used with antennas from 16 MHz to 2000 MHz providing penetration depths ranging from tens of m to a few cm.

The SUB-ECHO HBD 300 antenna operates at 300 MHz as central frequency. Its frequency boundaries of 3-dB bandwidth are 120-780 MHz. Front to back ratio stated around -14.5 dB. It weighs 4 kg and its dimension is (L x W x H) 720x360x160 mm.

a)

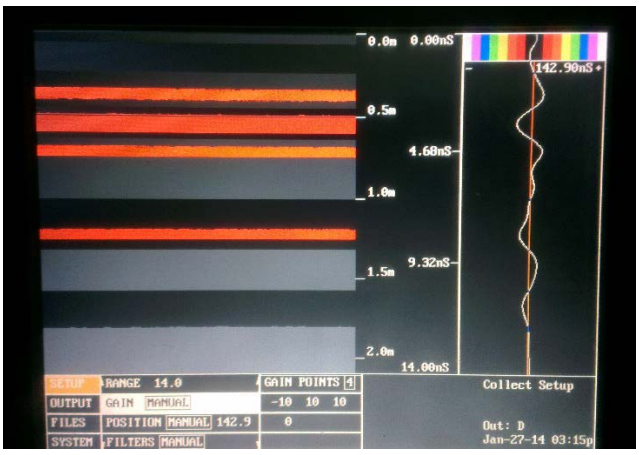

b)

c)

d)

Fig. 2 – Devices under test: (a) GPR GSSI SIR2000, (b) Detail monitor GPR device, (c) Radarteam SUB-ECHO HBD 300 antenna, (d) Setup antenna on rotating platform

For our test, we used the following equipment:

- Lecroy Wavemaster 8500A oscilloscope that allows measures up to 6 GHz;
- FSP30 spectrum analyzer by Rohde Schwarz operating in the range 9 kHz ÷ 30 GHz;
- E4440 spectrum analyzer by Agilent which works from 3 Hz to 26.5 GHz.

The measurement setup has been completed with:

- preamplifier HP8447F (9 kHz ÷1300 MHz);

- Shuner Sukoflex 100 microwave cables 104 & 106;
- Precision Conical Dipole (PCD) 8250 by Seibersdorf factory, like receiving antenna used in the frequency range 80 MHz ÷ 3 GHz, with a sensitivity that rises from 0.8 to 1.1 mV/m in the same frequency range.

We carried out measures inside an anechoic chamber "VECUVIA" of large dimension: 9x6x5.4 m. This chamber allows measurements in the frequency range 300 kHz÷18 GHz. Table I specifies its electric and magnetic shielding efficiency in different frequency ranges, and picture in Figure 3 shows setup of measure. A sketch of the same experimental setup is reported in Figure 4.

Tab. I – Electric and magnetic shielding efficiency of the anechoic chamber.

Frequency range	**Electric shielding efficiency (dB)**
300 kHz ÷ 30 MHz	120
30 MHz ÷ 400 MHz	105
400 MHz ÷ 18 GHz	100
Frequency	**Magnetic shielding efficiency (dB)**
10 kHz	60
100 kHz	90

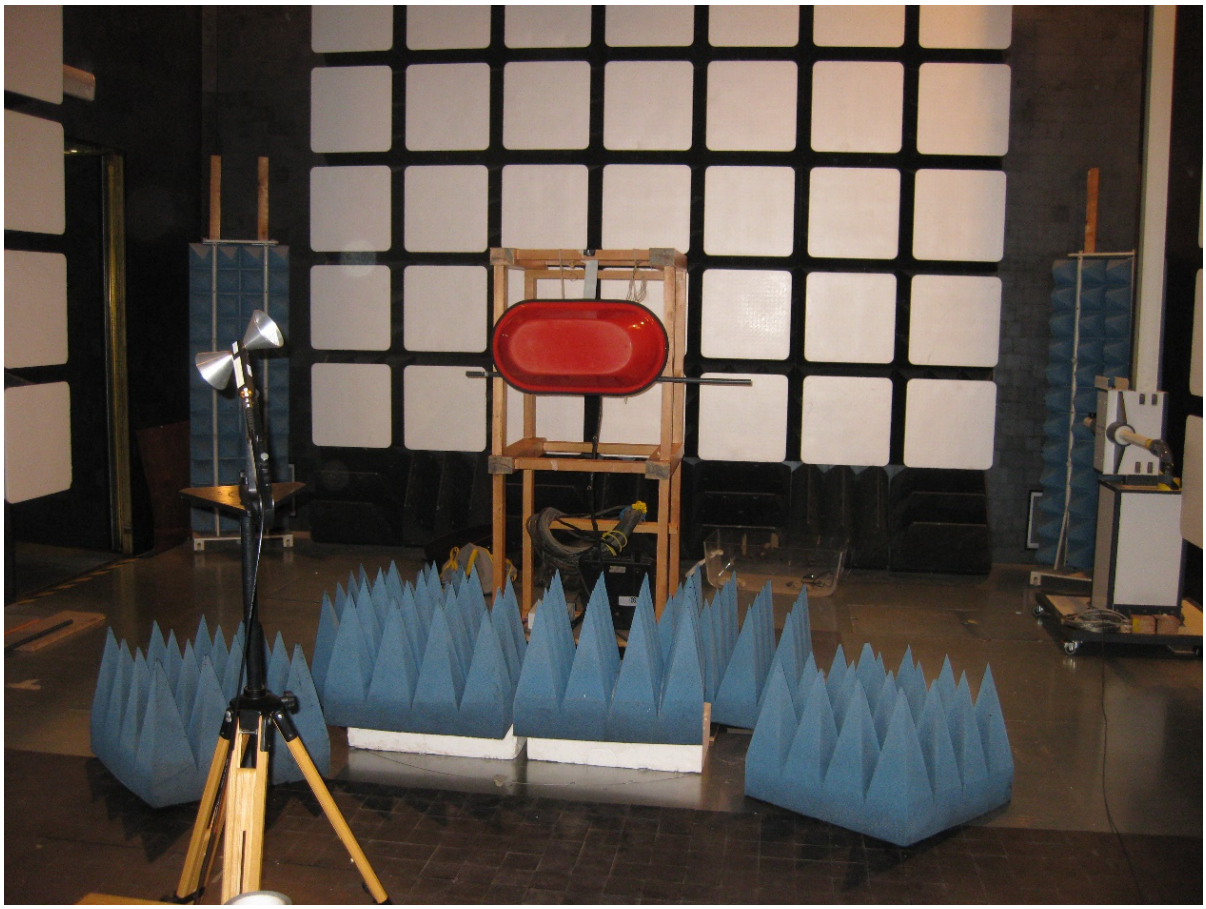

Fig. 3 – Anechoic chamber "VECUVIA"

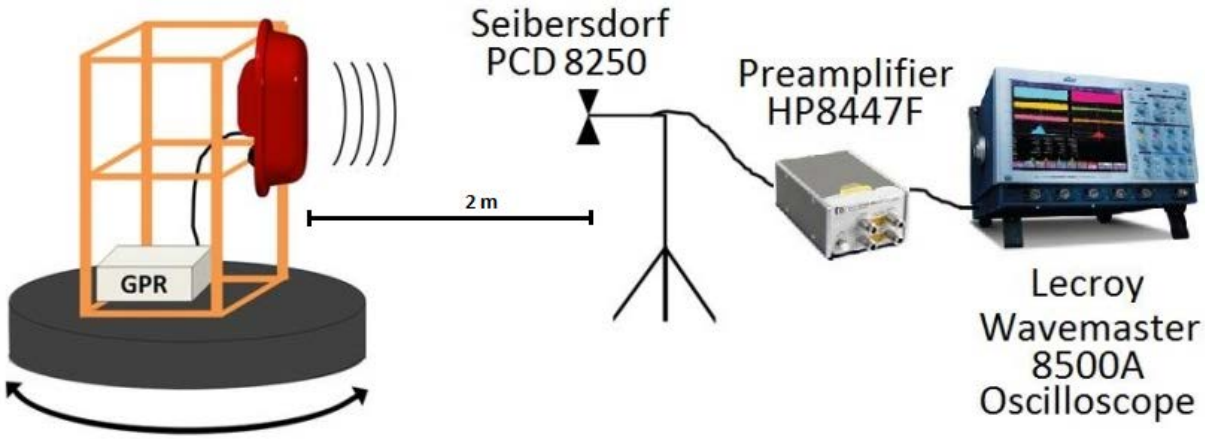

Fig. 4 – Sketch of the experimental setup

Normally, a GPR operator is exposed to the back lobe of the transmitting antenna, as well as to the signal reflected from soil under investigation. We

considered the worst case, evaluating the electric field transmitted from the GPR directly to a receiving antenna, located about at 2 m of distance.
The measured radiation pattern of the GPR antenna is shown in Figure 5.

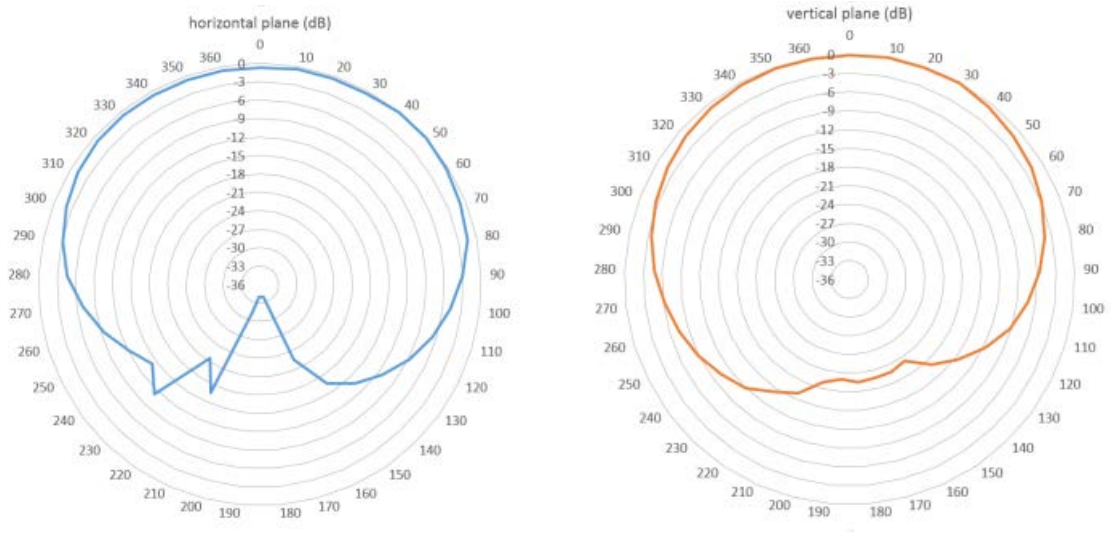

a) b)

Fig. 5 – Radiation patterns of the GPR antenna measured in dB units: (a) horizontal plane and (b) vertical plane

Results were collected by supposing that all radiated energy reaches the operator, along a direct line of maximum electromagnetic radiation, disregarding the back lobe transmission.

The intensity of the electric field E is evaluated by means of the following equation (1):

$$E = ACF \cdot V_a = ACF \cdot Att_{cable} \cdot V_r \quad (1)$$

where: V_a is the voltage value across output of receiving antenna, Att_{cable} defines the cable attenuation, V_r is the voltage intensity measured by the receiver, and ACF represents the antenna calibration factor.
By using a spectrum analyser (SA), we could measure the signal spectrum, identify its portion generated by the radar, and evaluate the peak and average

voltage intensity. Furthermore, by exploiting a suitable setting of the Resolution Bandwidth (RBW) of our SA, we could put in evidence the actual radar pulses. In Figure 6, typical pulses generated by the GPR are shown, in time and frequency domains. The SIR2000 GPR generates single pulses that have a time duration of about 2.7 ns and a variable Pulse Repetition Time (PRT = T). Measures carried out in the controlled room confirm the presence of spectral traces separated among them by a constant PRF = 1/T (Pulse Repetition Frequency), as shown in Figure 7.

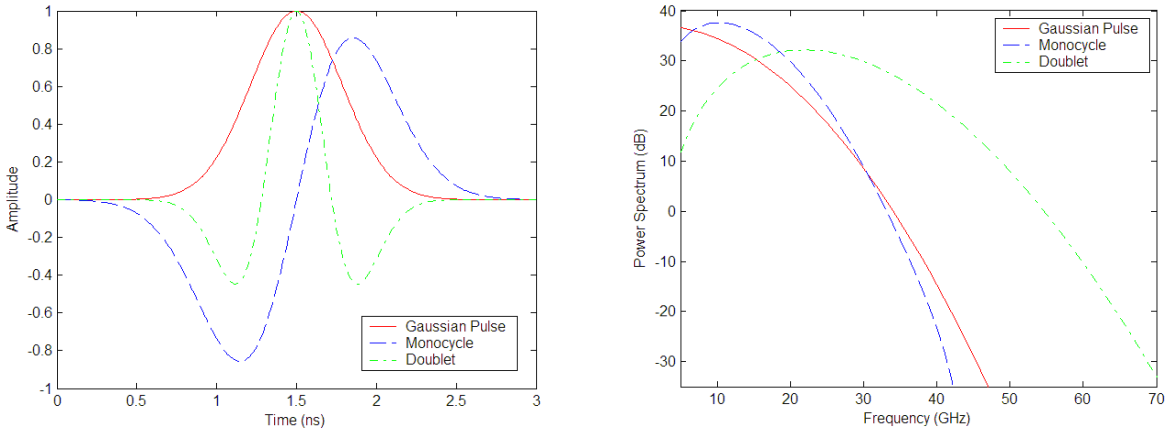

a) b)

Fig. 6 – Pulse generated by the GPR, in time (a) and spectral (b) domains

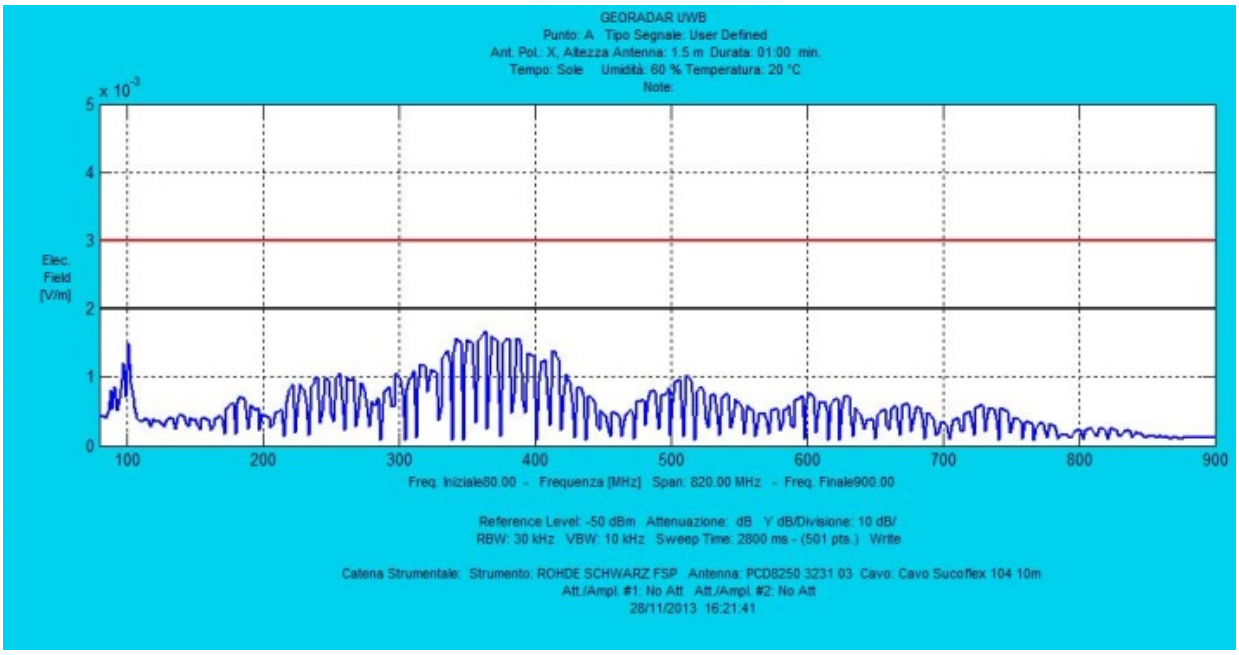

Fig. 7 – Measured spectrum

Two SA modes are possible, depending on the ratio between bandwidth at 3 dB of IF filter (RBW), and frequency distance between contiguous spectral rows, as shown in Fig. 8. These two procedures are named: line spectrum mode and pulse spectrum mode.

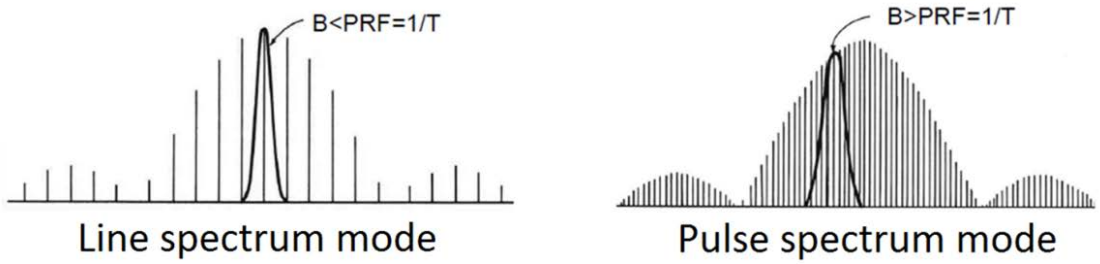

Fig. 8 – Spectral traces permitted

When we operate by using the line spectrum mode, the analyzer resolution allows us to display each single spectral component. In this case, the norm CEI 211-7B regulates how to measure the electric field peak: is the dB value, estimated by means of analyzer at carrier frequency, corrected by adding the de-sensitivity factor α_L:

$$\alpha_L = [dB] = -20 \cdot \log_{10}\left(\frac{\tau}{T}\right) \quad (2)$$

Where τ is the peak duration time.

DPCM (Decree of the President of the Council of Ministers of the Italian Republic) July 8, 2003 is the Italian rule regarding exposure of people to the electromagnetic fields. Nevertheless, it regulates only the cases of telecommunication fixed services (art. 1). However, in the case of pulsed signal, the same decree at subsection no. 4 recommends to adopt the European Recommendation (July 12, 1999). This rule, conformable to the ICNIRP (International Commission on Non-Ionizing Radiation Protection), evaluates maximum power density (S) as the average power density multiplied by factor 1000. This is equivalent to multiply the average electric field by the factor 32 for obtaining maximum electric field, at identical frequency obviously. Similarly, D. Lgs (Legislative Decree) 81-2008, conformable to the rule CE 2004/40, regulates worker exposure. Specifically, in the frequency range 10 MHz÷300 GHz, peak values are evaluated by multiplying the rms values by factors 32 and 1000, respectively for electric field and power density of the equivalent plane wave.

When the voltage receiver is expressed in dBm, we can use the equation:

$$E\left(\frac{dBV}{m}\right) = AFC(dB) + Att_{cable}(dB) + V_r(dBm) - 13 \quad (3)$$

In our experimental results, the value of electrical field peak has been measured equal to E_{peak} = 1.7 mV/m.

GPR's setup can be changed. In the case of setup as 900TAS, 300S, 2500HHS, we measured a PRT of 12 μs, different from that shown when setup is 500DPH (PRT=23.3 μs).

Consequently, the rms values of electrical field are:

$$E_{RMS} = E_{peak}\sqrt{\frac{\tau}{T}} = \begin{cases} 0.025\,\dfrac{mV}{\mathrm{m}}\text{ , for setup: 900 TAS, 300S, 2500HHS} \\ 0.018\,\dfrac{mV}{\mathrm{m}}\text{, for setup: 500DPH} \end{cases}$$

In any case, these measured values are very little, lower than limits imposed by rule. The following Figure 9 exemplifies the rules, by evaluating limits imposed respectively for average and for peak values of electric field.

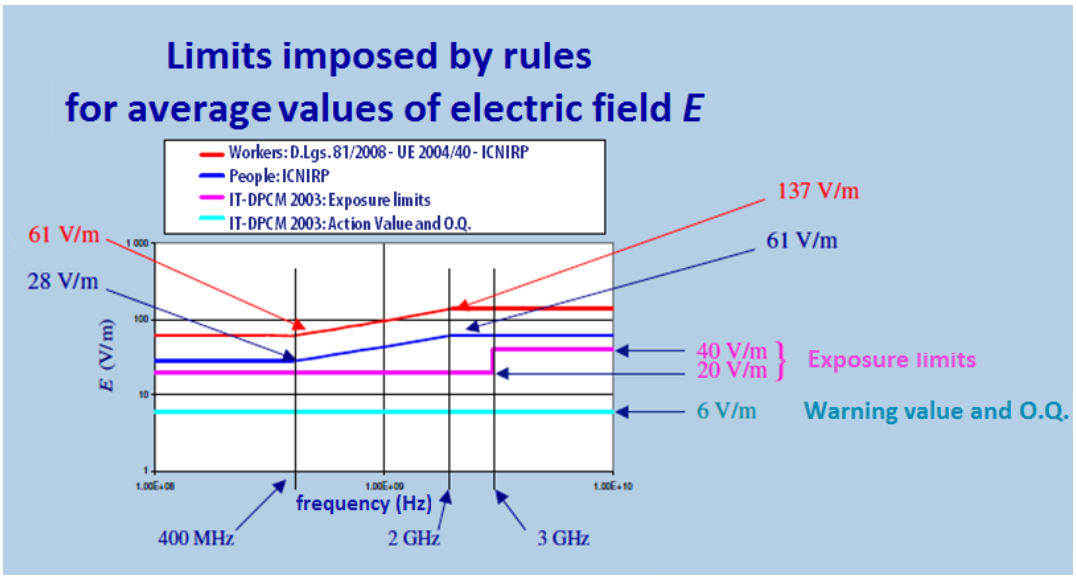

a)

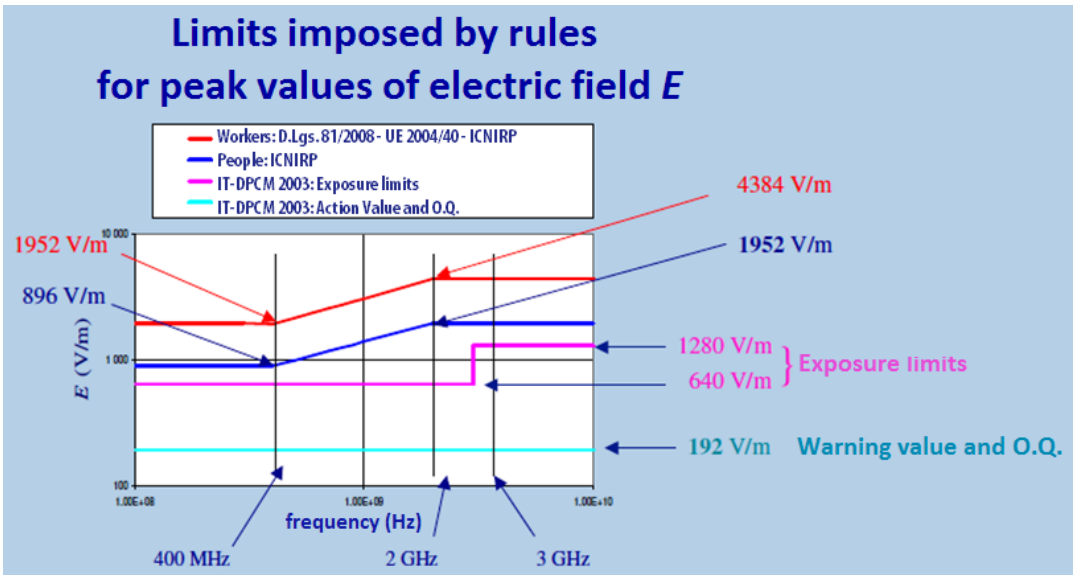

b)

Fig. 9 – Limits imposed by rules, respectively for average (a) and peak (b) values of electric field.

2. Interference Testing Analysis to Develop A GPR Application: Detection of People Under Avalanches

The detection and precise localization of people buried or trapped under avalanche or debris is an emerging field of application of GPR [6÷11]. In the last years, processing approaches and technological solutions have been developed to improve detection accuracy, speed up localization, and reduce

false alarms. In case of emergency scenario for avalanche, improvement of these three aspects is fundamental for increasing probability of survivals. Indeed, the survival time is very short, since the relative probability decreases to 90, 40 and 30 per cent, if the victim is removed from the snow within 15, 30 and 60 minutes, respectively. So, radar at direct contact with the snow surface is not a viable option. In fact, moving radar systems on a mountain slope run over by avalanche is particularly complicated, due to the presence of bulky slabs of ice mixed with snow. Therefore, placing the radar just on the snow is not fast enough for using it during emergency.

In order to solve this problem, since 2005 researchers have considered a GPR system mounted on an airborne platform [12÷14], e.g. helicopter shown in Figure 10, or UAV in the future. Especially for the last case, there is need to add electronic devices to the basic GPR system. These subsystems allow wireless communication between GPR and operating unit, located on the snowy surface or inside a control room.

In order to evaluate interferences generated by transmitters located near the GPR antenna, we organized two different measurements, in the presence of a cellular phone and of a XBee transceiver.

The first test concerned an UMTS cellular phone. The distance between the GPR antenna and the phone was 1.4 m. Figure 11 shows radargram output (3849 scans), in absence (a) and in presence (b) of the cellular transmission. Figure 12 shows the oscilloscope representation, allowing us to put in evidence a very limited spread of traces.

Fig. 10 – GPR system mounted on an airborne platform (from the Radarteam Sweden AB web-site)

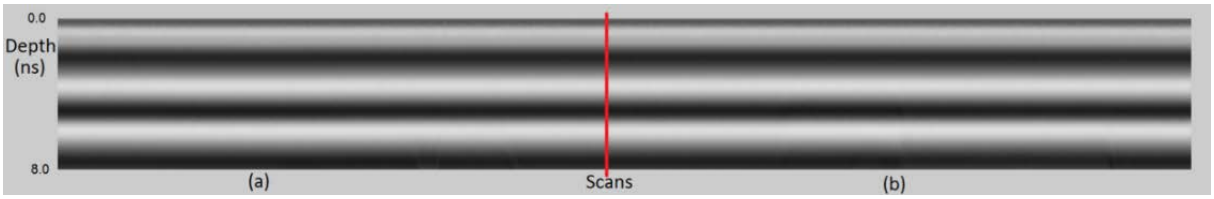

Fig. 11 – Radargram in absence (a) and in presence (b) of the cellular transmission

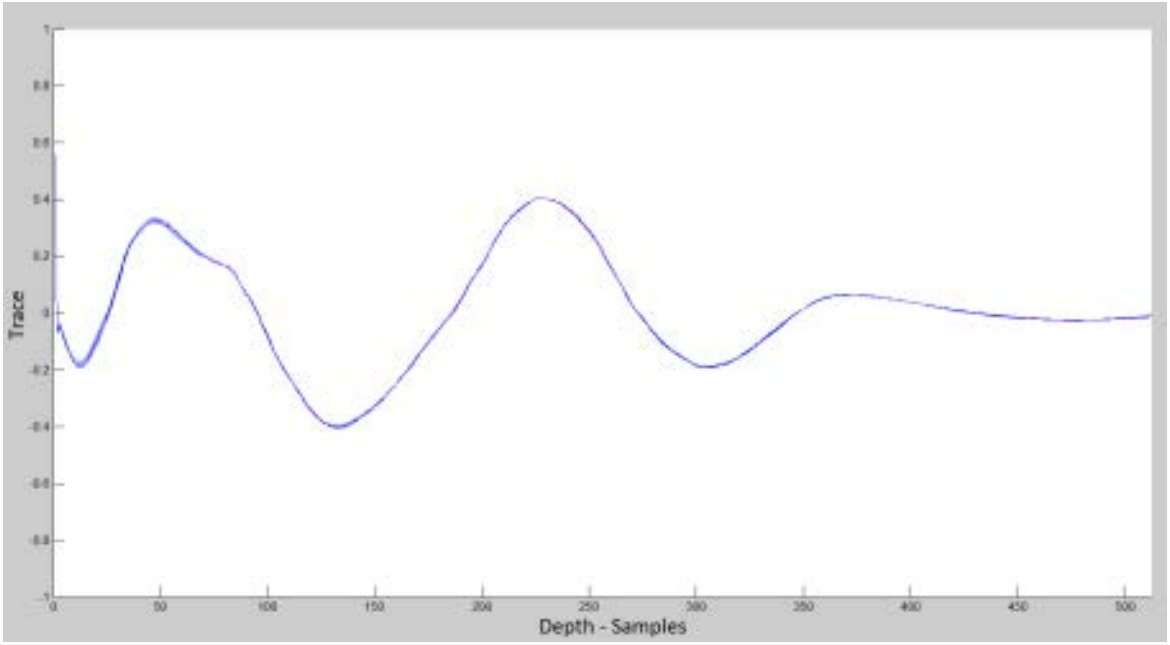

Fig. 12 – Oscilloscope representation

For the second test, a transceiver XBee PRO-S2 (international variant by Digi International), is arranged on the top at direct contact with GPR's antenna, as shown in Figure 13. Specifications of the RF module are: transmitting power output 10 mW, outdoor RF LOS range 1500 m, operating frequency band ISM 2.4 GHz, RF data rate 250 kbps, 14 direct sequence channels.

The radargram of Figure 14 shows a first interval of data acquisition with the XBee in off state, and a following interval characterized by the XBee continuously transmitting.

Both tests demonstrate a very low interference generated by the devices, due to the fact that their operating frequency bands are different from the GPR bandwidth. Therefore, the design for adding wireless communication devices to the GPR is justified.

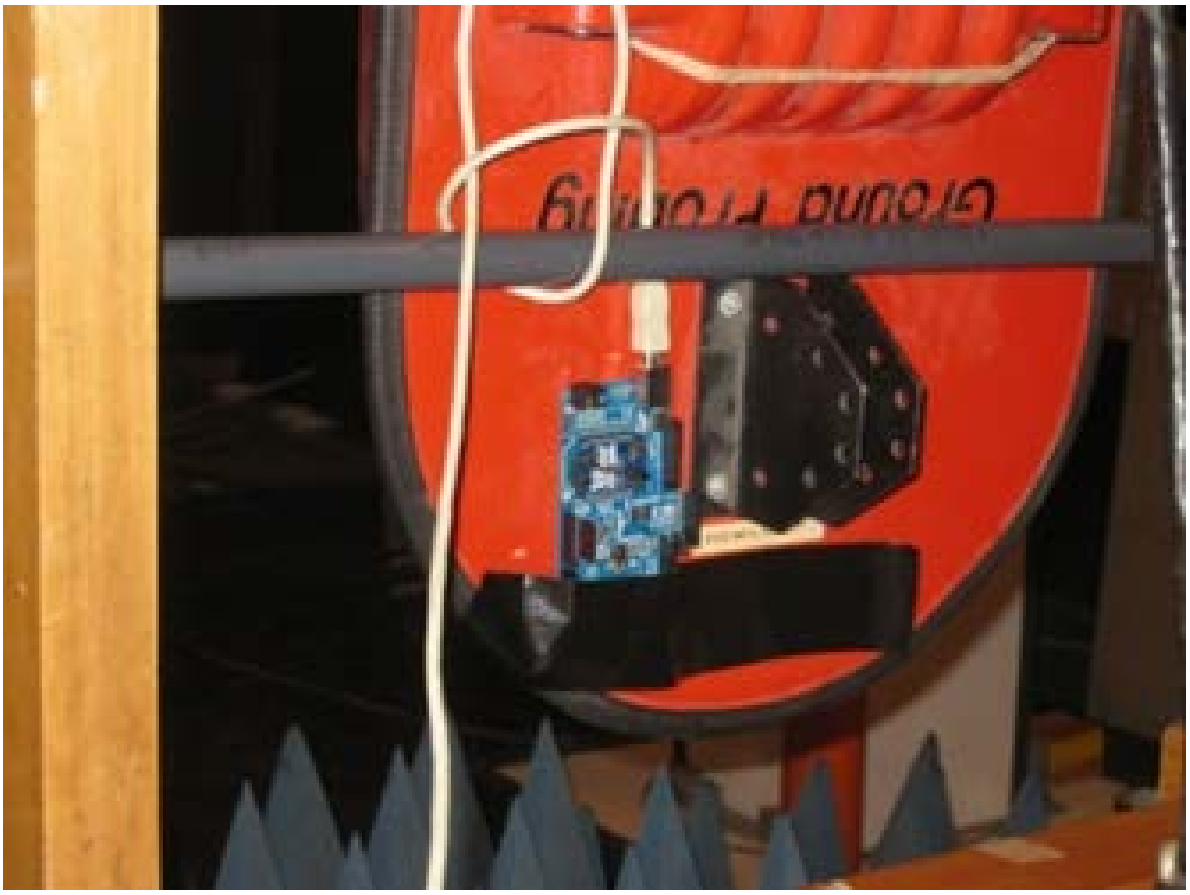

Fig. 13 – XBee transceiver on the top of the antenna.

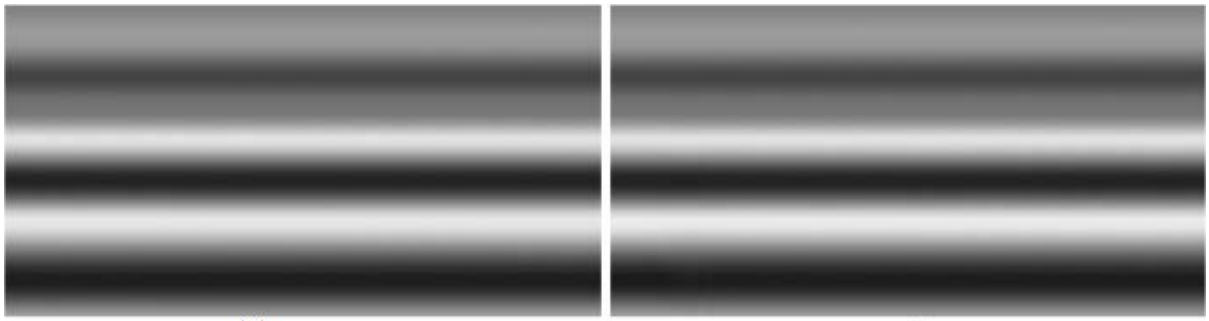

Fig. 14 – Radargram in presence (a) and in absence (b) of an operating XBee transceiver.

References

[1] A.P. Annan, N. Diamanti, and J.D. Redman, “GPR Emissions and Regulatory Limits,” 15th International Conference on Ground Penetrating Radar - GPR 2014, Brussels, Belgium, pp. 714-718, 2014.

[2] European Commission's Directorate-General for Enterprise and Industry, “Guide to the R&TTE Directive 1999/5/EC - Version of 20 April 2009”.

[3] CISPR 16-1: “Specifications for radio disturbance and immunity measuring apparatus and methods- Part I: Radio disturbance and immunity measuring apparatus”.

[4] ETSI Standard EN-302066-1 V1.2.l “Electromagnetic compatibility and Radio spectrum Matters (ERM); Ground- and Wall- Probing Radar applications (GPR/WPR) imaging systems; Part I: Technical characteristics and test methods”.

[5] ETSI Standard EN-302066-2 V1.2.l: “Electromagnetic compatibility and Radio spectrum Matters (ERM); Ground- and Wall- Probing Radar applications (GPR/WPR) imaging systems; Part 2: Harmonized EN covering essential requirements of article 3.2 of the R&TTE Directive”.

[6] C. Jaedicke, “Snow mass quantification and avalanche victim search by ground penetrating radar,” Survey in Geophysics, vol. 24, no. 5/6, 2003, pp. 431-445.

[7] A. Instanes, I. Lonne, and K. Sandaker, “Location of avalanche victims with ground penetrating radar,” Cold regions Sci. Technol., vol. 38, no. 1, 2004, pp. 55-61.

[8] J. Modroo and G. Olhoeft, “Avalanche rescue using ground penetrating radar,” in Proc. 10th Int. Conf. Ground Penetrating Radar, Delft, The Netherlands, 2004, pp. 785-789.

[9] E. Zaikov and J. Sachs, “UWB radar for detection and localization of trapped people,” Ultra Wideband, Boris Lembrikov (Ed.), ISBN: 978-953-307-139-8, InTech, 2010.

[10] J. Sachs, M. Helbig, R. Herrmann, M. Kmec, K. Schilling, E. Zaikov, and P. Rauschenbach, “Trapped victim detection by pseudo-noise radar,” in Proc. ACWR '11, 1st International Conference on Wireless Technologies for Humanitarian Relief, 2011, pp. 265-272.

[11] M. Loschonsky, C. Feige, O. Rogall, S. Fisun, and L. M. Reindl, “Detection technology for trapped and buried people,” IEEE MTT-S International Microwave Workshop on Wireless Sensing, Local Positioning, and RFID (IMWS 2009 - Croatia), 2009, pp. 1-6.

[12] M. Haltmeier, R. Kowar, and O. Scherzer, “Computer aided location of avalanche victims with ground penetrating radar mounted on a helicopter,” in Proc. 30th Workshop OAGM/AAPR Digital Imaging Pattern Recog., Obergurgl, Austria, 2005, pp. 19-28.

[13] A. Heilig, M. Schneebeli, and W Fellin, “Feasibility study of a system for airborne detection of avalanche victims with ground penetrating radar and a possible automatic location algorithm,” Cold Regions Sci. Technol., vol. 51, no. 2/3, 2008, pp. 178-190.

[14] F. Fruehauf, A. Heilig, M. Schneebeli, W. Fellin, and O. Scherzer, “Experiments and algorithms to detect snow avalanche victims using airborne ground-penetrating radar, “IEEE Trans. On Geoscience and Remote Sensing, vol. 47, no. 7, 2009, pp. 2240-2251.

Chapter I.3

Electromagnetic Wire-Grid Modelling for Ground Penetrating Radar Applications

Introduction

This chapter focuses on the electromagnetic wire-grid modelling of metallic cylindrical objects buried in the ground or embedded in a structure. In utility detection, quality controls of reinforced concrete, and many other GPR applications, the sought targets often are long and thin: in these cases, two-dimensional methods can be employed to model the scenario and solve the electromagnetic scattering problem. In this chapter, all the results are obtained by using GprMax2D [2], a well-known freeware tool implementing the Finite-Difference Time-Domain (FDTD) method.

Wire-grid modelling of conducting objects was introduced by Richmond in 1966 [3] and, since then, the method has been extensively used over the years to simulate arbitrarily-shaped objects and compute radiation patterns of antennas, as well as the electromagnetic field scattered by targets. For any wire-grid model, a better accuracy can be achieved with a larger number of wires; moreover, a fundamental question is the choice of the optimum wire radius and grid spacing. The most widely used criterion to fix the wire size is

the so-called equal-area rule (EAR) [3, 4]: the total surface area of the wires has to be equal to the surface area of the object being modelled. This rule comes from empirical observation and few authors have investigated its reliability for 2D objects through the years. Ludwig [4] studied the reliability of the rule by examining the canonical radiation problem of a transverse magnetic field by a circular cylinder in a vacuum, fed with a uniform surface current and compared with a wire-grid model; he concluded that the EAR is optimum and that too thin wires are just as bad as too thick ones. Paknys [5] investigated the accuracy of the rule for the modelling of a circular cylinder in a vacuum with a uniform current on it, continuing the study initiated in [4], or illuminated by a transverse magnetic monochromatic plane wave; he confirmed that the EAR is optimum and observed that the field inside the cylinder is most sensitive to the wire radius than the field outside the object. In [6], a circular cylinder was considered, embedded in a dielectric half-space and illuminated by a transverse magnetic monochromatic plane wave; the scattered near field was calculated by using the Cylindrical-Wave Approach (CWA) [7] and numerical results, obtained for different wire-grid models in the spectral domain, were compared with the exact solution; it was shown that more accurate results can be obtained with a wire radius shorter than what is suggested by the rule. More recently, both the acoustic and electromagnetic scattering problems by a periodic configuration of N wires distributed on a ring, modelling a circular cage, were studied [8]; it was demonstrated that, as N goes to ∞, the solution of the limiting problem is approached very slowly, as (N−1) log N.

1. FDTD Modelling of Cylindrical Objects

Several methods can be employed, to solve electromagnetic forward-scattering problems. One of the most versatile approaches is the well-known FDTD technique [11], based on a spatial and temporal discretisation of Maxwell's curl equations in differential form, commonly within a rectilinear Cartesian grid as originally proposed by Yee [12] in 1966. As mentioned in the introduction, the results presented in this chapter are obtained by using GprMax2D [2], a freeware FDTD tool for 2D numerical modelling, developed by Prof. A. Giannopoulos. In our simulations, the physical structure of the transmitter and receiver is not included in the model: the source is represented through a line of current, as a consequence of the assumption of the invariance of the problem in one direction, and the electric field impinging on the receiver is calculated. A first derivative of Gaussian pulse is emitted by the source, with 1 GHz centre frequency. All the involved media are assumed to be linear and isotropic, possibly lossy, and their constitutive parameters do not vary with frequency; metallic objects are assumed to be perfectly-conducting. In order to keep the errors associated with numerical-induced dispersion at a minimum, the spatial discretisation step is always at least ten times smaller than the smallest wavelength of the propagating electromagnetic fields; the highest frequency to be taken into account in the simulations is estimated as three times the center frequency of the pulse. To limit the effects of staircase approximation of continuous objects, circular cylinders are modeled by discretising their radius through at least twenty cells. Another crucial point in the FDTD approach is the approximation to be made in order to limit the computational space: to guarantee reliable results, we adopt Perfectly-Matched Layer boundaries as Absorbing Boundary Conditions, which are very effectively implemented in GprMax2D; we use ten

layers and put source and targets at least fifteen cells away from the most internal layer.

2. Numerical results

2.1 Accurate wire-grid modelling of objects buried in a soil

A perfectly-conducting circular cylinder is considered, embedded in a dielectric half-space representing a soil, as sketched in Figure 1a. The source is positioned at the air-soil interface and the emitted electric field is parallel to the target axis. The relative permittivity of the soil is $\varepsilon_r = 4$. The radius of the cylinder is R = 50 mm, its axis is in x = 250 mm, y = 100 mm. A wire-grid model of the object is shown in Figure 1b: it consists of N = 16 circular-section cylinders with radius r, arranged in a uniformly-spaced circular array. The best position for the wires is with axes lying on the surface of the cylinder to be modeled [6]; with a larger N, the behaviour of the array gets closer to that of the modelled object [7]. Our aim is to investigate the validity of the EAR. In our case, the rule imposes the condition r = R/N = 3.125 mm has to be satisfied. The good reliability of this criterion is apparent by the results shown in Figures 1c-1f. In particular, in Figures 1c and 1d, the B-scans obtained for the circular cylinder and its wire-grid model are presented, respectively. In Figures 1e and 1f, electric-field maps calculated in t = 2.2 ns are shown, for the circular cylinder and its wire-grid model (being t = 0 the time instant in which the source starts to emit the pulse). Here and in the following, according to a nomenclature widely accepted by the GPR community, the term 'A-scan' refers to an array of electric-field values calculated in a fixed spatial point and in T consecutive instants (a GPR trace); the term 'B-scan' corresponds to a matrix of electric-field values, calculated in T time instants and M different spatial points, meaning M A-scans (this is equivalent to assuming that a GPR 'stops' in M positions, for example along a line parallel to the air-soil interface,

gathering data in each of them; the B-scan is the comprehensive set of GPR traces). The B-scans presented in Figures 1c and 1d are obtained by shifting the source in M = 80 positions equally-spaced along the air-soil interface; the electric field is calculated on the interface at a distance d = 50 mm from the source. Small differences can be appreciated, between the results relevant to the circular-section cylinder and its wire-grid model: mainly, the array of wires causes the presence of a higher number of minor reflections. The electric-field maps in Figures 1e and 1f are calculated by putting the source in x = 240 mm, y = 250 mm. They reveal that the internal field is much more sensitive to the modelling configuration than the external one, in good agreement with [6]. In fact, the field inside the array of wires is not vanishing in Figure 1f; this suggests that more wires should be employed, when shielding effects are concerned. Despite the well-known rule of thumb yields good results, it can be verified that is far from being the optimum. In Figure 2a, results are shown for the same configuration as in Figure 1b, for various lengths of the wire radius, equal to, shorter, and longer than R/N. In particular, the absolute error on A-scans is plotted, defined as the magnitude of the difference between the exact A-scan (calculated in the presence of the circular cylinder) and the A-scan obtained for the wire-grid model.

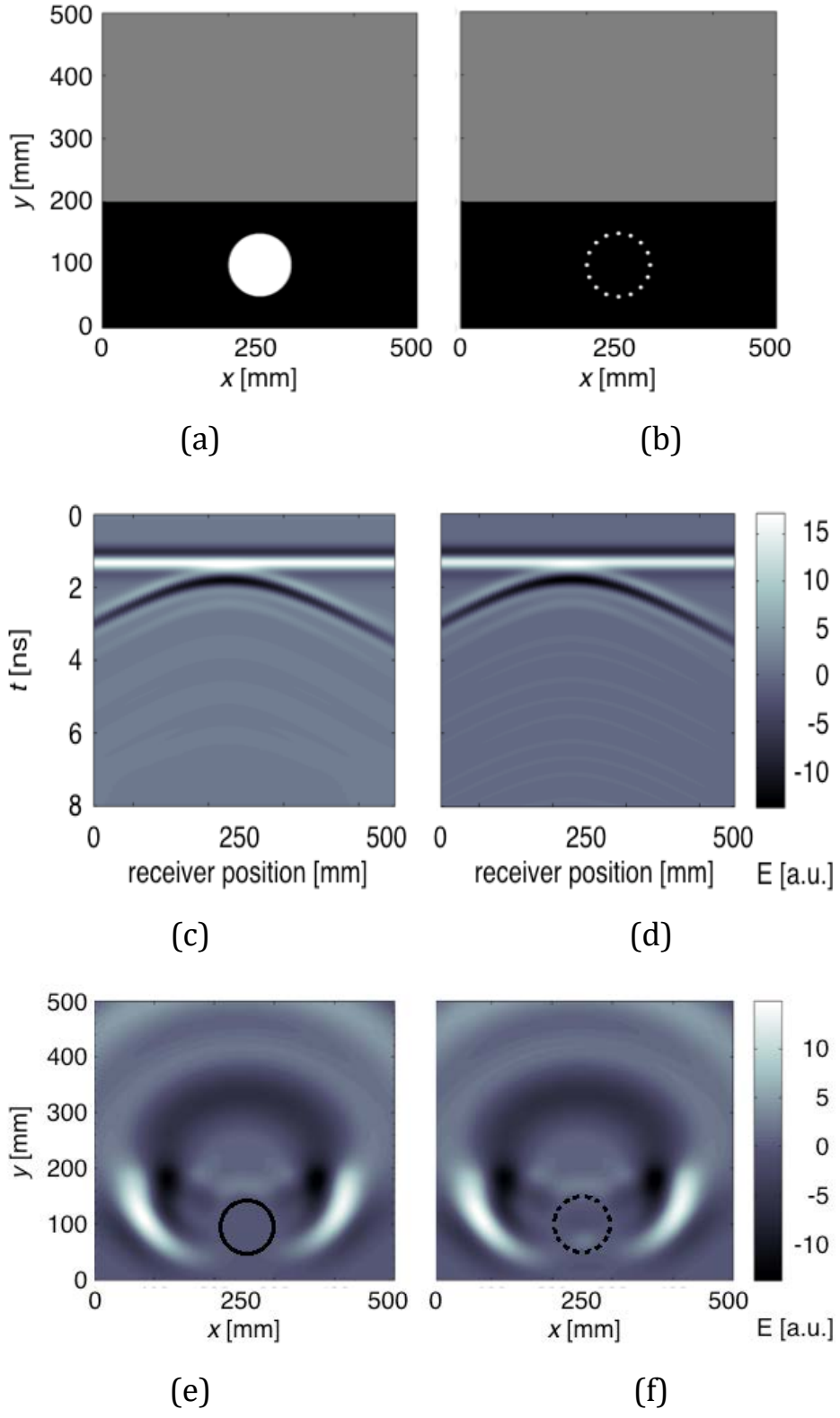

Fig. 1 – (a) and (b) geometry of the problem, (c) and (d) B-scans obtained for the circular cylinder, (e) and (f) electric-field maps for the circular section cylinder and its wire-grid model.

The source is in x = 240 mm, y = 250 mm and the field is computed in x = 250 mm, y = 250 mm. With a wire radius longer than the value suggested by the EAR, worse results are obtained; the lowest error is achieved when r = 0.9R/N. A refinement of this analysis is presented in Figure 2b: it can be noted that a shortening of about 12%, with respect to the well-known rule of thumb, gives the best results (the error is reduced of about one order of magnitude). In Figure 3, the same as in Figure 2 is reported, when N = 32. The error is slightly lower than when N = 16, as expected. The highest accuracy is achieved by shortening the radius of about 13%. Changing the radius of the modelled object and keeping fixed the size of the wires, or varying the object burial depth, we obtained analogous results. We now investigate whether similar results are obtained for a buried object with a different shape. To this aim, we consider a perfectly-conducting square-section cylinder, embedded in a dielectric half-space, as sketched in Figure 4a. The relative permittivity of the soil is again ε_r= 4. The side-length of the square is L = 100 mm, the axis is in x = 250 mm, y = 100 mm. A wire-grid model of the object is shown in Figure 4b: it consists of an array of N = 16 circular-section cylinders, with a spacing equal to 0.25L. To respect the EAR, the condition r = 2L/Nπ ≈ 3.979 mm has to be satisfied. In Figures 4c and 4d, B-scans obtained for the square-section cylinder and its wire-grid model are presented, respectively. In Figures. 4e and 4f, electric-field maps calculated in t = 2.2 ns are shown, for both the circular cylinder and its wire-grid model, when the source is in x = 240 mm, y = 250 mm. These results are in agreement with Figure 1; similar comments apply. In Figure 5, the absolute error on A-scans is shown. The source is in x = 240 mm, y = 250 mm, the field is computed in in x = 250 mm, y = 250 mm. With a wire radius longer than what was suggested by the EAR, worse results are obtained. A shortening of about 13-15%, instead, gives the best results. A general guideline for wire-sizing can be extracted, suggesting that the same-

area criterion is affordable, but a higher accuracy can be achieved with wires smaller than what suggested by the rule. A shortening of about 12-15 % is recommended.

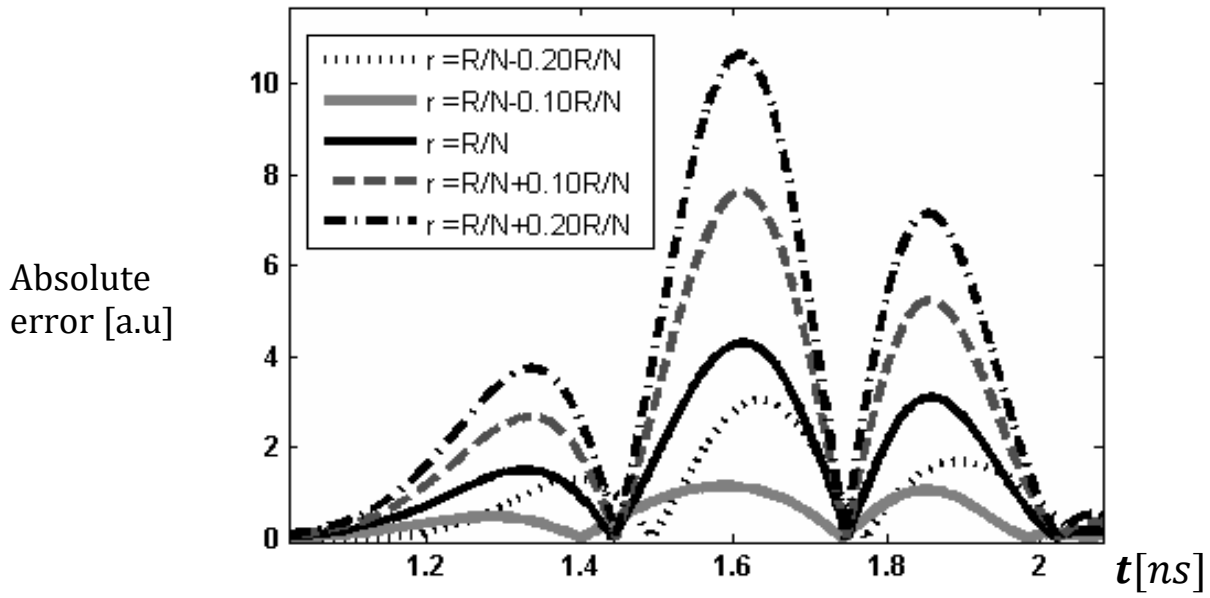

(a)

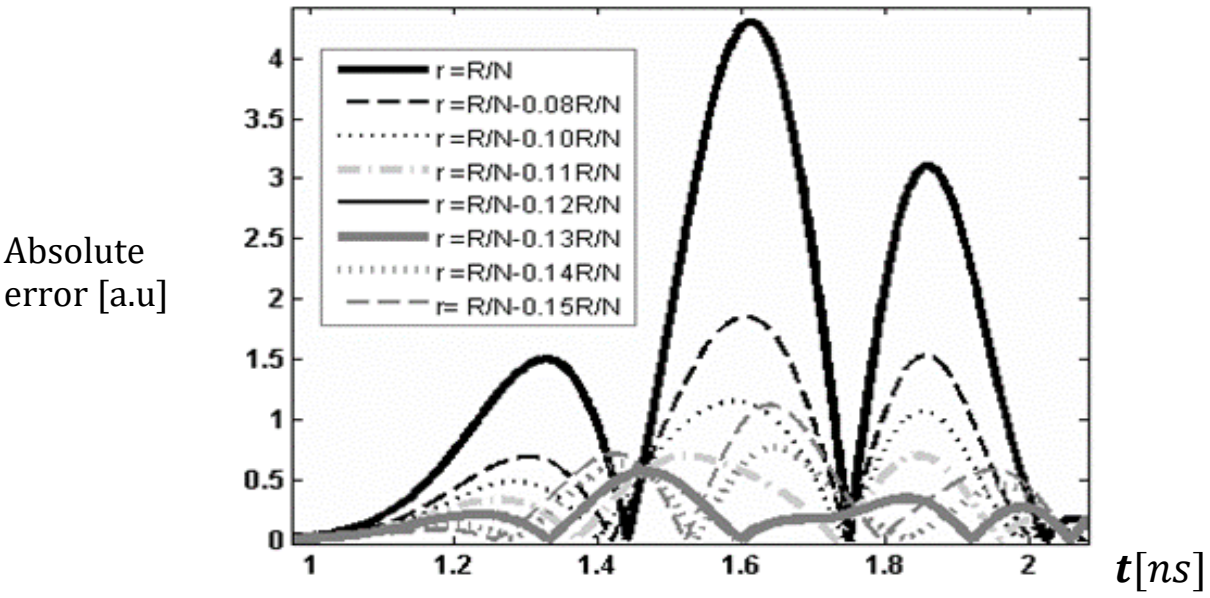

(b)

Fig. 2 – (a) Absolute error on A-scans, with N = 16 and for various lengths of the wire radius; (b) refinement of the analysis presented in (a).

2.2 Objects partially buried in different media

This sub-section deals with the simulation of objects partially buried in different media of a multilayered soil or structure. The considered scenario is depicted in Figure 6a: the upper half-space is a vacuum, the intermediate slab has a relative permittivity $\mathcal{E}_{r1}$ = 4 and is 300 mm thick, the lower half-space has a relative permittivity $\mathcal{E}_{r2}$ = 15. A perfectly-conducting circular cylinder is partially embedded in both the upper half-space and finite-thickness slab; the radius is R1 = 50 mm and the axis is in x = 250 mm, y = 780 mm. A larger cylinder is embedded in both the slab and lower half-space; the radius is R2 = 100 mm and the axis is in x = 600 mm, y = 500 mm. Both the cylinders are modeled by means of their equivalent wire-grid models, with N = 16; the wire radius is shortened of 13% with respect to the value suggested by the EAR. The B-scan presented in Figure 6c is obtained by shifting the source in M = 50 positions along a line parallel to the vacuum-slab interface, in y = 90 mm; the electric field is calculated on the same line at a distance d = 10 mm from the source. The aim of this example is just to remind and underline an interesting application of the wire-grid modelling: it allows to simulate partially-buried objects by using methods that cannot deal with geometries involving overlapping sub-domains, as the CWA.

2.3 Slotted objects

This sub-section deals with wire-grid modelling of slotted objects. In Figure 7a, the geometry of a perfectly-conducting slotted cylinder is shown: its radius is R = 50 mm, the axis is in x = 250 mm, y = 250 mm, the slot-length is πR/4, and the object is 2 mm thick. Figure 7b shows a wire-grid model of the object. The relative permittivity of the hosting half-space is $\mathcal{E}$r = 4. In Figure 8, A-scans calculated in x =250 mm, y = 450 mm are presented, for different values

of N; the exact curve is reported as reference. It can be noticed that the wire-grid models follow

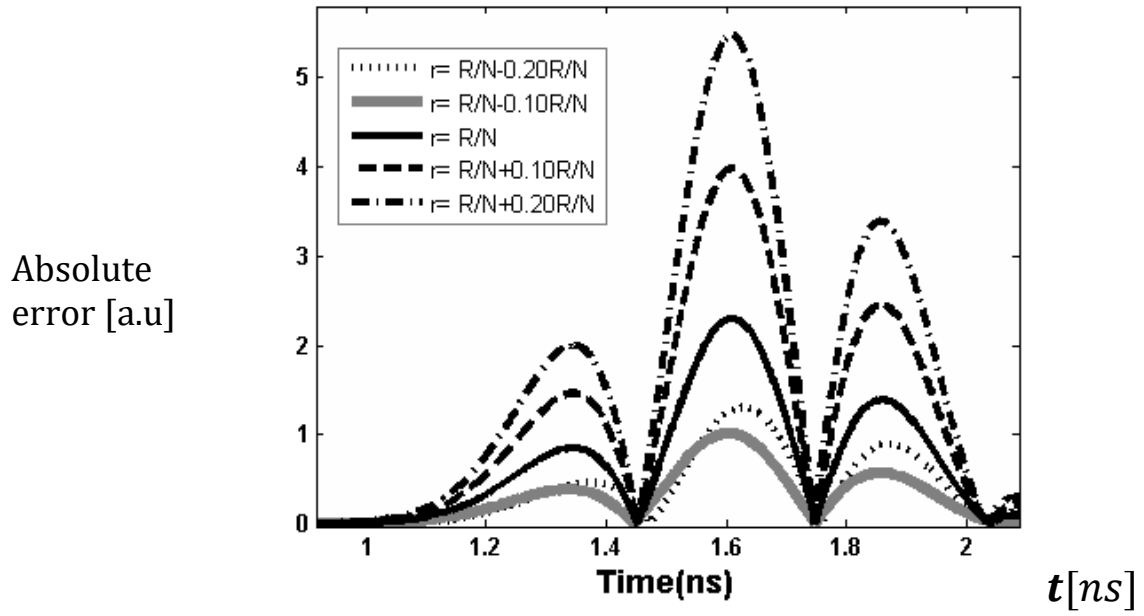

(a)

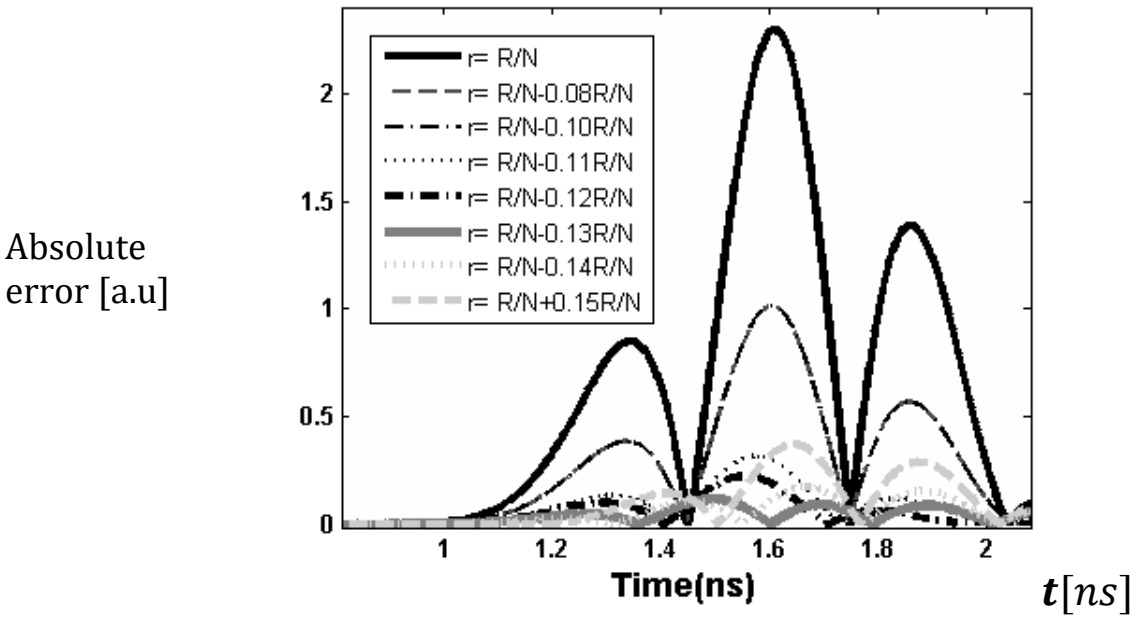

(b)

Fig. 3 – (a) Absolute error on A-scans, with N = 32 and for various lengths of the wire radius; (b) refinement of the analysis presented in (a).

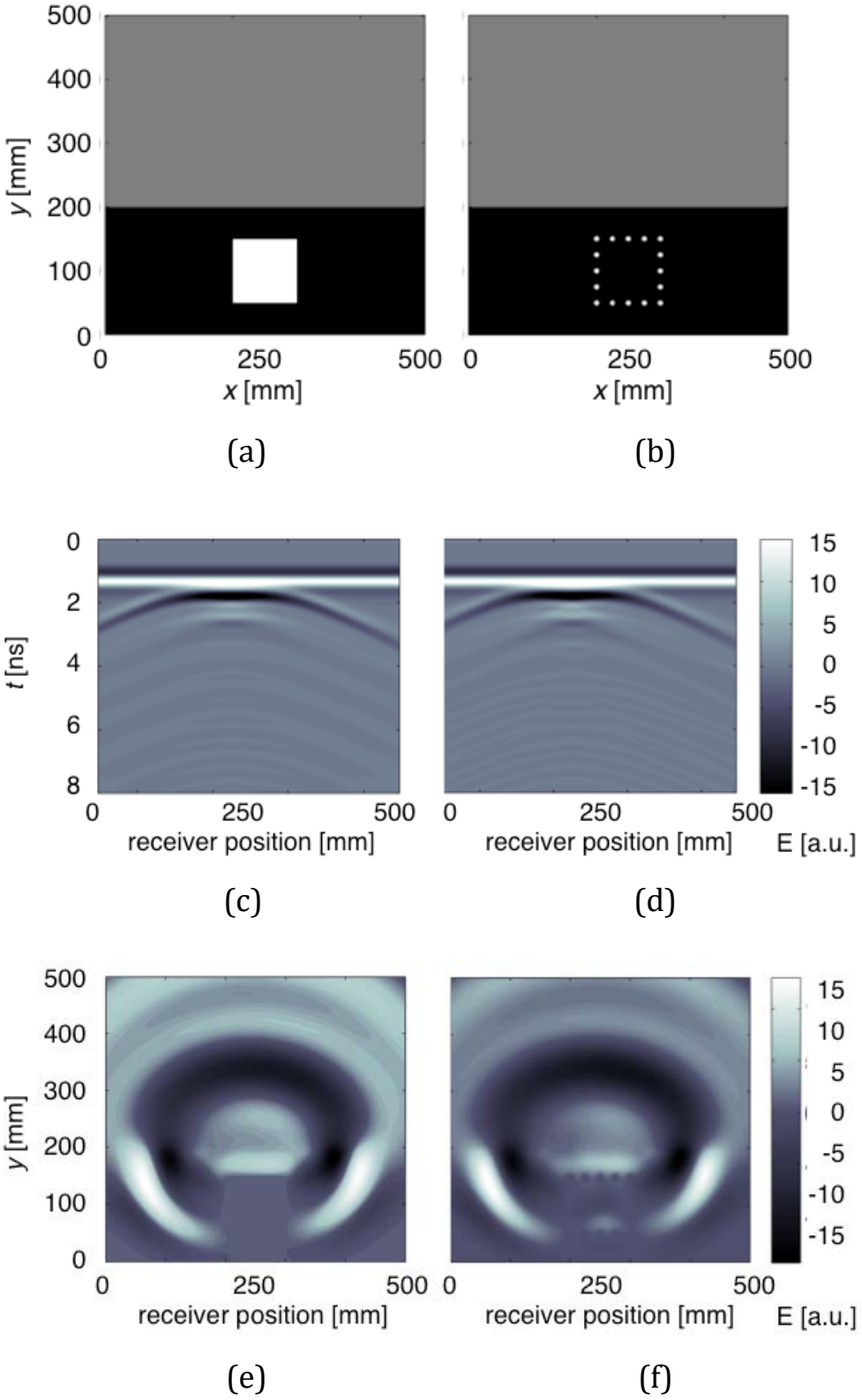

Fig. 4 – (a) Geometry of the problem; (b) B-Scans and (c) electric-field maps for the square-section cylinder and its wire-grid model.

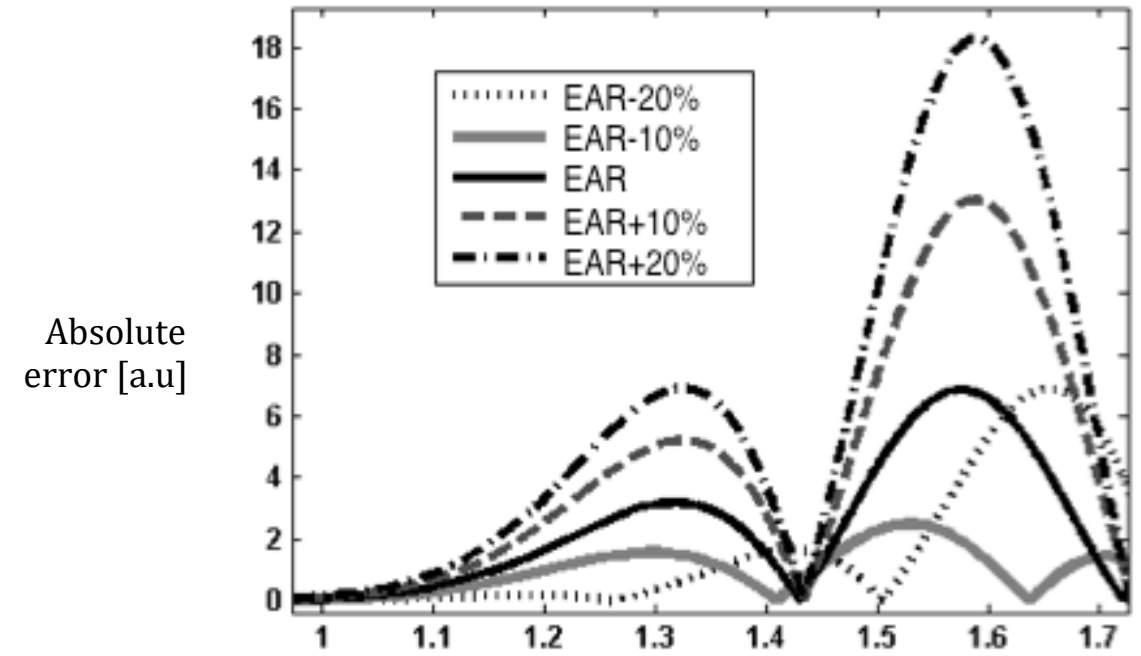

(a)

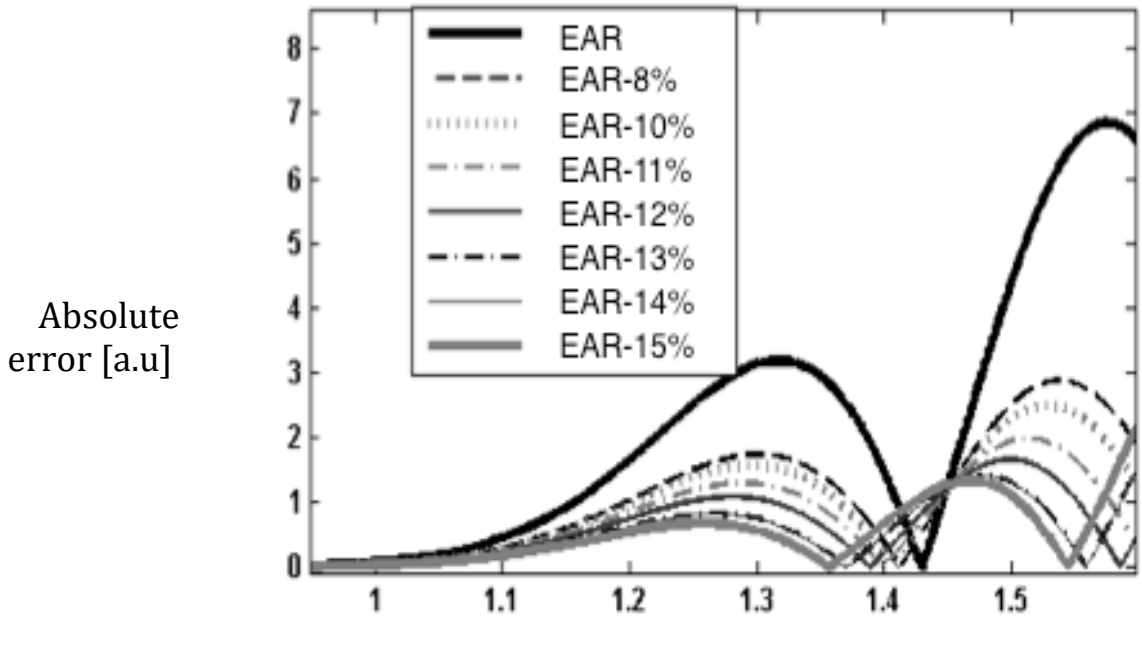

(b)

Fig. 5 – (a) Absolute error on A-scans, with N = 16 and for various lengths of the wire radius; (b) refinement of the analysis presented in (a).

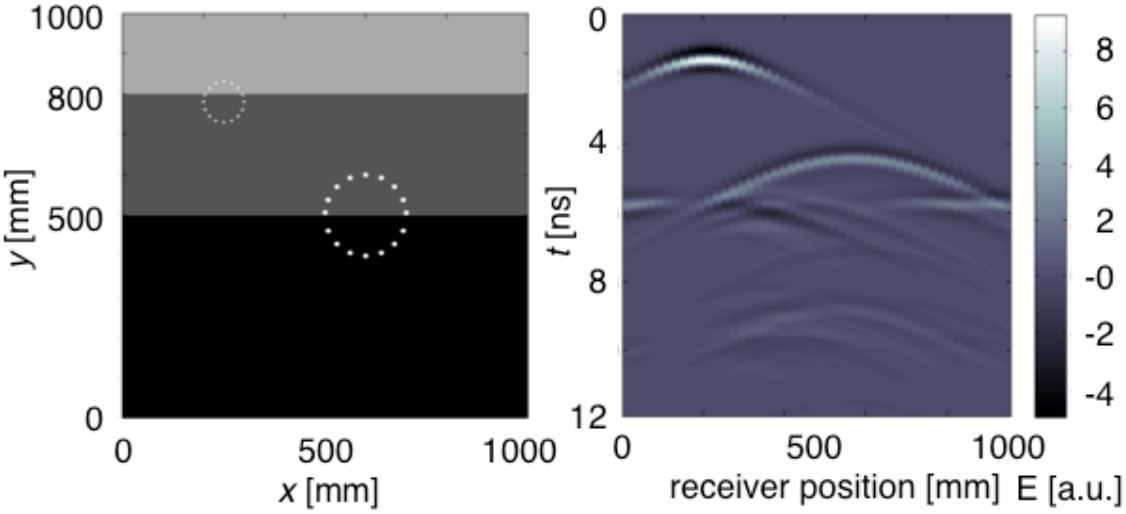

(a) (b)

Fig. 6 – (a) Geometry of the scattering problem for two partially buried cylinders, modelled with the wire-grid approach; (b) B-Scan.

the exact curve quite well for the first two reflections. However, the wire-grid reflections are delayed with respect to the exact ones, as if the slot was larger. The delay slightly reduces a larger N, for example the first reflection is delayed of 85, 75 and 70 ps when N = 16, 32 and 64, respectively.

We noticed that wire-grid results are much closer to exact results when the slot is longer. Moreover, we observed that in the presence of a short slot, as in Figure 7, the results are not much affected from the thickness of the object; for longer slots, instead, the thickness of the object has a stronger influence on the results and – in the wire-grid approach - more accurate results can be obtained by using two concentric arrays of wires, simulating both the inner and outer circle arcs of the object section.

This is an interesting topic that needs to be studied more in depth, in order to evaluate to what extent the wire-grid approach can be used for the modelling of slotted objects, and to extract simulation guidelines for this kind of geometries.

Conclusions

This chapter focused on the wire-grid modelling of buried cylindrical objects. Numerical results were obtained by using GprMax, a freeware and versatile tool implementing the Finite-Difference Time-Domain technique. We investigated the reliability of the well-known equal-area rule, showing that it yields affordable results but is quite far from being the optimum: higher accuracy can be achieved by using a wire radius 12-15% shorter than what is suggested by the rule. We considered circular-and square-section scatterers embedded in a half-space, in the presence of a line of current emitting an ultra-wide band pulse. Our results are in good agreement with [6], where the wire-grid modelling of a circular-section cylinder illuminated by a monochromatic plane wave was studied and preliminary spectral-domain results were presented, calculated by using the Cylindrical-Wave Approach.

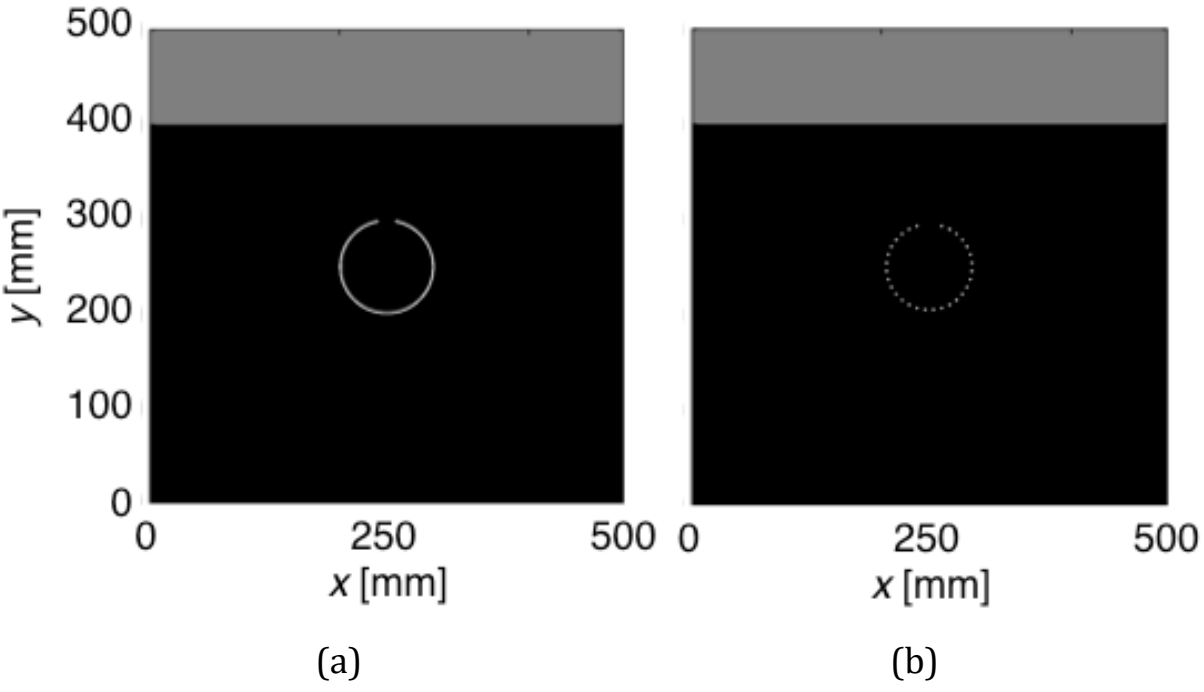

Fig. 7 – (a) Geometry of the scattering problem for a slotted cylinder (b) wire-grid model of (a), with 32 wires.

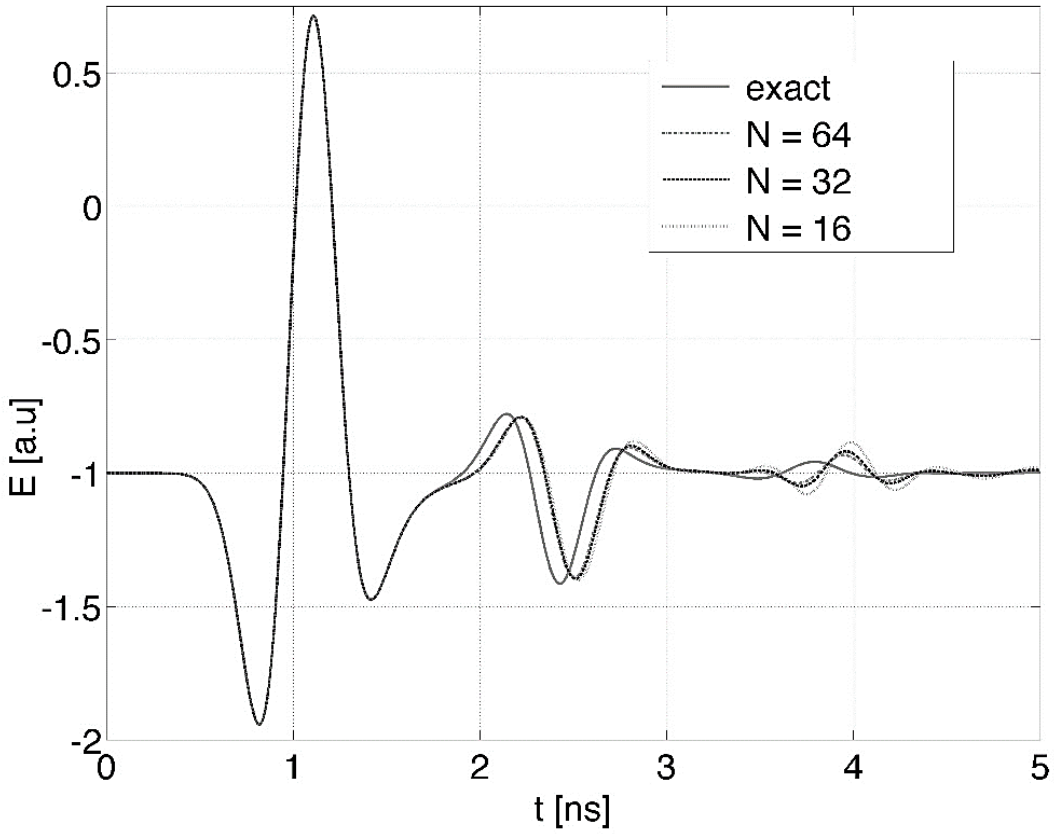

Fig. 8 – A-scan for the slotted cylinder and its wire-grid model.

Subsequently, we considered the wire-grid modelling of objects partially buried in different layers of a soil or structure. The aim of the reported example was to highlight that the wire-grid approach can significantly enhance the versatility of methods that can deal only with scatterers embedded in a homogeneous material. Finally, we investigated the wire-grid modelling of circular-section slotted objects and presented preliminary results. For small slots, the wire-grid results follow quite well the main reflections of the exact results, but with some delay. More accurate results are obtained in the case of larger slots. To model thick objects with large slots, it is recommended to use two concentric arrays of wires, simulating both the inner and outer circle arcs of the scatterer section.

This analysis is of particular interest for the electromagnetic simulation of

Ground Penetrating Radar scenarios. It may also be useful for shielding applications [13], and in the measurement of electromagnetic properties of materials through the use of coaxial cages [14].

References

[1] D. J. Daniels, "Ground Penetrating Radar," Institution of Engineering and Technology, 2nd ed., 2004.

[2] A. Giannopoulos, "Modelling ground penetrating radar by GprMax," Construction and Building Materials, vol. 19, 2005, pp. 755–762.

[3] J. H. Richmond, "A wire-grid model for scattering by conducting bodies," IEEE Trans. Antennas Propagat., vol. 14, 1966, pp. 782–786.

[4] A.C. Ludwig, "Wire grid modeling of surfaces," IEEE Trans. Antennas Propagat., vol. 35, 1987, pp.1045–1048.

[5] R.J. Paknys, "The near field of a wire grid model," IEEE Trans. Antennas Propagat., vol. 39, 1991, pp. 994–999.

[6] F. Frezza, L. Pajewski, C. Ponti, G. Schettini, "Accurate wire-grid modelling of buried conducting cylindrical scatterers," Nondestructive Testing and Evaluation, vol. 27, 2012, pp. 199–207.

[7] M. Di Vico, F. Frezza, L. Pajewski, G. Schettini, "Scattering by a finite set of perfectly conducting cylinders buried in a dielectric half-space: a spectral-domain solution," IEEE Trans. Antennas Propagat., vol.53, 2005, pp. 719–727.

[8] P. A. Martin, "On acoustic and electric Faraday cages," Proc. Royal Society, vol. 470, 2014, 20140344.

[9] X. B. Xu, C. M. Butler, "Scattering of TM excitation by coupled and partially buried cylinder at the interface between two media," IEEE Trans. Antennas Propagat., vol.35, 1987, pp. 529–538.

[10] M. Zampolli, A. L. Espana, K. L. Williams, P. L. Marston, "Low- to mid-frequency scattering from submerged targets partially buried in the sediment at an oblique angle," J. Acoustical Society Am., vol. 131, 2012, pp. 3393-3393.

[11] A. Taflove, "Computational Electrodynamics: The Finite-Difference Time-Domain Method," Artech House, 1995.

[12] K. Yee, “Numerical solution of initial boundary value problems involving Maxwell’s equations in isotropic media,” IEEE Trans. Antennas Propagat., vol.14, 1966, pp. 302–307.

[13] S. Celozzi, R. Araneo, G. Lovat, “Electromagnetic shielding,” Wiley-IEEE Press, 2008.

[14] E. Mattei, S. E. Lauro, E. Pettinelli, G. Vannaroni, “Coaxial-Cage Transmission Line for Electromagnetic Parameters Estimation,” IEEE Trans. Instrumentation and Measurements, vol. 62, 2013, pp. 2938-2942.

Part II

Electromagnetic techniques for the evaluation of the dielectric permittivity of media

Chapter II.1

Measurement System for Evaluating Dielectrics Permittivity of Granular Materials in the 1.7-2.6 GHz Band

Introduction

The development of dielectric spectroscopy techniques, with particular emphasis on those operating in the microwave frequency range, has attracted an increasing interest in the last few years [1]. Such techniques permit measurement of the frequency-dependent complex permittivity of a material sample. Knowledge of this quantity can prove useful for quality-control purposes [2], [3] or for understanding the interaction of the material with an electromagnetic wave and the corresponding heating effect [4]. A specific field of application of microwave heating, especially at the 2.45-GHz industrial, scientific and medical (ISM) frequency, is road maintenance [5]. Indeed, by heating the asphalt concrete through the use of microwaves, it is possible to perform on-site repairs of holes or cracks present on the road surface. Still, microwaves might even be employed in the production stage of the asphalt concrete, as a substitute to conventional ovens currently exploited for drying and heating the mineral aggregates, which are subsequently bound together with asphalt. Microwave heating might also help for the recycling process of

reclaimed asphalt pavement. Mineral aggregates used inside the asphalt concrete mixture have different sizes, typically ranging from less than 1 up to 25 mm in diameter. They are obtained from basalt or calcareous rocks. In the final concrete, they are bound together by asphalt (or bitumen), which is usually refined from petroleum. The key data needed for studying the feasibility of a microwave system for asphalt concrete production or recycling are the complex permittivities of the concrete components (asphalt and mineral aggregates) and the concrete itself. Therefore, an accurate system suitable to perform complex permittivity measurements around 2.45 GHz on both compact and granular materials is needed. The most common solutions in this frequency range exploit open-ended coaxial probes [6], whose tip is placed in contact with the material [7]. However, such systems are not suitable to perform measurements on granular materials and have a sensitive area that is definitely too small to allow a correct characterization of asphalt concrete, which is a mixture whose granular components can also be several tens of millimeters in diameter. To overcome such limitation, transmission/reflection solutions can be adopted, where the material is placed inside a suitable section of transmission line [8]. However, currently, implemented systems are based on a coaxial structure [9], [10] and operate in a frequency region well below the ISM band at 2.45 GHz. On the other hand, the most widespread waveguide measurement systems are based on the WR90 standard waveguide, allowing measurements in the 8–12-GHz band (X-band).

In this chapter, the design and the metrological characterization of a waveguide system, suitable to perform complex permittivity measurements on material samples of

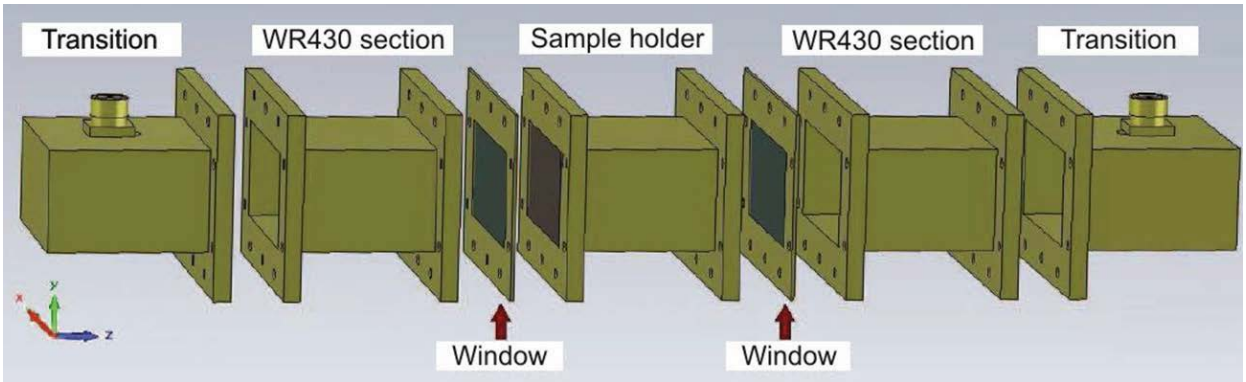

(a)

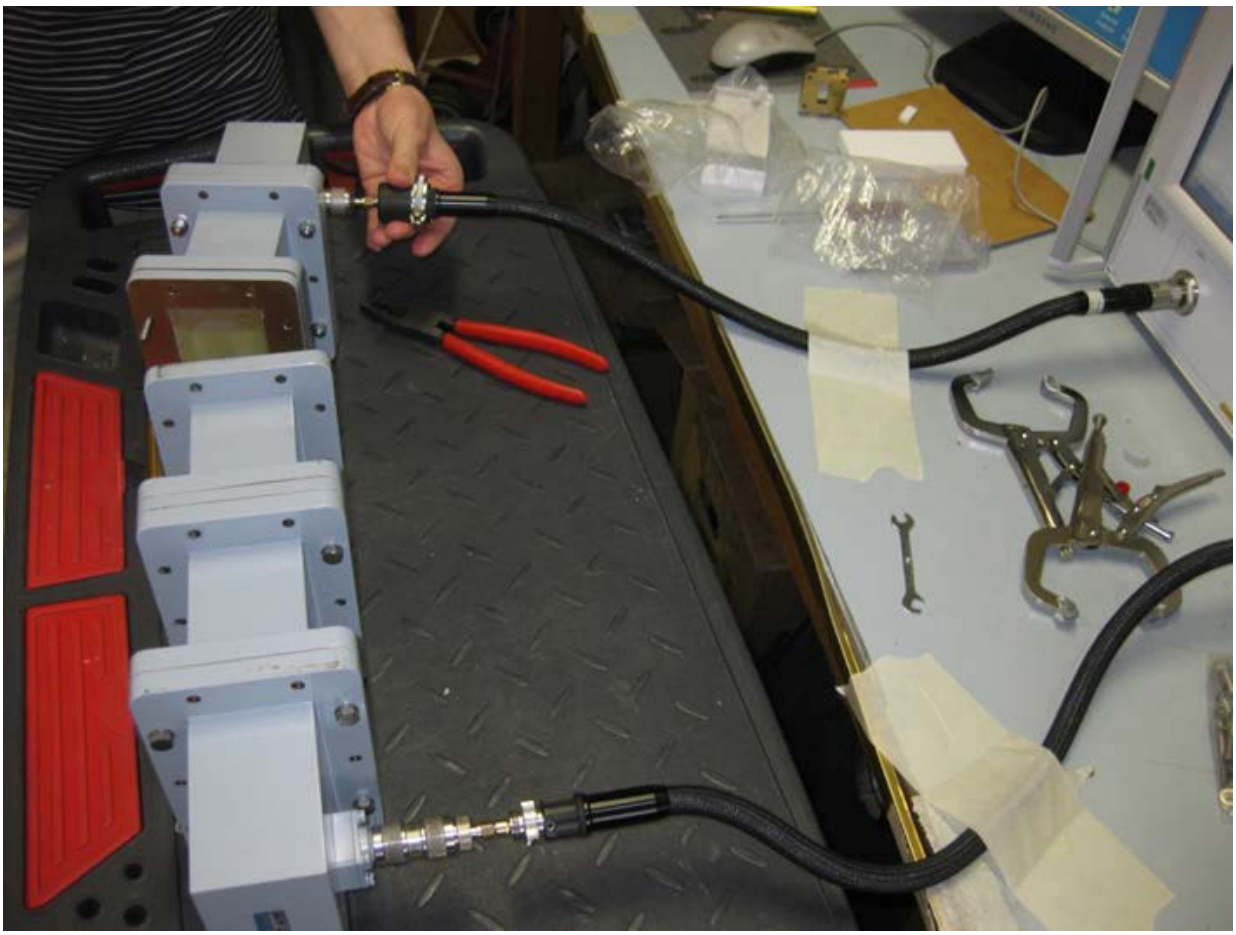

(b)

Fig. 1 – (a) Sketch and (b) picture of the WR430 measurement system.

adequate size, are presented. The system is developed with the aim of providing an accurate and affordable solution for measurement on granular and compact materials in the frequency range around 2.45 GHz.

1. Design of the waveguide system

As reported in [11], the design goal of achieving a permittivity measurement system suitable to characterize adequately sized material samples (possibly granular), suggested the use of a transmission/reflection system based on rectangular waveguides. Among the different standardized waveguides, the WR430 waveguide, spanning the 1.7–2.6-GHz region, was used. The choice of this waveguide over other standard waveguides with partially overlapping operating frequency range (i.e., the WR340) was due to its larger cross-sectional dimensions (approximately 109 mm × 55 mm), thus accommodating samples with sufficient volume to accurately characterize the asphalt concrete mixture and components. The whole system was designed through electromagnetic full-wave simulations, performed employing Computer Simulation Technology (CST) Microwave Studio software. A sketch of the designed system is shown in Fig. 1a. The system is composed of a couple of coaxial (N-type) to rectangular waveguide (WR430) transitions; two standard WR430 waveguide sections (long enough to ensure that higher order modes are sufficiently damped); and a sample holder, 10 cm in length. Typically, waveguide systems are employed for measurements on solid and compact materials, which can be cut in a parallelepiped shape and inserted in the sample holder. However, one of the goals of the proposed measurement system is the characterization of granular materials (such as the mineral aggregates). Therefore, to allow the insertion of granular samples in the sample holder, two pressurization windows were added, directly connected to the sample holder ends, which are filled by epoxy and confine the material inside the holder. The windows are designed so as to bear up to 1 kg of material. Due to the presence of the epoxy dielectric, a shunt capacitive load is added to the waveguide, thus creating an impedance-mismatch effect. Even

though this can be compensated for through standard vector error correction procedures, the windows were equipped with a printed inductive copper iris. Such an iris, typically realized through two thin rectangular metal patches protruding from the narrow walls of the waveguide (so as to reduce its effective width), is designed to provide a shunt inductance able to cancel, through resonance, the capacitive mismatch at the target frequency of 2.45 GHz [12]. To slightly enlarge the matching bandwidth, the iris was designed with an elliptically shaped (rather than straight) contour, whose eccentricity was optimized through specific electromagnetic simulations. The whole structure is made of brass, with copper-plated inner walls. To make the system practically usable for performing reflection/transmission measurements with a vector network analyzer, it is necessary to apply the vector error correction procedure at the sample holder ports [13]. Such procedure permits compensation for most of the systematic errors and requires a specific calibration kit. The most simple calibration standards to be employed for waveguide systems are the short circuit (i.e., a metallic end plate) and a waveguide section of known length (typically equal to one-fourth of the wavelength computed in the middle of the operating frequency band). This set of standards accommodates the thru-reflect-line (TRL) vector error correction procedure. Fortunately, there are several waveguide calibration kits available on the market; however, to the best of authors' knowledge, none of them is suitable for the WR430 waveguide format. Therefore, the short circuit and waveguide section standards were built as part of the whole project. Starting from their geometrical and electrical characterization, a custom model for the developed calibration kit was implemented and added to the network analyzer data base [14].

2. Measurement model and uncertainty

In transmission/reflection measurements, the sample is placed inside the waveguide and an electromagnetic wave is launched at the waveguide port. By measuring the scattering parameters at the waveguide ports, it is possible to retrieve the complex permittivity of the sample through an appropriate measurement model. Historically, the first works that proposed permittivity measurements with the transmission/reflection technique date back to the mid-20th century [15]–[17]. However, it was only in the early 1970s that a new model was developed in [18] and further optimized in [19]: such model, known as Nicolson–Ross–Weir (NRW), accurately operates only at frequencies far from the sample resonances, which occur whenever the sample length becomes an integer multiple of half wavelength computed inside the sample. An alternative model for evaluating the complex permittivity of the sample, starting from the measured scattering parameters, has been developed by the National Institute of Standards and Technology (NIST) [8], [20]: such a model employs a mathematical formulation that largely limits errors related to sample resonances. In this chapter, measurements were performed using an Agilent E8363C vector network analyzer, equipped with Agilent 85071E permittivity measurement software [21]. In particular, this software provides different measurement models, including the aforementioned NRW and NIST models. The measurement results reported herein have been obtained employing the NIST model, which has been proved to be the most accurate for nonmagnetic materials, like the ones of interest for this chapter.

2.1 Uncertainty Contributions

A theoretical evaluation of permittivity measurement uncertainty for the NIST model can be found in [8] and [20]. Applying such evaluation to the proposed system, the following main uncertainty contributions can be identified: 1) uncertainty in scattering parameters; 2) air gaps between sample and holder; 3) dimensional uncertainty in the sample holder; 4) uncertainty in sample length; and 5) uncertainty in the exact sample positioning inside the holder. In measurements on solid and compact materials, many of these contributions were made negligible thanks to the chosen mechanical tolerances in the system realization and to the accurate milling of the material samples. Therefore, the main remaining contributions are likely those related to scattering parameters and to the sample length. In particular, the uncertainty in sample length is mainly the result of the imperfect planarity of the sample surface, especially for pliable materials. Exploiting the results reported in [8] for the sensitivity coefficients, using uncertainty figures taken from the network analyzer datasheets for scattering parameter measurements, and assuming a worst case uncertainty of 0.05 mm in sample length (on the basis of the measured nonplanarity), the combined uncertainty on the real part of the measured permittivity is about 2% (average value over the entire frequency band). This result is in optimum agreement with typical uncertainty stated in the 85071E software specifications [21]. Clearly, for measurements on granular materials, some of the aforementioned uncertainty contributions may become more prominent. For example, the sample length is harder to be accurately evaluated. In addition, inhomogeneities in the sample may lead to the propagation of higher order modes. Higher order mode propagation, in particular, is responsible for a deterioration in the accuracy of scattering parameter measurements, which become affected by spurious oscillations. These artifacts on the scattering parameters can lead to an increased

uncertainty in estimated permittivity, especially around sample resonances, where the sensitivity coefficients for the NIST model tend to become rather large. However, as long as an average value of the permittivity is of interest, because no significant relaxation processes are expected in the measurement bandwidth, artifacts around sample resonances are not of great concern and should not decrease measurement accuracy in a significant way.

3. Experimental characterization of the proposed system

To characterize the presented WR430 custom system, measurements were performed on a set of different solid materials. Unfortunately, while for reference liquid materials, very accurate databases of permittivity are available [22], it is more complex to obtain reliable reference solid materials. Therefore, we used low-permittivity solid materials that are known to exhibit an extremely flat permittivity over the entire microwave frequency band. In this way, it was possible to validate the system through a comparison with measurements performed on the same materials employing a standard WR90 waveguide system operating between 8.2 and 12.4 GHz, and used as a reference. Indeed, the WR90 waveguide system is entirely based on commercial components (with the exception of the sample holder, realized with a milling machine with 0.005 mm repeatability), and it is an excellent candidate to be used as a reference for comparing the WR430 custom system measurements, thanks to its stated typical worst case uncertainty equal to 2% [21]. For the characterization of the system, the following materials were chosen: 1) low-density polyvinyl chloride; 2) polytetrafluoroethylene; 3) polymethyl methacrylate; and 4) polycarbonate. These test materials were chosen to satisfy the following criteria: 1) flat permittivity spectrum so as to allow a direct comparison between the results obtained with the WR430 and the WR90 systems; 2) low permittivity (real part less than 8), in order to

better represent permittivities of asphalt concrete main components; 3) ease of mechanical processing for preparing the parallelepiped samples. For each material, two different samples were machined (both taken from the same material block): 1) one to be inserted in the WR430 and 2) the other in the WR90 waveguides. The experimental setup for the WR430 measurement system is shown in Figure 1b. Measurements in both frequency bands were performed using the Agilent E8363C precision network analyzer (PNA). In all the measurements, the TRL error correction procedure was applied, thus compensating for possible nonidealities (such as spurious reflections, wall losses, and electrical delay introduced by the sample holder).

Table I – Values of the real part of the dielectric permittivity, as measured through the WR430 waveguide and the standard WR90 system, for the reference solid materials. the percentage difference is also reported

Material	$\varepsilon'_{m,WR430}$	$\varepsilon'_{m,WR90}$	$\%\Delta\varepsilon'_m$
LD-PVC	1.619	1.608	0.7%
PTFE	2.056	2.038	0.9%
PMMA	2.592	2.591	0.04%
PC	2.822	2.809	0.5%

Throughout the experimental session, the environmental temperature, monitored through a thermistor sensor, was within the (26.5±1.0) °C range. Table I summarizes the measurement results for the different material samples. In particular, for each tested material, the average value measured for the real part of the permittivity, throughout the entire frequency bandwidth, and the corresponding percentage differences are reported. The results obtained with the proposed WR430 and with the traditional WR90

systems are in good agreement; in fact, the percentage differences between the average permittivities measured through the two systems are below 1%.

References

[1] E. Piuzzi et al., "A comparative analysis between customized and commercial systems for complex permittivity measurements on liquid samples at microwave frequencies," IEEE Trans. Instrum. Meas., vol. 62, no. 5, pp. 1034–1046, May 2013.

[2] A. Cataldo, E. Piuzzi, G. Cannazza, E. De Benedetto, and L. Tarricone, "Quality and anti-adulteration control of vegetable oils through microwave dielectric spectroscopy," Measurement, vol. 43, no. 8, pp. 1031–1039, 2010.

[3] A. Cataldo, E. Piuzzi, G. Cannazza, and E. De Benedetto, Classification and adulteration control of vegetable oils based on microwave reflectom- etry analysis," J. Food Eng., vol. 112, no. 4, pp. 338–345, 2012.

[4] J. M. Osepchuk, "A history of microwave heating applications," IEEE Trans. Microw. Theory Techn., vol. 32, no. 9, pp. 1200–1224, Sep. 1984.

[5] R. G. Bosisio, J. Spooner, and J. Granger, "Asphalt road maintenance with a mobile microwave power unit," J. Microw. Power, vol. 9, no. 4, pp. 381–386, 1974.

[6] M. Adous, P. Quéffélec, and L. Laguerre, "Coaxial/cylindrical transition line for broadband permittivity measurement of civil engineering materials," Meas. Sci. Technol., vol. 17, no. 8, pp. 2241–2246, 2006.

[7] M. A. Stuchly and S. S. Stuchly, "Coaxial line reflection methods for measuring dielectric properties of biological substances at radio and microwave frequencies-A review," IEEE Trans. Instrum. Meas., vol. 29, no. 3, pp. 176–183, Sep. 1980.

[8] J. Baker-Jarvis, M. D. Janezic, J. H. Grosvenor, Jr., and R. G. Geyer, "Transmission/reflection and short-circuit line methods for measuring permittivity and permeability," NIST, Boulder, CO, USA, Tech. Note 1355-R, 1992.

[9] J. Q. Shang, "Effects of asphalt pavement properties on complex permittivity," Int. J. Pavement Eng., vol. 3, no. 4, pp. 217–226, 1999.

[10] J. Q. Shang, J. A. Umana, F. M. Bartlett, and J. R. Rossiter, "Measurement of complex permittivity of asphalt pavement materials," J. Transp. Eng., vol. 125, no. 4, pp. 347–356, 1999.

[11] E. Piuzzi et al., “Design and characterization of a measurement system for dielectric spectroscopy investigations on granular materials in the 2.45 GHz ISM band,” in Proc. IEEE Int. Instrum. Meas. Technol. Conf. (I2MT), Pisa, Italy, May 2015, pp. 734-738.

[12] N. Marcuvitz, Waveguide Handbook. New York, NY, USA: Dover, 1951. [13] “Applying error correction to network analyzer measurements,” Agilent Technol., Santa Clara, CA, USA, Appl. Note 1287-3, 2002.

[14] “Specifying calibration standards and kits for Agilent vector network analyzers,” Agilent Technol., Santa Clara, CA, USA, Appl. Note 1287-11, 2011.

[15] A. R. von Hippel, Ed., Dielectric Materials and Applications. New York, NY, USA: Wiley, 1954.

[16] M. Sucher and J. Fox, Eds., Handbook of Microwave Measurements. New York, NY, USA: Polytechnic Institute of Brooklyn, 1963.

[17] C. G. Montgomery, Ed., Technique of Microwave Measurements. Boston, MA, USA: Boston Technical Publishers, 1964.

[18] A. M. Nicolson and G. F. Ross, “Measurement of the intrinsic properties of materials by time-domain techniques,” IEEE Trans. Instrum. Meas., vol. 19, no. 4, pp. 377-382, Nov. 1970.

[19] W. B. Weir, “Automatic measurement of complex dielectric constant and permeability at microwave frequencies,” Proc. IEEE, vol. 62, no. 1, pp. 33–36, Jan. 1974.

[20] J. Baker-Jarvis, E. J. Vanzura, and W. A. Kissick, “Improved technique for determining complex permittivity with the transmission/reflection method,” IEEE Trans. Microw. Theory Techn., vol. 38, no. 8, pp. 1096-1103, Aug. 1990.

[21] “Materials measurement software: Technical overview,” Agilent Technol., Santa Clara, CA, USA, Tech. Rep. 85071E, 2012.

[22] A. P. Gregory and R. N. Clarke, “Tables of the complex permittivity of dielectric reference liquids at frequencies up to 5 GHz,” Nat. Phys. Lab., Teddington, U.K., Tech. Rep. MAT 23, 2009.

Chapter II.2

Experimental results on granular inert materials

Introduction

To test the performance of the proposed in chapter I, measurements were also carried out on typical materials used for asphalt, moistened at different water content levels. Finally, different dielectric mixing models were investigated and their suitability for the considered materials was verified.

1. Results on basaltic and calcareous materials

To test the suitability of the proposed WR430 system for dielectric spectroscopy investigations on asphalt materials, measurements were performed on two materials that are typically used in the asphalt industry: 1) calcareous and 2) basaltic aggregates. Both these materials were screened so as to obtain stones with a diameter ranging from 2 to 4 mm.

The total porosity (ϕ), defined as the total pore space per unit volume of granular material (including both air contained inside the single grains and air filling the empty spaces between grains) [23], was estimated as follows. A volume of dry material (V_{dry}) equal to the one required to fill the sample holder was placed in a container. Some water was placed in another container

and weighed with an electronic balance (W_b). The water was poured inside the material sample, until the material sample was filled with water. The remaining water was then weighed (W_f). The volume of the added water ($V_{a.w.}$) was evaluated as $(W_b - W_f)/\rho_{water}$, where ρ_{water} is the density of water. Finally, the porosity was estimated as $\phi = V_{a.w.}/ V_{dry}$ [24]. In this way, the ϕ values of the two materials were estimated to be ϕ_{calc} = 41.8% for the calcareous material and ϕ_{bas} = 49.3% for the basaltic material. The same samples used for estimating porosity were subsequently employed for permittivity measurements. For each material, the dielectric spectroscopy measurements were carried out as follows. Starting from the oven-dried material, the sample was moistened at progressively higher values of volumetric water content (θ_{ref})

$$\theta_{ref} = \left(\frac{V_w}{V_{dry}}\right) \times 100 \quad (1)$$

where V_w is the volume of the added water.

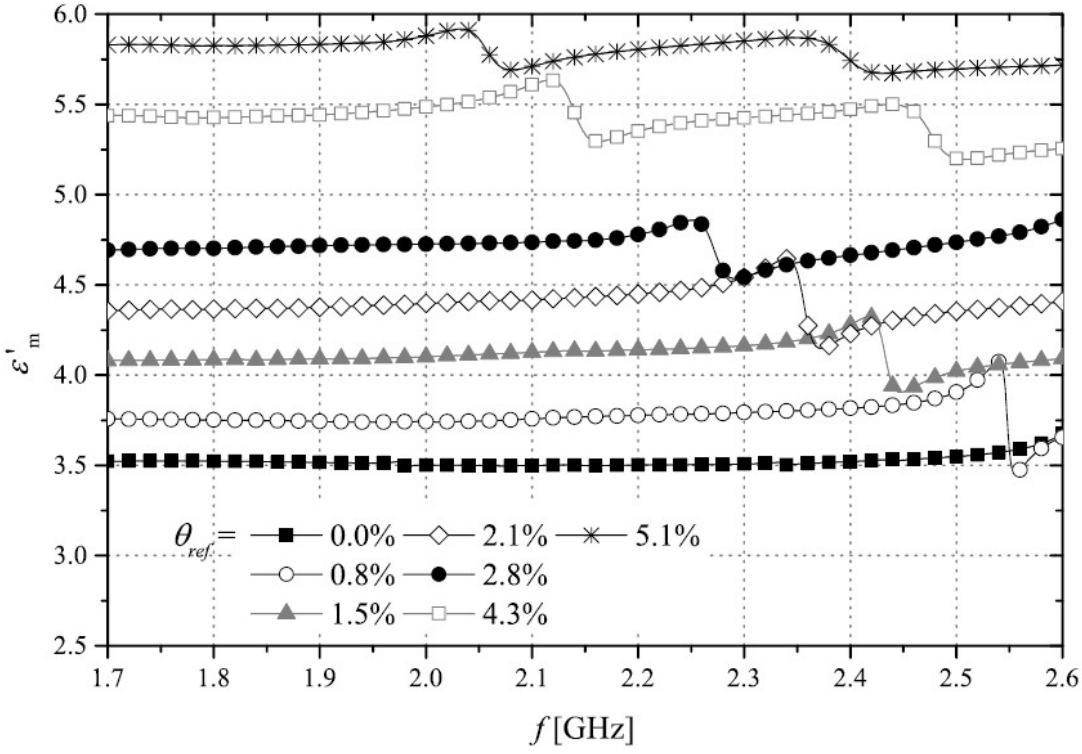

(a)

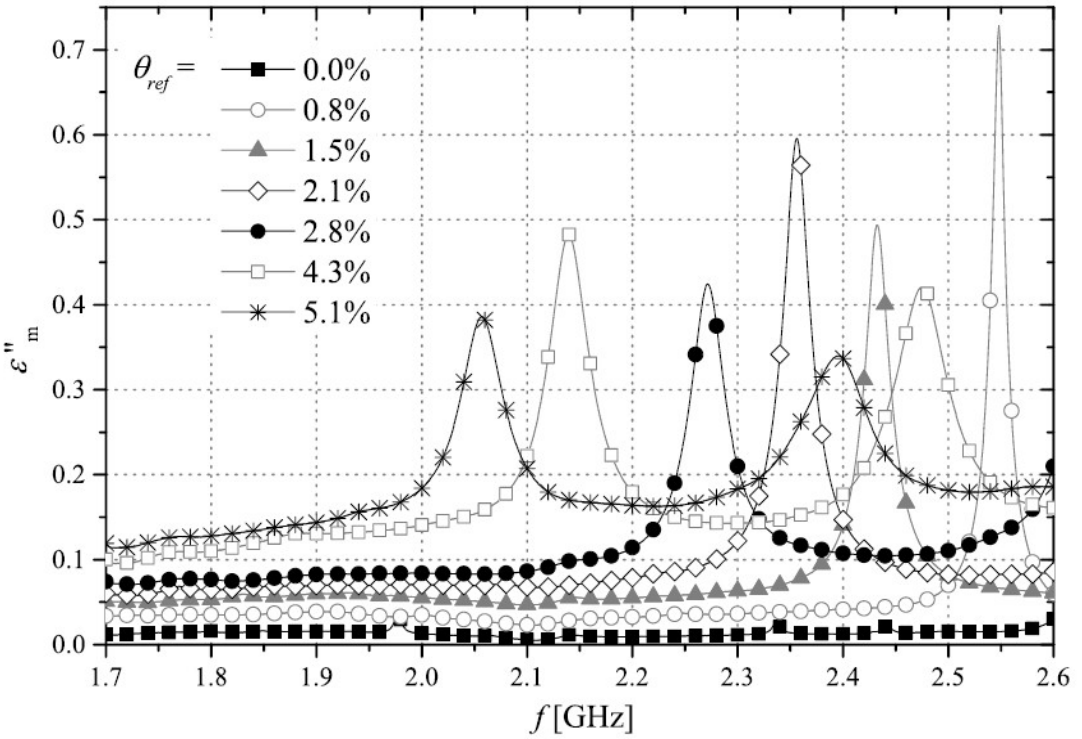

(b)

Fig. 2 – Measurement results on the calcareous aggregate for different water content leves. (a) Real and (b) imaginary parts of the relative dielectric permittivity.

For each moistening step, the sample was inserted in the sample holder and shaken so as to ensure that its volume was constant, and the corresponding real part ε'_m and imaginary part ε''_m of the relative dielectric permittivity were measured with the WR430 system. The actual water content was estimated by weighing the sample immediately after its removal from the sample holder. With regard to the calcareous aggregate, starting from the oven-dried condition, it was moistened at θ_{ref} = 0.8%, 1.5%, 2.1%, 2.8%, 4.3%, and, finally, 5.1% (this final value corresponding to near saturation). Figures 2a and 2b shows the ε'_m and ε''_m results in the considered frequency range, respectively.

Similar experiments were performed on the basaltic material. Starting from the oven-dried material, the sample was moistened at θ_{ref} = 0.9%, 1.8%, 3.0%, 4.2%, 6.3%, and, finally, 7.1%. Also in this case, this final value corresponds to near saturation. Figures 3a and 3b shows the ε'_m and ε''_m results in the considered frequency range, respectively. For both the considered materials and for each considered θ_{ref} value, the corresponding permittivity values are generally constant in the considered frequency range, thus showing a low dispersivity of the material. Indeed, some fluctuations and abrupt variations are present. As previously discussed, they are attributable to the sample resonances and are unavoidable

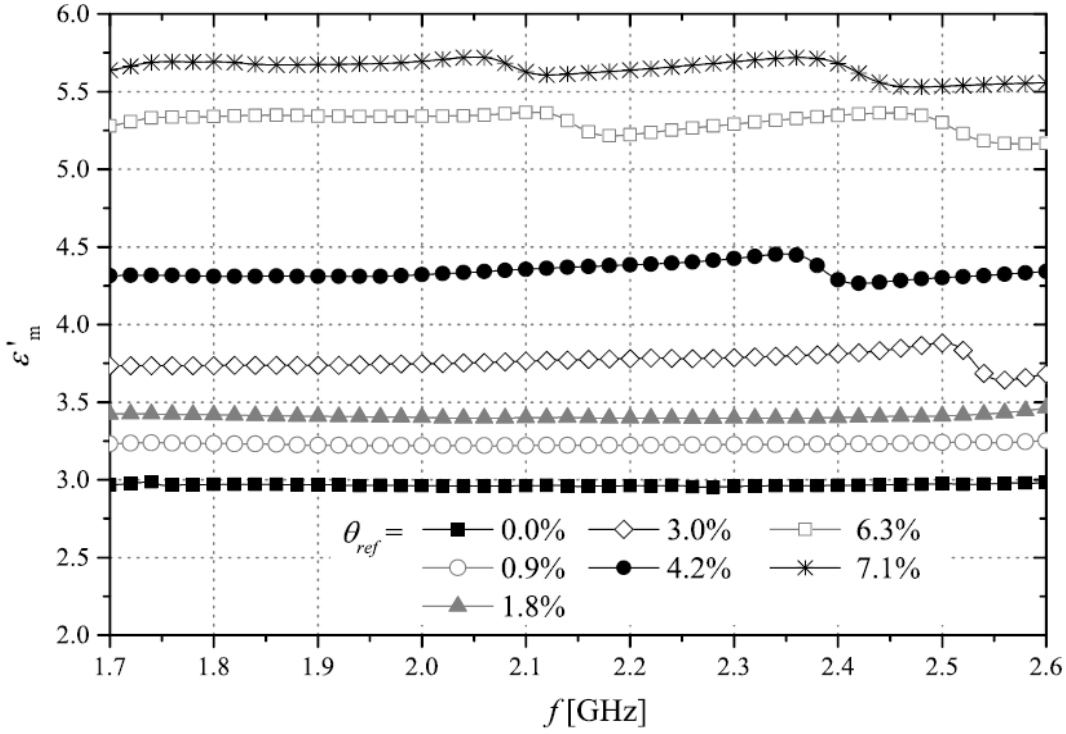

(a)

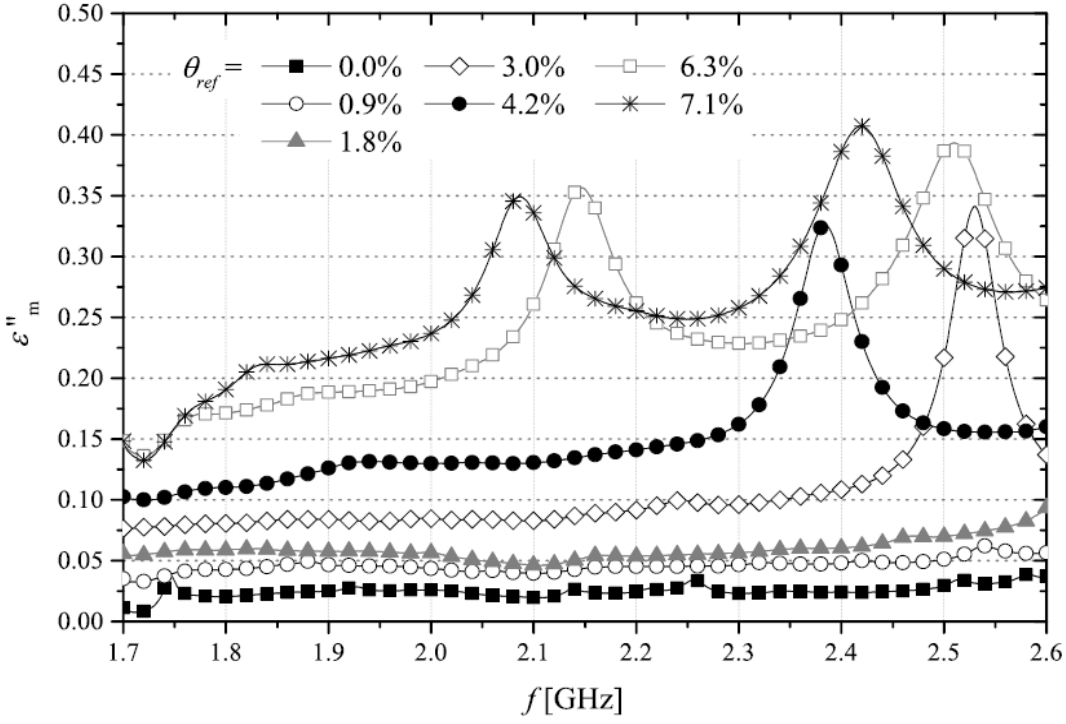

(b)

Fig. 3 – Measurement results on basaltic material for different moisture levels. (a) Real and (b) imaginary parts of the relative dielectric permittivity.

Table II – Summarized results of the measured permittivity values (ε'_m) obtained for calcareous aggregate, for pre-established values of θref. the frequency values ($f$res) of the resonance phenomena that occur are also reported

θ_{ref}	ε'_m	f_{res} values (GHz)
0.0%	3.5	1.76; 2.51
0.8%	3.8	1.69; 2.41
1.5%	4.1	1.63; 2.32
2.1%	4.4	2.24
2.8%	4.7	2.17
4.3%	5.4	2.02; 2.65
5.1%	5.8	1.95; 2.55

propagation of higher order modes. To better clarify this aspect, the permittivity value (real part) for each sample has been obtained as an average over the entire frequency band, neglecting the regions affected by the resonances. The ε'_m values are reported in Tables II and III for the calcareous and basaltic aggregates, respectively. Tables II and III also report the approximate resonance frequencies given by the following equation (by neglecting losses):

$$f_{res,k} \cong \sqrt{\frac{1}{\varepsilon'_r}\left[\left(\frac{k \cdot c_0}{2 \cdot L}\right)^2 + f_{c_0}^2\right]} \quad (2)$$

Tab. III– Summarized results of the measured permittivity values (ε'_m) obtained for basaltic material, for the pre-established values of θref. The frequency values ($f$res) of the resonance phenomena that occur are also reported.

θ_{ref}	ε'_m	f_{res} values (GHz)
0.0%	3.0	1.90
0.9%	3.2	1.84; 2.63
1.8%	3.4	1.79; 2.55
3.0%	3.7	1.71; 2.44
4.2%	4.3	2.27
6.3%	5.3	2.04; 2.67
7.1%	5.7	1.97; 2.58

where C_0 is the speed of light in vacuum, ε'_r is the real part ofthe dielectric permittivity of the propagation medium, f_{c0} is the cutoff frequency of the waveguide in air, L is the length of the sample, and k = 1, 2, 3, . . . , n is the order of the resonance.

The computed resonance frequencies agree well with the position of the artifacts on the measured permittivity spectra, appearing as relaxation-like behaviors both in the real and imaginary parts of permittivity. It is worth noting that, in some cases (e.g., dry calcareous aggregate), an apparently impossible increase in permittivity with frequency is visible at the upper edge of the band. However, from the previously computed resonances, it is immediate to verify that such unrealistic behavior is once more the effect of a sample resonance occurring just at the upper edge of the operating frequency band.

Altogether, it can be concluded that, when the system is used for measurements on aggregate materials, the predicted 2% measurement uncertainty is compromised around sample resonance frequencies, but an

average permittivity value can still be safely and accurately estimated. Clearly, the system would not be suitable to characterize materials with relaxation phenomena and sample resonances within the explored frequency band. As a last note, some experiments have been performed to assess measurement repeatability, which was always better than 1%. Also system drift, assessed through a measurement in air (empty sample holder) carried out at the end of the measurement session (which could last up to 6 h), showed values of the order of 0.1%.

2. Identification and validation of the $\theta - \varepsilon$ dielectric mixing models

The following step regarded the identification of dielectric mixing models that could suitably describe the θ–ε relationship for the considered materials; in particular, three different models were considered as candidates:

1) a semiempirical model (i.e., the four-component α-model [25], [26]);
2) a probabilistic model (i.e., Ansoult's model [27], [28]);
3) an empirical model (i.e., Topp's equation [29]).

These models adopt different approaches to infer the θ–ε relationship. Semiempirical dielectric mixing models [25], [26], [30], [31] are largely used for granular materials. In these models, several parameters are taken into account (such as porosity of the material and distinction of free water from bound water), which are crucial for an accurate physical description of the considered materials, and are sometimes neglected by more general dielectric models.

The probabilistic Ansoult's model, instead, is based on the random propagation of the pulse in a porous medium that is represented as an array of capacitors. In this approach, the granular material is schematized as a set of three capacitors, each associated with the dielectric constants of the different material constituents (neglecting bound water). A computational algorithm,

with a fine-tuning of the so-called degrees of freedom, is used to evaluate the overall equivalent dielectric constant [28].

Finally, empirical approaches simply fit mathematical expressions to measured data: no assumption is made about the state of water in porous materials. In this chapter, the well-known Topp's model was used [29]; hence, a third-order polynomial regression equation was used to represent the θ–$\mathcal{E}$ relationship.

To comparatively assess the robustness and suitability for the specific materials, the following procedure was carried out. First, the θ values were considered as independent variables of the model, and the corresponding permittivity values $\mathcal{E}_{m,mod}$ were evaluated from the α-model and from Ansoult's model. These values were then compared with the $\mathcal{E}_m$ values, directly measured through the WR430 system.

Successively, the dielectric mixing models were inverted. In this way, the measured $\mathcal{E}_m$ values were considered as independent variables, and the corresponding water content levels θ_{mod} were evaluated from the rearranged α-and Ansoult's models. The obtained θ_{mod} values were then compared with the known (reference) θ values. In this case, also Topp's model was used.

2.1 Dielectric Mixing Models

The semiempirical four-component α-model is described by the following equation [26], [30], [31]:

$$\mathcal{E}_m^{\alpha} = (\theta - \theta_{bw})\mathcal{E}_{fw}^{\alpha} + (1 - \phi)\mathcal{E}_s^{\alpha} + \theta_{bw}\varepsilon_{bw}^{\alpha} + (\phi - \theta)\varepsilon_a^{\alpha} \quad (3)$$

where α is a parameter that takes into account the geometry and the polarization, ϕ is the total porosity, $\mathcal{E}_m$ is the measured permittivity, $\mathcal{E}_s$ is the permittivity of the solid material (i.e., without air), $\mathcal{E}_{\mathrm{fw}}$ is the permittivity of free water (which is equal to 78, at the controlled environmental temperature 27±1 °C), $\mathcal{E}_a$ is the permittivity of air, $\mathcal{E}_{\mathrm{bw}}$ is the permittivity of bound water

(which was considered equal to 35 [26]), θ_{bw} is the volumetric content of (only the) bound water, and, finally, θ is the total volumetric water content. In particular

$$\theta_{bw} = \begin{cases} \theta & for \theta \leq \theta_{bw,max} \\ \theta_{bw,max} & for \theta > \theta_{bw,max} \end{cases}$$

where $\theta_{bw,max}$ is the saturation value of bound-water content.

The value of $\mathcal{E}$s can be calculated from the permittivity of the dry material ($\mathcal{E}_{m,dry}$), by applying (3) and considering $\theta_{bw} = 0$ and $\theta = 0$

$$\mathcal{E}s = \left(\frac{\varepsilon_{m,dry}^{\alpha} - \phi \cdot \varepsilon_{a}^{\alpha}}{1 - \phi} \right)^{\frac{1}{\alpha}} \quad (4)$$

In this chapter, the values of α and $\theta_{bw,max}$ were evaluated applying a least-squares fitting procedure of the experimental data to (3) and (4). Overall, the following parameter values were obtained: $\mathcal{E}s$ = 5.38; α = 0.74; and $\theta_{bw,max}$ = 3% for the basaltic aggregate, and $\mathcal{E}s$ = 5.75; α = 0.71; and $\theta_{bw,max}$ = 0.2% for the calcareous aggregate.

It is worth mentioning that the saturation value for bound water could be linked to geometrical characteristics of the grains [26], and thus theoretically computed. On the other hand, also the value assigned to bound water permittivity is somewhat arbitrary, since the different layers of bound water show a progressively increasing permittivity value, and it could be optimized as well. Overall, the obtained values must be considered as a set of best-fitting parameters, suitable to derive a predictive model, rather than representative of the actual geometric structure of the grains.

Starting from these considerations, for each material and for each pre-established volumetric water content level (θ), the corresponding relative dielectric permittivity $\mathcal{E}'_{m,\mathrm{mod}}$ was calculated from (3), obtaining the solid line reported in Figures 4a and 4b for calcareous and basaltic samples, respectively. Successively, Ansoult's model was applied. In this case, the model requires two inputs, namely, the permittivity of the solid material and the number of degrees of freedom. These parameters were evaluated through a minimization procedure. The obtained number of degrees of freedom was 19 for both materials, while the obtained values of $\mathcal{E}s$ were 5.40 and 4.32 for calcareous and basaltic aggregates, respectively. Results of application of the optimized Ansoult's model are reported in Figures 4a and 4b.

Comparing the performances of the two models against the measured values (square markers in Figure 4), it is immediately evident that both models are suitable for materials, like the tested calcareous aggregate, where bound water plays a minor role (less than 0.2% maximum volumetric content). On the other hand, the four-compartment α model proves superior in cases (like the tested basaltic aggregate) where bound water is a significant fraction (volumetric content up to 3%). In particular, for the calcareous material, the maximum percentage error of the α model evaluated as

$$\Delta\varepsilon\% = \left(\left|\varepsilon'_{m,mod} - \varepsilon'_m\right| \cdot 100\right)/\varepsilon'_m \qquad (5)$$

is less than 1%, while it goes up to 1% for Ansoult's model. For the basaltic sample, instead, the error is less than 1% for the α model and exceeds 10% for Ansoult's model, which, however, shows performances similar to the α model for volumetric moisture above 3%. It is worth noting that the comparison has been carried out for a range of moisture levels below 10%, while similar comparisons in the literature consider much higher water contents. This is because usually such models are applied to soils, which can be soaked

following rain or irrigation. On the other hand, an aggregate used for civil applications, once taken from a stack, can at most be saturated. Therefore, the results point toward the applicability of a four-compartment semiempirical model as a suitable mixing model to describe mineral aggregates used in the asphalt industry in the moisture conditions expected under typical scenarios.

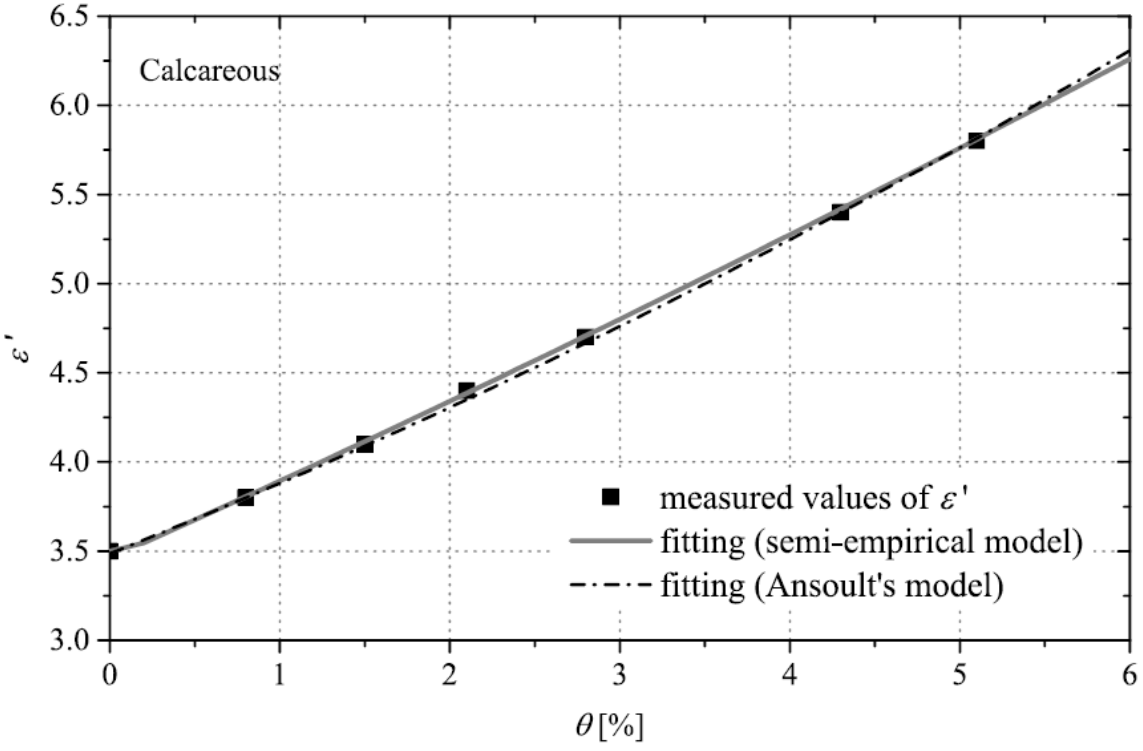

(a)

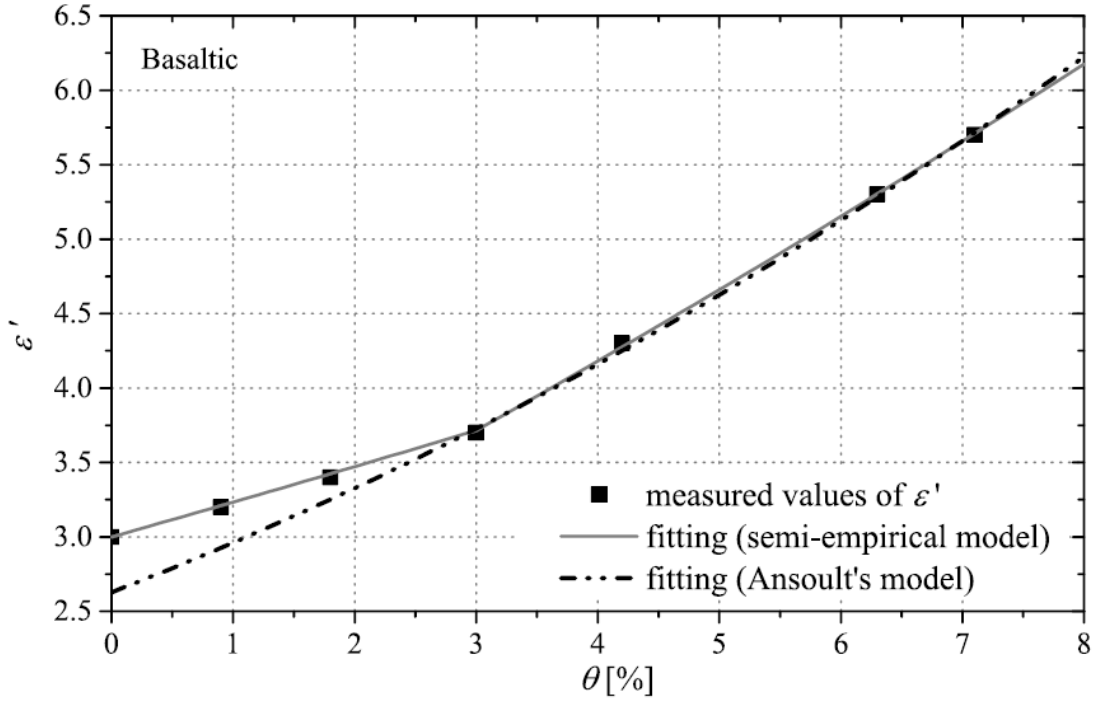

(b)

Fig. 4 – Comparison of the results obtained applying different dielectric models. (a) Calcareous and (b) basaltic aggregates.

2.2 Moisture content estimation

As aforementioned, to test the robustness of the considered dielectric mixing models, the α model and Ansoult's models were inverted so as to have $\mathcal{E}m$ as an independent variable. In particular, with regard to the α-model, the inversion of (3) leads to the following equations:

$$\theta = \begin{cases} \dfrac{\varepsilon_m^\alpha - \varepsilon_s^\alpha \cdot (1-\phi) - \phi \cdot \varepsilon_a^\alpha}{\varepsilon_{bw}^\alpha - \varepsilon_a^\alpha} & if \quad \theta \le \theta_{bw,max} \\ \dfrac{\varepsilon_m^\alpha - \varepsilon_s^\alpha \cdot (1-\phi) + \theta_{bw,max} \cdot \left(\varepsilon_{fw}^\alpha - \varepsilon_{bw}^\alpha\right) - \phi \cdot \varepsilon_a^\alpha}{\varepsilon_{fw}^\alpha - \varepsilon_a^\alpha} & if \quad \theta > \theta_{bw,max} \end{cases}$$

In this case, the $\mathcal{E}_{\mathrm{m}}$ values were considered as independent variables, thus calculating the corresponding water content values derived from the model (θ_{mod}).

As for Ansoult's model, to circumvent the fact that its algorithm requires θ as input (independent variable) and gives $\mathcal{E}$ as output (dependent variable), without possibility of switching input/output [28], an iterative procedure was carried out. More specifically, different values of θ were given as input to the algorithm, until the output value of $\mathcal{E}$ equaled the measured value of the permittivity. Finally, in addition to the α and Ansoult's models, a totally empirical model (i.e., Topp's model) was used to estimate moisture content. Topp's model is based on a simple

Tab. IV – Comparison between water content levels evaluated through the dielectric models ($\theta\alpha$, θans , θTopp) and the pre-established water content levels (θref), for calcareous aggregate, in correspondence with different values of measured permittivity (ε'_m)

ε'_m	θ_{ref}	θ_{α}	θ_{Ans}	θ_{Topp}
3.5	0.0%	0.01%	0.03%	0.03%
3.8	0.8%	0.79%	0.80%	0.78%
4.1	1.5%	1.47%	1.52%	1.48%
4.4	2.1%	2.13%	2.21%	2.15%
4.7	2.8%	2.79%	2.87%	2.80%
5.4	4.3%	4.26%	4.30%	4.27%
5.8	5.1%	5.08%	5.07%	5.11%

Table V – Comparison between water content levels evaluated through the dielectric models ($\theta\alpha$, θans , θtopp) and the pre-establishedwater content levels (θref), for basaltic material, in correspondence with different values of measured permittivity (ε'_m)

ε'_m	θ_{ref}	θ_{α}	θ_{Ans}	θ_{Topp}
3.0	0.0%	0.00%	1.11%	-0.09%
3.2	0.9%	0.86%	1.66%	0.88%
3.4	1.8%	1.70%	2.19%	1.72%
3.7	3.0%	2.94%	2.94%	2.75%
4.3	4.2%	4.25%	4.31%	4.22%
5.3	6.3%	6.29%	6.33%	6.04%
5.7	7.1%	7.08%	7.07%	6.95%

third-order polynomial fitting of experimental data. The obtained θ_{mod} values for the three models were then compared with the pre-established (true) values of θ.

Tables IV and V summarize the results for the calcareous sand basaltic materials, respectively. The results show that, for calcareous aggregate, the three models provide accurate estimates of the water content, while, as expected, Ansoult's model fails for low-moisture contents in the case of the

basaltic material. It is worth highlighting that the simple polynomial model (Topp's equation), suitably fitted to experimental data, provides very robust estimations of water content for very different types of materials.

Conclusions

The experimental characterization of the system was completed by performing dielectric permittivity measurements on inert materials that are typically used in the production of asphalt (calcareous and basaltic aggregates). Finally, to analytically characterize the relationship between water content of the granular materials and the corresponding permittivity values, three different dielectric models (i.e., α model, Ansoult's model, and Topp's equation) were comparatively assessed. Experimental tests were performed to identify the most suitable ones in describing the water content and dielectric permittivity relationship for the considered materials. The results not only suggest the need to use a four-compartment model for accurate characterization of the water/aggregate mixture, but also highlight that, as far as moisture estimation from the measured permittivity is the main aim, a third-order polynomial fitting proves an excellent candidate for a simple and ready-to-use model. The obtained measurement results demonstrate the flexibility and practical usability of the system for possible applications in the road-maintenance related industry. Compared with standard waveguide systems, the proposed custom solution is characterized by the large sample holder volume, the optimized operating frequency range allowing measurements around the ISM frequency of 2.45 GHz, and the presence of the pressurization windows making the system suitable for granular samples. Overall, the costs for manufacturing the custom-made waveguide components are below €1000, making it a competitive and cost-

effective solution. Finally, it is worth emphasizing that the application of the proposed system is not limited to the aggregate materials used in the asphalt production; on the contrary, it could also be used for dielectric spectroscopy of granular materials in general (with application, for example, in the agri-food industry).

References

[23] R. Lal, Ed., Encyclopedia of Soil Science, vol. 1, 2nd ed. Boca Raton, FL, USA: Taylor & Francis, 2005.

[24] P. F. Hudak, Principles of Hydrogeology, 3rd ed. Boca Raton, FL, USA: CRC Press, 2005.

[25] J. R. Birchak, C. G. Gardner, J. E. Hipp, and J. M. Victor, "High dielectric constant microwave probes for sensing soil moisture," Proc. IEEE, vol. 62, no. 1, pp. 93–98, Jan. 1974.

[26] M. C. Dobson, F. T. Ulaby, M. T. Hallikainen, and M. A. El-Rayes, "Microwave dielectric behavior of wet soil-Part II: Dielectric mixing models," IEEE Trans. Geosci. Remote Sens., vol. 23, no. 1, pp. 35–46, Jan. 1985.

[27] M. Ansoult, L. W. De Backer, and M. Declercq, "Statistical relationship between apparent dielectric constant and water content in porous media," Soil Sci. Soc. Amer. J., vol. 49, no. 1, pp. 47–50, 1985.

[28] P. Todoroff and P. Langellier, "Comparison of empirical and partly deterministic methods of time domain reflectometry calibration, based on a study of two tropical soils," Soil Tillage Res., vol. 45, nos. 3–4, pp. 325–340, 1998.

[29] G. C. Topp, J. L. Davis, and A. P. Annan, "Electromagnetic determination of soil water content: Measurements in coaxial transmission lines," Water Resour. Res., vol. 16, no. 3, pp. 574–582, 1980.

[30] G. P. de Loor, "Dielectric properties of heterogeneous mixtures containing water," J. Microw. Power, vol. 3, no. 2, pp. 67–73, Mar. 1968.

[31] A. Cataldo, L. Tarricone, M. Vallone, G. Cannazza, and M. Cipressa, "TDR moisture measurements in granular materials: From the siliceous sand test case to the applications for agro-food industrial monitoring," Comput. Standards Interfaces, vol. 32, no. 3, pp. 86–95, 2010.

Ringraziamenti

Desidero ringraziare con autentica gratitudine il Prof. Fabrizio Frezza relatore di questa tesi, per la disponibilità, incoraggiamento e la particolare sensibilità dimostratami

Un sentito e distinto ringraziamento alla Prof.ssa Lara Pajewski per il prezioso aiuto fornito durante tutto il mio percorso di Dottorato

Un grazie di cuore ai Professori
Francesco Benedetto e Raffaele Persico

Grazie alla COST Action TU1208
"Civil Engineering Applications of Ground Penetrating Radar"

Table of Contents